FORMATION OF AN EXON-DEFINED A COMPLEX SPLICEOSOME

INTERMEDIATE RESULTS IN CD45 EXON REPRESSION

APPROVED BY SUPERVISORY COMMITTEE

Kristen W. Lynch, Ph.D.

Kevin Gardner, Ph.D.

Melanie Cobb, Ph.D.

Qinghua Liu, Ph.D.

DEDICATION

In honor of my grandfather, Lloyd B. Murphy

FORMATION OF AN EXON-DEFINED A COMPLEX SPLICEOSOME

INTERMEDIATE RESULTS IN CD45 EXON REPRESSION

by

AMY ELIZABETH HOUSE

DISSERTATION

Presented to the Faculty of the Graduate School of Biomedical Sciences

The University of Texas Southwestern Medical Center at Dallas

In Partial Fulfillment of the Requirements

For the Degree of

DOCTOR OF PHILOSOPHY

The University of Texas Southwestern Medical Center at Dallas

Dallas, Texas

October 2007

ACKNOWLEDGEMENTS

FORMATION OF AN EXON-DEFINED A COMPLEX SPLICEOSOME

INTERMEDIATE RESULTS IN CD45 SPLICING REPRESSION

AMY ELIZABETH HOUSE, Ph.D.

The University of Texas Southwestern Medical Center at Dallas, 2007

KRISTEN W. LYNCH, Ph.D.

Alternative splicing is a common means for genetic regulation in higher eukaryotes, and variability in splicing patterns results in a significant increase in protein diversity. Of particular interest is how the splicing machinery is regulated to allow for alternative splicing while maintaining accurate splicing fidelity. CD45 is a trans-membrane tyrosine phosphatase that is expressed on the surface of hematopoetic cells. The CD45 gene contains three variable exons that are partially repressed in naïve T cells and are preferentially skipped upon T cell

activation. Importantly, it has been shown that the alternative splicing of CD45 pre-mRNA affects the resultant protein's function within the cell emphasizing the importance of this RNA processing event. As such, CD45 provides an excellent model system in which to study signal-responsive alternative splicing.

Pre-mRNA splicing is catalyzed by the spliceosome, a macromolecular complex that assembles *de novo* on a pre-mRNA template in a stepwise and highly dynamic process. The inherent dynamic nature of the spliceosome suggests the potential for regulation at numerous points along the assembly pathway. Previously, a 60-nucleotide exonic silencer (ESS1) was identified within variable exon 4 of the CD45 gene. ESS1 is bound by at least three hnRNP proteins (hnRNP L, PTB, hnRNP E2) of which hnRNP L is the main functional component. Subsequent work showed that ESS1 does not regulate CD45 exon 4 splicing by the typical mechanism of preventing exon definition. Instead, spliceosome assembly is stalled after the exon has been recognized by the spliceosome such that both U1 and U2 are bound to the splice sites suggesting that the stalled complex represents an A-like exon-defined complex (AEC). Additionally, hnRNP L is sufficient to block spliceosome assembly at the AEC. Further biochemical analysis of the AEC suggests that the stall in assembly may be due to altered interactions between the spliceosomal snRNAs and/or proteins and the pre-mRNA substrate. Overall, this inhibition represents a new

mechanism for splicing regulation, and suggests that the formation of an AEC

intermediate is an important transition in the spliceosome assembly pathway.

TABLE OF CONTENTS

PRIOR PUBLICATIONS

House, A.E. and K.W. Lynch. (2007) Regulation of Alternative Splicing: More than just the ABCs? *J. Biol. Chem.*, accepted.

House, A.E. and K.W. Lynch (2006) An exonic splicing silencer represses spliceosome assembly after ATP-dependent exon recognition. *Nat. Struct. Mol. Biol.*, 13: 937-944.

Rothrock, C.R.*, **House, A.E.***, and K.W. Lynch (2005) HnRNP L represses exon splicing via a regulated exonic splicing silencer. *EMBO J*. 24: 2792-2802. (*co-first author)

ABSTRACTS

House, A. and K. W. Lynch. *In Vitro* Recapitulation of Signal-Induced Alternative Splicing (poster). Ninth Annual Meeting of the RNA Society, 2004.

House, A. and K. W. Lynch. Mechanism of Regulated Exon Inclusion in CD45 Alternative Splicing (oral presentation). Tenth Annual Meeting of the RNA Society, 2005.

House, A. and K. W. Lynch. Structural and Proteomic Characterization of Regulated Exon-defined A Complex (poster). Eleventh Annual Meeting of the RNA Society, 2006.

LIST OF FIGURES

LIST OF APPENDICES

LIST OF DEFINITIONS

α – Anti

A – Adenosine

AEC – A-like Exon-definition Complex

AMT – Aminomethyltrimethyl

AMV RT – Avian Myeloblastosis Virus Reverse Transcriptase

ARS – Activation Responsive Sequence

ASF/SF2 – Splicing Factor, Arginine/Serine-rich 1

ATP – Adenosine Triphosphate

Bi – Biotin

bp - Basepair

BPS – Branch Point Sequence

BSA – Bovine Serum Albumin

C – Cytidine

CGRP – Calcitonin-Gene Related Peptide

CP – Phosphocreatine

dNTP – Deoxyribonucleotide Triphosphate

ddATP – Dideoxyadenosine Triphosphate

ddCTP – Dideoxycytidine Triphosphate

ddGTP – Dideoxyguanosine Triphosphate

ddNTP – Dideoxyribonucleotide Triphosphate

ddTTP – Dideoxythymidine Triphosphate

ddseq – Dideoxysequencing

DExD/H – family of RNA helicases, containing Asp-Glu-X-Asp/His motif

DMEM – Dulbecco's Modified Eagle's Medium

DTT – Dithiotreitol

EDTA – Ethylenediaminetetraacetic acid

eNOS – Endothelial Nitric Oxide Synthase gene

Erk1/2 – Extracellular Signal Related Kinase

ESE – Exonic Splicing Enhancer

ESS – Exonic Splicing Silencer

FPLC – Fast Protein Liquid Chromatography

FR – Fold Repression

G – Guanosine

GAR – Guanosine-Adenosine Rich

GDP – Guanosine Diphosphate

GST – Glutathione-S-Transferase

GTP – Guanosine Triphosphate

HIV – Human Immunodeficiency Virus

HnRNP – Heterogeneous Nuclear Ribonuclear Protein

HPLC – High Performance Liquid Chromatography

IPTG – Isopropyl-beta-D-thiogalactopyranoside

ISE – Intronic Splicing Enhancer

ISS – Intronic Splicing Silencer

JSL1 – Jurkat Splicing Line 1

KCl – Potassium Chloride

kD – kilo Dalton

KH – K Homology RNA Binding Domain

LB – Luria's Broth

MBP – Maltose Binding Protein

$MgCl_2$ – Magnesium Chloride

MgOAc – Magnesium Acetate

MMLV RT – Maloney Murine Leukemia Virus Reverse Transcriptase

mRNA – Messenger RNA

MS2 – Bacteriophage Coat Protein

NaCl – Sodium Chloride

NaOAc – Sodium Acetate

NE – Nuclear Extract

NF-1 – Neurofibromin 1 gene

NRS – Negative Regulator of Splicing

nt- Nucleotides

oligo – Oligonucleotide

PAGE – Polyacrylamide Gel Electrophoresis

PCA – Phenol Chloroform Isoamyl Alcohol

PCR – Polymerase Chain Reaction

PHA – Phytohemagglutinin

PK – Proteinase K

PMA – Phorbol 12-myristate 13-acetate

PMSF – Phenylmethanesulphonylfluoride

PPT – Polypyrimidine Tract

pre-mRNA – Precursor Messenger RNA

PSF – PTB Associated Splicing factor

PTB – Polypyrimidine Tract Binding Protein

PVA – Polyvinyl Alcohol

Py – Pyrimidine

RNA – Ribonucleic Acid

RNAi – RNA Interference Mechanism

RNase – Ribonuclease

RRM – RNA Recognition Motif

RS – Arginine-Serine Rich Domain

RT – Reverse Transcription

RT-PCR – Reverse Transcription Polymerase Chain Reaction

SC35 – Splicing factor, Serine/Arginine-rich 2

SCID – Severe-Combined Immune Deficiency

SDS – Sodium Dodecyl Sulfate

SELEX – Systematic Evolution of Ligands by Exponential Enrichment

SFK – Src Family Protein Tyrosine Kinase

SHAPE – Selective 2' Hydroxyl Acylation analyzed by Primer Extension

siRNA – Small Interfering RNA

snRNA – Small Nuclear RNA

snRNP – Small Nuclear Ribonucleoprotein Particle

SPF45 – Human Splicing Factor 45 kDa

ss- Splice Site

Sxl – Sex-lethal

T – Thymidine

TCA – Trichloroacetic Acid

TCR – T Cell Receptor

Tra – Transformer Protein

Tri-snRNP – U5/U4•U6 Small Nuclear Ribonucleoprotein Particle

U – Uridine

U2AF – U2 Auxiliary Factor

YB-1 – Y-Box Binding Protein

CHAPTER ONE

Introduction and Literature Review

After the sequencing of the human genome, the unexpectedly small number of estimated genes emphasized the importance of other means by which we generate a diverse proteome. Among these mechanisms are the use of alternate transcription and translation start sites, alternative 3' end processing, RNA editing and alternative pre-mRNA processing (Black, 2003; Hui and Bindereif, 2005). Alternative splicing, however, is predicted to occur in the vast majority of mammalian genes making it perhaps the most common mechanism of generating protein diversity (Blencowe, 2006). A genome-wide survey of alternative splicing in more than 50 human cell types estimated that over 70% of human genes are regulated in this manner (Johnson et al., 2003).

The CD45 gene was previously reported to be subject to regulation by alternative splicing (Birkeland et al., 1989; Hermiston et al., 2002; Hermiston et al., 2003). CD45 contains three variable exons that are partially repressed in resting T cells and then preferentially repressed upon T cell activation by antigen challenge (Lynch and Weiss, 2000). Analysis of the mechanisms governing CD45 splicing has identified a regulatory element that is required for repressing the use of these exons under resting conditions (Lynch and Weiss, 2001; Rothrock et al., 2003). However, the auxiliary factors involved and the mechanism by

which these factors function to block recognition of the exons by the spliceosome remained unaddressed in these studies. In this document, work identifying the regulatory trans-acting factors and the mechanism by which they function to repress splicing are presented. The repressed exon is bound by a specific hnRNP silencer binding complex, of which hnRNP L acts as the main functional component to prevent splicing (Rothrock et al., 2005). Further, hnRNP L blocks splicing by stalling spliceosome assembly at an unusual step (House and Lynch, 2006). Importantly, the stalled complex is both a previously unreported point of splicing regulation and a very poorly understood transition in spliceosome assembly. As such, preliminary characterization of the stalled A-like exon-defined complex (AEC) provides unique insight into important aspects of the splicing reaction. In this introduction, I review important previous work in order to provide the necessary background required for understanding of the mechanism of regulated splicing reported in subsequent chapters.

Alternative splicing patterns

Constitutive splicing is the removal of intronic sequence and the ligation of exonic sequence from a pre-mRNA to create a mature, protein-coding RNA transcript. It follows that alternative splicing is the differential inclusion or exclusion of exons to generate distinct mRNA isoforms from the same precursor. There are five major classes of alternative splicing events, which include: cassette exon skipping, mutually exclusive cassette exons, use of alternative 5' or 3' splice

sites, and intron retention (Figure 1-1)(Black, 2003). Upwards of 70-90% of

alternative splicing events are predicted to alter the coding sequence of the

protein (Johnson et al., 2003; Modrek and Lee, 2002), making alternative splicing
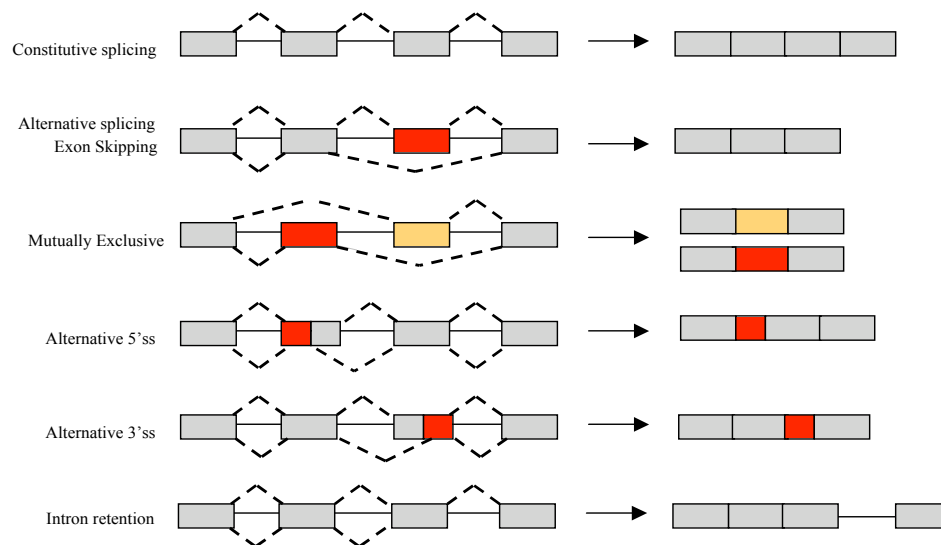
Modified from Black, 2003.

Figure 1-1. Common patterns of pre-mRNA alternative splicing. Alternative splicing generates several different mRNA transcripts from a single precursor. The most common patterns of alternative splicing are shown along with the change in the resulting alternate product as compared to the constitutively spliced product. Exons are depicted as boxes, and introns as lines. Dashed lines indicate the splice sites used in the splicing reaction.

an incredibly important tool for regulating protein activity as well as diversity.

Changing the protein coding sequence can have profound effects on all aspects of

the molecule's behavior and function, including, but certainly not limited to its

localization, enzymatic activity, allosteric regulation, post-translational

modification, and ability to bind target substrate or ligand (Black, 2003).

The regulation of gene expression via alternative splicing is known to

occur in response to a number of different biological processes. Often several

mRNA isoforms from the same gene are generated in the same cell, and the ratio of these isoforms with respect to one another may be altered by the cell or tissue type, developmental stage or gender (Lynch, 2007; Tarn, 2007). In particular, alternative splicing processes are subject to regulation by signal transduction pathways which are regulated by changes in a cell's environment. Signal-induced alternative splicing is especially common in the immune system and the nervous system, both of which must undergo rapid and robust changes in response to extracellular stimuli (Black, 2003; Li et al., 2007; Lynch, 2004b).

The spliceosome and the splicing reaction

The general mechanism for splicing of eukaryotic nuclear pre-mRNA transcripts proceeds through a two-step transesterification reaction, similar to that used by self-splicing introns (Sharp, 1987). First, the branch point A launches a nucleophilic attack on the 5'ss, leading to release of the upstream exon and formation of the lariat-downstream exon intermediate (Figure 1-2). Then, the released exon attacks the phosphate at the 3' end of the intron resulting in exon ligation and release of the lariat intermediate. However, in eukaryotes, splicing requires external factors, both RNA and protein, that associate to form a multi-component enzyme known as the spliceosome, which functions to catalyze the reaction. The spliceosome is comprised of five snRNAs (U1, U2, U4, U5 and U6) that associate with a number of proteins to form a ribonucleoparticle called a "snRNP" (Black, 2003). The catalytic conformation of the spliceosome (so-called

5'ss   BPS   PPT   3'ss

Exon 1 GU — A —(Py)n — AG Exon 2   pre-mRNA

Cleaved upstream exon   Exon 1 -OH +   GU / A —(Py)n — AG Exon 2   Lariat-downstream exon

Lariat   GU / A —(Py)n —AG   +   Exon 1 Exon 2   Ligated exons
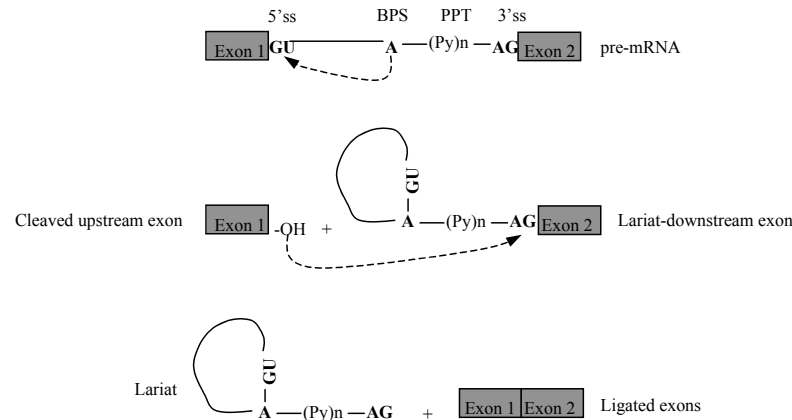
Modified from Black, 2003.

Figure 1-2. Splicing proceeds through a two-step transesterification reaction. The first reaction results in upstream exon release and lariat intermediate formation. The second reaction results in lariat release and exon ligation. Conserved splicing consensus sequences within the 5' splice site (5'ss) and 3' splice site (3'ss) of the pre-mRNA are shown. BPS, branch point sequence that contains the bulged adenosine residue (A). PPT, polypyrimidine tract where Py indicates a pyrimidine residue.

"C" complex) does not exist de novo in its final structure but rather forms in a highly dynamic process best described by a step-wise pathway involving several intermediate complexes (E-A-B) that have been identified and characterized *in vitro* and *in vivo* (Figure 1-3)(Matlin and Moore, 2007; Tardiff and Rosbash, 2005). The earliest known complex committed to the splicing pathway (E) is defined by U1 snRNP bound to a 5' splice site, with direct base-pairing between the U1 snRNA and the 5' splice site sequence of the pre-mRNA, and U2 auxiliary factor (U2AF) as well as SF1 bound to a corresponding 3' splice site (Figure 1-3)(Das et al., 2000). U2AF is a hetero-dimer composed of the U2AF35 and U2AF65 subunits, which recognize and bind to the terminal AG and the PPT within the 3' splice site respectively, while SF1 is associated with the branch-

point sequence (Black, 2003). E complex is then chased into the pre-spliceosome A complex by the stable addition of U2 snRNP at the 3' splice site facilitated by base-pairing between the U2 snRNA and the pre-mRNA branch-point (Figure 1-3) (Black, 2003). Importantly, this A complex represents the first characterized ATP-dependent step in the assembly of the spliceosome. A complex is converted into B complex by the ATP-dependent recruitment and addition of the U4-U6/U5 tri-snRNP, which contains the remaining spliceosome subunits, followed by the release of U2AF35 and U2AF65 (Figure 1-3) (Black, 2003). Finally, C complex forms by extensive remodeling of both the snRNA and the protein components that are present in B complex, including loss of both the U4 and U1 snRNPs (Figure 1-3)(Black, 2003). These rearrangements produce an active site in C complex that is now capable of catalyzing the transesterification chemistry required for exon ligation and lariat release. The release of U1 and U4 snRNPs, as well as many other molecular rearrangements required for assembly, are promoted by the action of a series of DExD/H box ATPase proteins (Staley and Guthrie, 1998; Valadkhan, 2007). By definition, the complexes described above represent a spliceosome formed around an intron, in an orientation described as "intron-defined". This definition is based on the early use of genes from *S. cerevisiae* or artificial metazoan model substrates in studies of spliceosome assembly, which typically contain a single short intron. However, the subsequent use of more complex splicing substrates has lead to the conclusion that, at least
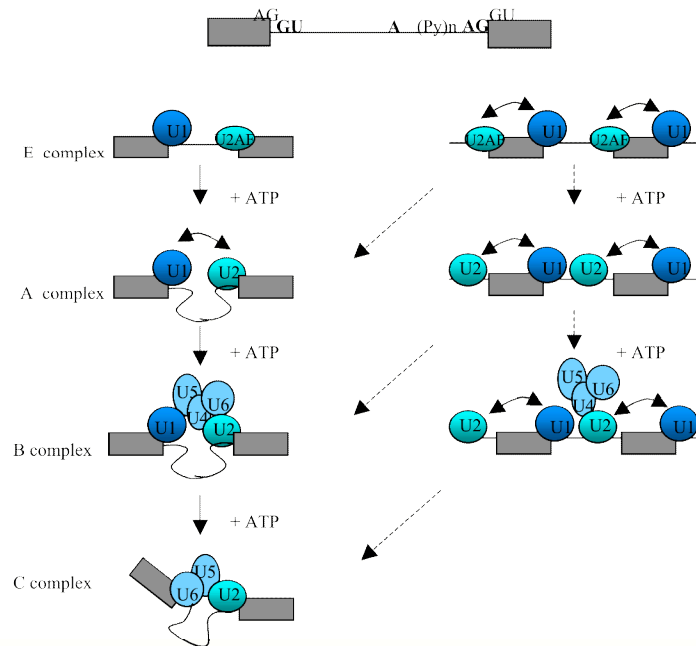
Figure 1-3. The spliceosome assembles in a step-wise and dynamic process. Unspliced and unassembled pre-mRNA is shown at the top. The spliceosomal snRNP components recognize and bind the conserved sequence elements at the exon-intron boundary. The known intermediates (E-A-B) along the assembly pathway and the snRNP components of these complexes are shown. Spliceosome assembly initiates by forming a complex across the exon, but must transition to forming an intron-defined complex by catalysis (C complex). Canonical intron-defined intermediates are shown on the left, while possible exon-defined intermediate are shown on the right. Arrows indicate the association of snRNPs.

during the earliest steps in assembly, the metazoan spliceosome is built around the exon in a manner termed "exon-definition" (Figure 1-3, right-hand column)(Berget, 1995; Hertel, 2007). The final C complex must be formed around the intron for proper catalysis, however, how long the exon-defined conformation persists during spliceosome assembly remains an open question. While kinetic studies have suggested that the commitment of splice site pairing occurs at the A complex stage in assembly (Lim and Hertel, 2004), it has also been demonstrated that U1 and U2 snRNP can bind the 5' and 3' splice sites flanking an isolated

exon to form a stable complex that is subsequently capable of splicing *in trans* to a separate exon (Chiara and Reed, 1995).

It is possible that the stage at which the growing spliceosome transitions from exon-definition to intron-definition differs between substrates in a manner determined by factors such as intron length, auxiliary regulatory proteins or splice site strength. Moreover, cross-exon and cross-intron interactions between snRNP components also may not be mutually exclusive, but rather may occur simultaneously via distinct faces of the snRNPs to assist in the overall assembly of the spliceosome. Finally, it is worth noting that the complexes shown in Figure 1-3 are almost certainly not a comprehensive description of spliceosome assembly. As our ability to isolate and characterize the spliceosome increases, so does our appreciation of previously unidentified transition states in the assembly pathway (Matlin and Moore, 2007).

Auxiliary sequences and non-snRNP proteins in alternative splicing

While the splice sites within the pre-mRNA function to direct the splicing machinery, these sequence elements in higher eukaryotes are highly degenerate and often imbedded within introns that are significantly longer than exons. Thus, frequently as few as a handful of nucleotides mark the ends of an intron often tens of thousands of bases long (Black, 1995). Recent work estimates that the information provided by the canonical pre-mRNA splice sites are less than half of that required for accurate and efficient splicing suggesting that these sequences

are inadequate to direct the splicing machinery (Lim and Burge, 2001). Therefore, it is not surprising that sequence elements outside of the splice sites can strongly affect metazoan pre-mRNA splicing. Cis-acting auxiliary sequences are defined by their activities, such that sequences which promote recruitment of the spliceosome and exon inclusion are termed splicing enhancers, and sequences that disrupt assembly of the splicing machinery and cause exon skipping are referred to splicing silencers. Both types of regulatory sequences can occur within exons and introns, refining their identification as either intronic splicing enhancers (ISE), intronic splicing silencers (ISS), exonic splicing enhancers (ESE) or exonic splicing silencers (ESS) (Black, 2003).

The initial identification and characterization of splicing regulatory elements relied on the development of model system minigene constructs, based on known alternatively spliced genes. Sequences within the minigene context were deleted and/or inserted, and the resulting splicing activity was monitored. One of the best characterized splicing regulatory sequences, purine rich GAR enhancers, were identified using minigene analysis (Watakabe et al., 1993). These enhancers are often bound by ASF/SF2 and Tra2, of which both are members of the SR protein family (Liu et al., 1998; Tacke and Manley, 1999). However, RNA regulatory sequences are often poorly conserved with respect to the ideal consensus sequence (Black, 2003), emphasizing the importance of a thorough understanding of what constitutes these sequence elements. Toward this end, more generalized

methods have been developed to identify novel enhancer and silencer elements. SELEX (systematic evolution of ligands by exponential enrichment) analysis, in combination with *in vivo* and *in vitro* selection protocols, has identified several different ESE elements (Coulter et al., 1997; Liu et al., 2000; Liu et al., 1998; Schaal and Maniatis, 1999a; Woerfel and Bindereif, 2001). More recently, a study screened a 10-mer library *in vivo* using a splicing reporter identified and confirmed several new splicing silencer elements (Wang et al., 2004). In addition, bioinformatics approaches have also been employed to identify new auxiliary sequences that influence splicing. The development of new and improved computational methods has identified over 20 novel ESEs and ESSs, many of which have been confirmed to have function *in vivo*, emphasizing the range of splicing regulatory elements (Stadler et al., 2006). Also, several groups of hexameric enhancer sequences were identified using bioinformatics (Fairbrother et al., 2002). Continued use of these systematic approaches, in combination with specific minigene studies, has greatly enhanced our understanding of splicing regulatory sequence elements and their functions.

While a few regulatory sequences have been shown to function by directly creating RNA secondary structures that alter splice site recognition (Buratti et al., 2004; Graveley, 2005; Hertel, 2007; Singh et al., 2007), the majority act primarily as platforms for binding of non-snRNP regulatory proteins. To a first approximation, the best characterized of the regulatory elements are ESEs, which

most commonly bind a family of proteins known as Serine/Arginine-rich proteins

(SR proteins) (Figure 1-4A). Members of the SR protein family contain a RRM

(RNA recognition motif) RNA binding domain and a region rich in Arg-Ser

dipeptides (RS domain) involved in making protein-protein interactions (Lin and

Fu, 2007). Previous reports have shown that at least one member of the SR

protein family must be present for efficient splicing in cell extracts (Black, 2003).

While this suggests functional redundancy *in vitro*, as the addition of any SR

protein resulted in the same outcome, the role of a particular SR protein is likely

more important *in vivo* (Black, 2003; Wang et al., 2001). ASF/SF2 has been

shown to interact with U170K, a non-SR protein component of the U1 snRNP, in

a large SR protein complex that functions to promote splicing (Kohtz et al., 1994;
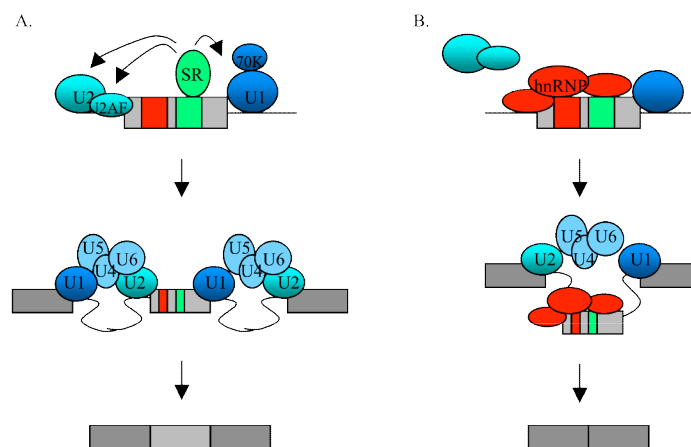
Figure 1-4. Cis-acting regulatory sequences and their cognate binding proteins regulate patterns of alternative splicing. (A) Splicing enhancer elements typically bind to members of the SR protein family. Binding of SR proteins facilitates recruitment and assembly of the spliceosome resulting in increased exon inclusion. (**B**) Splicing silencer elements most often bind to proteins in the hnRNP family. Binding of hnRNPs to the exon results in inhibition of spliceosome assembly and thus exon skipping.

Wu and Maniatis, 1993). In addition, several other large SR protein complexes also require the binding of additional RS domain containing proteins, such as U2AF35, SRm160 and SRm300, and are believed to show specificity in their protein interactions, suggesting that individual SR proteins likely have specific as well as general functions *in vivo* (Blencowe et al., 1998; Eldridge et al., 1999; Li and Blencowe, 1999; Zuo and Maniatis, 1996).

By contrast to ESEs, ESSs typically function to repress exon inclusion by recruiting members of the hnRNP family of proteins (Figure 1-4B). The hnRNP family of proteins was initially defined based on their association with unspliced RNA and their functions in RNA processing (Dreyfuss et al., 1993). As such, they are a structurally diverse set of RNA binding proteins although all members contain either the KH domain or the RRM RNA binding motif (Martinez-Contreras et al., 2007). While most members of the hnRNP family are predominantly localized to the nucleus, several hnRNP proteins have been reported to shuttle between the nucleus and cytoplasm (Nakielny and Dreyfuss, 1999). While SR and hnRNP proteins do not always correlate strictly with enhancers and silencers respectively, this simplification helps illustrate the important emerging concept of a splicing "code" in which the splicing pattern of a gene is determined by the interplay of proteins along a nascent transcript (Fu, 2004; Han et al., 2005; Hertel, 2007; Matlin et al., 2005). Additional splicing regulatory proteins have also been identified that have similar activity to SR and

hnRNP proteins but do not fall cleanly into one of these two protein families (Darnell, 2006; Forch et al., 2002; Ishiura et al., 2005; Lin and Fu, 2007). Such non-SR/hnRNP splicing regulatory proteins further increase the complexity of the splicing regulatory machinery.

Combinatorial control of alternative splicing

A critical aspect of splicing regulation is the concept of combinatorial control by cooperative or dueling cis-acting elements. Most hnRNP and SR proteins are expressed ubiquitously, implying that the precise balance of negative and positive factors in any given cell can have a profound influence on the ultimate choice of alternative splicing patterns (Black, 2003). An increasing number of regulated splicing events under the control of both splicing enhancer and silencer elements are being reported. Alternative splicing of CD45 exon 5 was shown to require both an ESE and an ESS, but the mechanism by which this regulation occurs remains unclear (Tong et al., 2005)(L. Motta-Mena and K.W. Lynch, UTSWMC). Exon N1 in the c-src gene is spliced in a tissue specific manner, such that N1 is included in neurons but excluded in all other cell types (Black, 2003). Splicing of the N1 exon is regulated by the collective binding of factors to an ESE as well as several ISSs and ISEs located both upstream and downstream of the exon (Modafferi and Black, 1997; Modafferi and Black, 1999; Rooke et al., 1999). Again, the specific details of splicing regulation remain

vague, but the importance of combinatorial control in regulating mammalian splicing is clear.

Regulation of splice site recognition

Perhaps the best characterized splicing enhancers and silencers are those that control the earliest steps of spliceosome assembly, namely the association of the U1 snRNP, U2AF and the U2 snRNP with the 5' and 3' splice sites respectively (Lin and Fu, 2007; Martinez-Contreras et al., 2007; Matlin et al., 2005). SR proteins have been shown to interact with both the U1 snRNP and the U2AF heterodimer, recruiting these spliceosomal components to a particular exon (Figure 1-4A)(Lin and Fu, 2007). Furthermore, the RS domains of SR proteins stabilizes RNA base-pairing interactions between the U2 snRNA and the BPS (Shen and Green, 2006). SR proteins are thought to bind to most exons to promote basic exon definition interactions even for constitutive (non-alternative) exons (Lin and Fu, 2007). However, the association of SR proteins with ESEs is often relatively weak and thus can be promoted or blocked by neighboring proteins to regulate exon inclusion. For example, the *Drosophila* female-specific splicing regulatory protein Tra stabilizes the binding of SR proteins to an ESE to facilitate recruitment of the U2AF heterodimer to the weak female-specific PPT of the Doublesex gene (Lynch and Maniatis, 1996; Zuo and Maniatis, 1996). By contrast, inclusion of HIV-1 tat exon 2 is inhibited by hnRNP A1 competing with the SR protein SC35 for binding to an overlapping ESE/ESS element, thereby

preventing SR-dependent recruitment of U2AF to a weak 3' splice site (Figure 1-5A)(Zahler et al., 2004).

In addition to the ability of hnRNPs to directly compete with SR proteins, there have been several well-studied examples of hnRNPs functioning directly to repress U1 or U2 binding to a exon (Figure 1-4B). In the simplest model, binding of an hnRNP to an ESS, or an ISS located close to the exon, causes a direct steric block in the ability of a spliceosomal component to bind to an overlapping sequence, similar in concept to the competition between hnRNPs and SR proteins described above. For example, binding of hnRNP H to the extreme 3' end of NF-1 exon 3 blocks U1 binding to the adjacent 5' splice site (Buratti et al., 2004). Dimerization or oligomerization of hnRNPs bound to the pre-mRNA can further affect spliceosomal binding to sites distal to the primary location of hnRNP association. For example, hnRNP A1 binds an ESS at the 3' end of the HIV-1 tat exon 3, and subsequently oligomerizes to essentially coat the repressed exon thereby preventing U1 and U2 snRNP association (Figure 1-5B)(Zhu et al., 2001). However, hnRNP A1-mediated repression is alleviated in the presence of ASF/SF2, which binds an ESE within the HIV-1 tat exon 3, further emphasizing the importance of combinatorial control in splicing (Figure 1-5B). Alternatively, hnRNPs bound to distant sequences can "loop out" the intervening sequence, as is observed in the autoregulation of hnRNP A1 in which A1 molecules bound to the introns flanking variable exon 7B, interact across the exon to sequester it from the
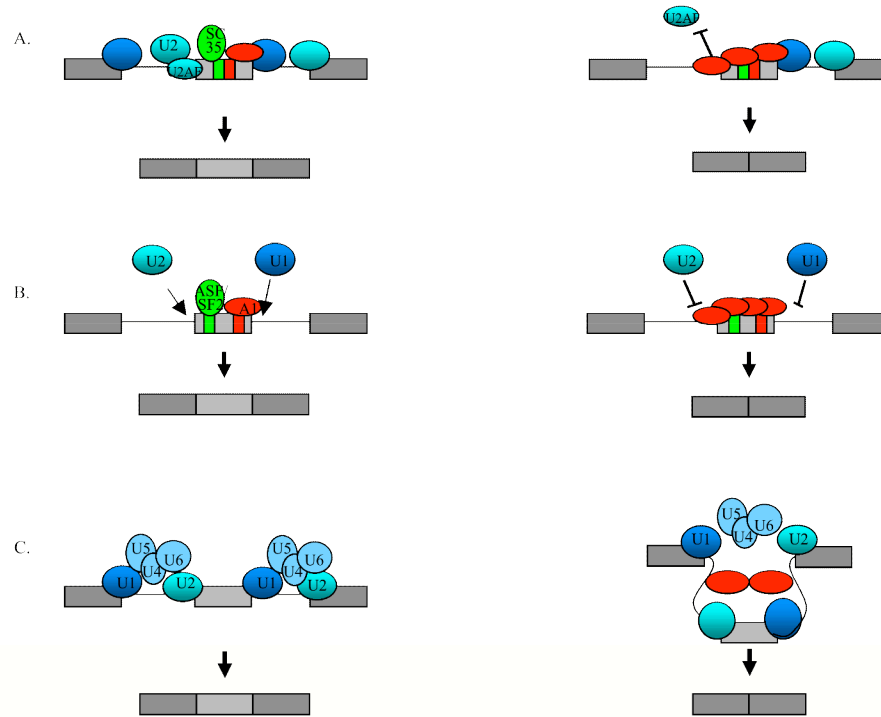
Figure 1-5. Mechanisms of hnRNP A1 regulated spliceosome assembly. The mechanisms of hnRNP A1 mediated exon repression are shown on the right, while events promoting exon inclusion are depicted to the left. (**A**) Binding of hnRNP A1 to a silencer element within HIV-1 tat exon 2 prevents the SC35-dependent recruitment of U2AF to a weak 3'ss resulting in exon repression. (**B**) Oligomerization of hnRNP A1 across the HIV-1 tat exon 3 sterically blocks binding of U2 snRNP causing exon repression. The presence of ASF/SF2 prevents multimerization of hnRNP A1 and promotes exon inclusion. (**C**) Binding of hnRNP A1 to its own transcript upstream and downstream of variable exon 7B results in the "looping out" of the sequence and exon skipping.

rest of the pre-mRNA transcript (Figure 1-5C)(Blanchette and Chabot, 1999; Nasim et al., 2002). It should be noted, however, that whether such looping blocks initial access to the splice sites by the snRNPs, or prevents appropriate pairing between snRNPs remains an open question.

Regulation of pre-spliceosomal transitions and molecular rearrangements

The examples of regulation outlined above, and other similar studies, initially led to the general belief that the vast majority of splicing regulation

occurs prior to the first ATP dependent step in spliceosome assembly. However, as discussed both above and below, spliceosome assembly is highly dynamic throughout the entire substrate recognition and catalytic cycle. Therefore, it seems likely that many or all of the interactions that are formed and broken throughout assembly are potential points of regulation. Indeed, a growing body of work has now demonstrated regulation of alternative splicing at several points in assembly downstream of the ATP-dependent binding of U2 to the branch-point sequence.

Enhancement of snRNP pairing has been proposed as a mechanism for activation of splicing by hnRNPs A1 or H when positioned at distal sites within a long intron. In this case A1 and H are not predicted to directly contact the snRNPs, but rather to dimerize and loop out intervening intron sequences, thus bringing together the snRNPs bound to the 5' and 3' splice sites (Martinez-Contreras et al., 2006). Therefore, the looping out of a variable exon may not only decrease use of the "sequestered" exon as discussed above, but also promote the alternative pairing of the flanking exons (Figure 1-5C). Furthermore, looping out of an exon by flanking hnRNPs is unlikely to simply block access of snRNPs to the repressed exon, since in both the autoregulation of hnRNP A1 discussed above (Figure 1-5C), and in repression of the N1 exon of n-src by binding of the hnRNP PTB to the flanking introns, association of U1 snRNP to the repressed exon is not inhibited (Blanchette and Chabot, 1999; Sharma et al., 2005). Interestingly, detailed analysis of the regulation of n-src demonstrates that
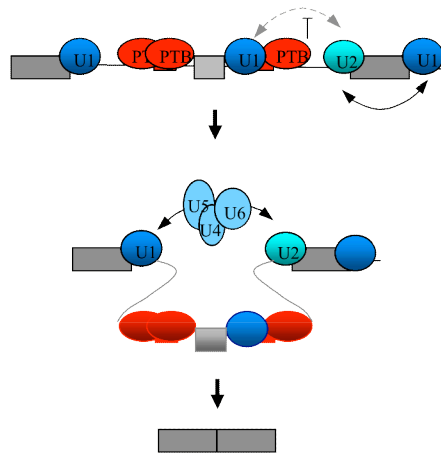
Figure 1-6. PTB blocks the spliceosome transition from an exon- defined to an intron-defined complex. The regulatory protein PTB binds to intronic sequences flanking the variable exon N1 of the c-src pre-mRNA, and prevents exon inclusion by blocking the cross intron association of the U1 and U2 snRNPs.

intronic binding of PTB blocks pairing of the repressed N1 exon with the downstream exon, even after formation of a U1 and U2-containing exon definition complex (Figure 1-6)(Sharma et al., 2005)(S. Sharma and D. Black, personal communication). The transition in spliceosome assembly that is blocked upon formation of the stalled complex on the repressed n-src exon is analogous to that reported herein for CD45 exon 4 (House and Lynch, 2006). Thus exon pairing can be regulated by proteins bound within the intron as well as the exon, and likely represents a more widespread mechanism for alternative splicing than previously recognized.

In addition to exon pairing, appropriate recruitment of tri-snRNP is necessary for progression through spliceosome assembly and is also susceptible to regulation. In addition to their role early in assembly, SR proteins have been

shown to promote U6 snRNA association with the 5'ss and can influence spliceosome formation at this later stage in assembly (Roscigno and Garcia-Blanco, 1995; Shen and Green, 2006, 2007). In contrast, the negative regulator of splicing (NRS) within the retroviral gag gene prevents proper tri-snRNP recruitment (Giles and Beemon, 2005). This NRS functions as a pseudo-5' splice site that sequesters the downstream 3' splice site into a nonfunctional spliceosome complex. Analysis of the NRS-mediated aberrant spliceosome found that while all required spliceosome subunits (U1, U2, tri-snRNP) were present for active complex assembly, tri-snRNP was positioned in such a way as to preclude splicing (Giles and Beemon, 2005). Inappropriate binding of U6 can also influence early steps in spliceosome assembly to alter splice site choice, as shown for regulation of the human calcitonin/CGRP gene (Zhu et al., 2003). Finally, binding of U1 and U2 to non-splice sites within the pre-mRNA has also been implicated in alternative splicing, suggesting that correct conformation of snRNPs can be a common regulatory event in spliceosome assembly (Kan and Green, 1999; Siebel et al., 1992).

More generally, given the fact that most metazoan genes contain multiple exons any partial stall in assembling a proper spliceosome likely permits competing splice sites to pair and excise the stalled exon. On the other hand, an increase in the rate of assembly might promote use of an otherwise weak splice site. Such a kinetic model for regulation is similar to a proposed kinetic

proofreading model for general splicing (Mayas et al., 2006; Query and Konarska, 2006; Valadkhan, 2007), and predicts that altering the efficiency at any step during spliceosome assembly could result in a change in splice site choice. With regards to general spliceosome assembly, recent work has demonstrated the importance of DExD/H box ATPases in regulating the kinetics of many RNA rearrangements (Query and Konarska, 2006) and suggests that the regulation of these proteins likely plays a role in alternative splicing.

Elegant genetic work by two groups has shown that toggling between two mutually exclusive structures of the U2 snRNA (stem-loop structures IIa and IIc) promotes distinct steps in both the assembly and catalytic phases of the splicing cycle (Hilliker et al., 2007; Perriman and Ares, 2007). The DExD/H-box ATPases Prp5 and Prp16, as well as the U2 snRNP protein Cus2, have all been implicated in regulating these U2 snRNA rearrangements and the progression of spliceosome assembly (Hilliker et al., 2007; Perriman and Ares, 2007). Similarly, the DExD/H box protein Prp28 is required for the release of U1 snRNA and exchange for U6 snRNA at the 5'ss; this activity is particularly important in cases where the 5'ss deviates significantly from the consensus (Staley and Guthrie, 1999). Finally, the GTPase Snu114 and the associated DExD/H protein Brr2 are required for the dissociation of U4 and U6 that is necessary during the transition to C complex (Small et al., 2006). Interestingly, Snu114 activity in promoting spliceosome assembly is clearly susceptible to regulation by control of its GTP vs. GDP

binding state (Small et al., 2006). More broadly, one can easily imagine that substrate-bound proteins could alter the local recruitment or activity of any of the "checkpoint" DExD/H box proteins mentioned above, thereby increasing or decreasing spliceosome assembly on a nearby exon to regulate its inclusion in the final mRNA. Indeed, a recent knock-down of several DExD/H proteins in *Drosophila* revealed specific changes in the alternative splicing of some, but not all, variable exons tested (Park et al., 2004), providing experimental evidence for a kinetic model of regulation.

Regulation of splice site choice during catalysis

In addition to altering pre-spliceosome formation, regulation of the spliceosome by DExD/H-box proteins also occurs during catalysis (Query and Konarska, 2006). Strikingly, while binding of U2AF35 to the 3' AG of an intron is typically required for efficient exon definition and for recruiting the U2 snRNP
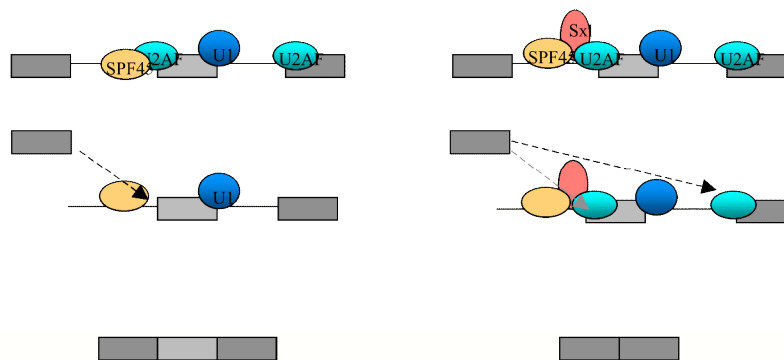
Figure 1-7. Binding of SPF45 to the Sex-lethal transcript influences the second step of catalysis. In male flies, SPF45 binds a proximal 3' AG upstream of the 3'ss AG bound by U2AF and marks the site of exon ligation. In female flies, however, the Sex-lethal (Sxl) protein is expressed and binds on either side of the exon thereby promoting inclusion. Under these conditions, catalysis is blocked at the second step and use of the exon in the final product is repressed.

to the BPS, several studies have shown that the identity of the 3' AG for exon ligation is not irreversibly determined until the actual second catalytic step (Chua and Reed, 1999; Soares et al., 2006). In other words, the 3'AG bound early in spliceosome assembly by U2AF35 is not necessarily the same dinucleotide at which the intron is cleaved from the downstream exon.

One of the determinants of the eventual site of second step cleavage is the spliceosomal protein SPF45, which binds to the 3' AG that is ultimately used for catalysis. In the *Drosophila* Sex-lethal transcript, SPF45 binds to a 3'AG upstream from that initially bound by U2AF35 to direct splicing to this proximal site (Lallena et al., 2002). In the absence of SPF45, splicing switches to the downstream 3'AG with no significant loss of efficiency; however, when the Sex-lethal (Sxl) protein interacts with SPF45 at the proximal 3'AG it results in complete inhibition of the second step of splicing in this region, and results in exon skipping (Lallena et al., 2002). Presumably, the association of Sxl with SPF45 stalls catalysis with sufficient local efficiency that eventually a rearrangement occurs to bring the 3'ss upstream of the next exon into the catalytic pocket of the spliceosome (Figure 1-7), again consistent with a kinetic model of splicing regulation. Recently, contacts between SR proteins and RNA in the catalytic core of the spliceosome were demonstrated to rearrange (Shen and Green, 2007), suggesting that SR proteins may function to modulate assembly beyond the initial step of exon definition.

CD45 signal-induced alternative splicing

The CD45 gene encodes a hematopoetic cell specific transmembrane protein tyrosine phosphatase, and serves as an excellent model system for studying the signal-induced alternative splicing. Despite the relatively small change in isoform expression upon T cell activation, on the order of 3 to 5 fold, the physiological importance of this event is underscored by the correlation between naturally-occurring mutations within the CD45 gene and increased susceptibility a number of autoimmune diseases and viral infections (Dawes et al., 2006; Lynch, 2004a; Tackenberg et al., 2003; Tchilian et al., 2001). CD45 is expressed on the surface of all nucleated hematopoetic cells, such that the phosphatase domain is intracellular while both the fibronectin repeats and the cytosine-rich domain are localized external of the cell (Figure 1-8). The three variable exons encode a portion of the N terminal region of the extracellular domain, which is subject to O-linked glycosylation (Hermiston et al., 2003).

CD45 is known to be a critical component in immune cell biology, but the exact mechanism of the protein in T cell regulation remains controversial. While

Figure 1-8. Domain structure of alternate CD45 protein isoforms. CD45 is a transmembrane protein that is oriented such that the two phosphatase domains are localized with the cell, whereas the three fibronectin repeats are extracellular. The variable exons encode a portion of the extracellular N terminal region of the protein that is differs between the alternate protein isoforms (R456 versus R0).

loss of CD45 expression caused severe-combined immune deficiency (SCID) in mice and humans (Byth et al., 1996; Kishihara et al., 1993; Kung et al., 2000; Mee et al., 1999), the remaining T cells studied did not display the typical autoimmune response (Hermiston et al., 2003). Meanwhile, many studies focused on understanding the phosphatase activity of CD45 to identify substrates that might provide insight into CD45 function. Lck and Fyn, members of the Src family protein tyrosine kinases (SFKs), were both shown to be targets of CD45 tyrosine phosphatase activity. These kinases act to mediate signaling events that occur soon after the T cell receptor (TCR) is engaged by antigen (Hermiston et al., 2003). CD45 has been reported to target the inhibitory phosphorylation sites on both Lck and Fyn, suggesting CD45 may stimulate signaling at the TCR by alleviating inhibition; however, a loss of CD45 expression was reported to result in an increase of SFK activity (Hermiston et al., 2003). A recent study suggests that CD45 expression is necessary for the de-phosphorylation of a particular site on Lck (p56 pTyr-394), which results in suppressed T cell hyperactivity (McNeill et al., 2007). Overall, the role of CD45 in regulating the immune response, while of obvious importance, remains poorly understood.

As we have known for many years that the CD45 gene is alternatively spliced (Birkeland et al., 1989; Hermiston et al., 2002; Hermiston et al., 2003), the expression of the resulting isoforms and the effect of this processing on the resultant protein function has been well characterized. The CD45 gene contains

three variable exons (4, 5 and 6) that are alternatively spliced in T cells (Figure 1-9A). RT-PCR analysis of CD45 isoform expression in primary lymphocytes has shown that the variable exons are preferentially included in resting cells; however, in the days following treatment of these cells with PHA, to mimic antigen challenge, the variable exons become preferentially skipped (Figure 1-9B)(Lynch and Weiss, 2000). Five CD45 isoforms have been shown to be expressed at both
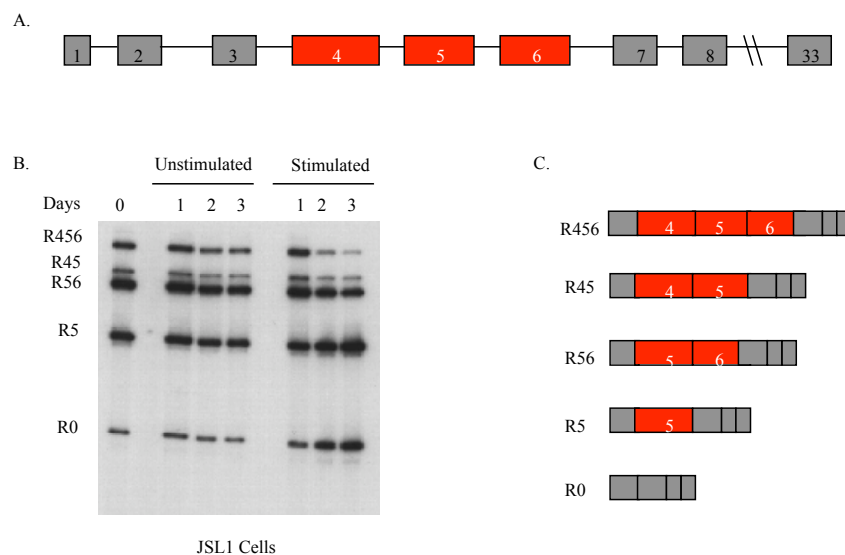
Modified from Lynch and Weiss, 2000.

Figure 1-9. CD45 undergoes signal-induced alternative splicing. (**A**) The CD45 gene contains three variable exons (4, 5 and 6) that are alternatively spliced in T cells. (**B**) RT-PCR analysis of mRNA isoforms expressed in primary human lymphocytes under resting and PHA-activated conditions. Variable exons are partially skipped under resting conditions, but become preferentially skipped following T cell activation. (**C**) Schematic of the five CD45 isoforms that are expressed at both the RNA and protein level.

the RNA and protein level in humans, and the level of protein expression has been reported to correlate with changes in splicing, such that following activation there was an increase in the expression of larger isoforms and a decrease in the expression of smaller isoforms (Trowbridge and Thomas, 1994).

The different CD45 protein isoforms have distinct functions within the cell. The larger isoform has been shown to exist predominantly as a monomer with increased CD45 phosphatase activity, while an increase in the expression of the smaller isoforms results in dimerization of CD45 molecules and a decrease in phosphatase activity (Hermiston et al., 2003; Xu and Weiss, 2002). So then, primary T cells preferentially express the monomeric, high molecular weight

Phosphatase ON   Phosphatase OFF
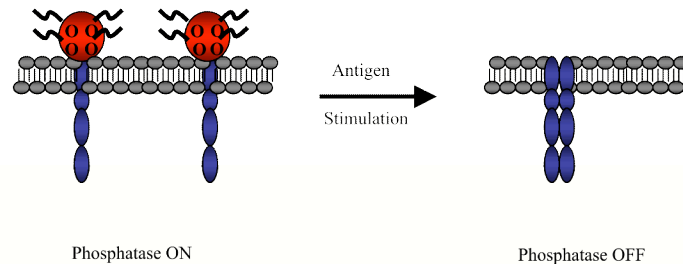
Figure 1-10. Alternative splicing of CD45 pre-mRNA results in altered protein function. The larger isoforms of CD45, containing the region encoded by the variable exons, exist predominantly in the monomeric state with increased phosphatase activity. The smaller isoforms of CD45 tend to dimerize thereby dampening phosphatase activity.

CD45 isoform with enhanced phosphatase activity such that the TCR is poised to signal upon antigen challenge (Figure 1-10). Once activated, the T cell adjusts the splicing profile to promote exon skipping and increase expression of the dimeric, low molecular weight CD45 isoform with diminished phosphatase activity thereby dampening signaling at the TCR and maintaining T cell homeostasis (Figure 1-10). Taken together, the switch in expression of CD45 alternatively spliced isoforms provides the T cell with a rapid and effective means by which to respond to the changing environment.

Given the biological relevance of the regulation of CD45 isoform expression, the mechanisms governing CD45 splicing are tremendously important and have been the primary focus of the Lynch lab over the past several years. As CD45 signal-induced alternative splicing is a T cell specific event, the JSL1 cell line was generated to recapitulate the splicing pattern seen in primary human lymphocytes. Treatment of the cells with the phorbol ester PMA mimics antigen challenge and resulted in an activation-induced decrease in the amount of variable exon inclusion in the endogenous CD45 gene (Lynch and Weiss, 2000). Analysis of the auxiliary sequences within the CD45 variable exons identified both silencer and enhancer elements within each of the regulated exons (Lynch and Weiss, 2000; Rothrock et al., 2003; Tong et al., 2005).

Initial mutational analysis was performed using a minigene context that consisted of variable exon 4 flanked by CD45 constitutive exons 3 and 7 (WT). Splicing of this minigene in the JSL1 cell line showed partial repression under resting conditions and preferential skipping upon activation, thus mimicing splicing of the endogenous CD45 gene (Figure 1-11, WT)(Rothrock et al., 2003). A 60-nucleotide exonic splicing silencer, termed ESS1, was identified within variable exon 4 (Figure 1-11, alt-ESS)(Lynch and Weiss, 2001). Subsequently, ESS1 was shown to be both necessary and sufficient for both basal and signal-induced splicing regulation (Figure 1-11, alt-ESS and glo-ESS)(Rothrock et al., 2003). Both variable exons 5 and 6 were shown to contain ESS1-like elements
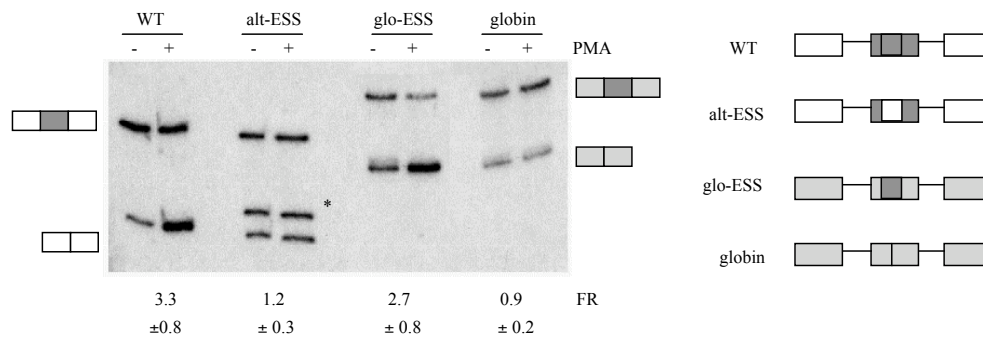
Figure 1-11. Minigene analysis identified the ESS1 element as both necessary and sufficient for exon repression. RT-PCR analysis of the splicing of minigenes that were stably expressed in JSL1 cells under resting (-PMA) or activated (+PMA) conditions. The WT minigene contains variable exon 4 flanked by CD45 constitutive exons 3 and 7. The alt-ESS minigene is identical with the exception of a 60-nucleotide deletion within variable exon 4; the region is replaced with sequence from CD45 constitutive exon 14. The asterisk indicates a cryptic splice product. The glo-ESS minigene consists of exon and intron sequence from the non-signal responsive human β-globin gene with the 60-nucleotide region of variable exon 4 inserted as shown. The globin minigene consists of all sequence from the human β-globin gene and serves as a control. Fold repression (FR) is calculated as the change in the ratio of 3-exon product to 2-exon product between resting and activated conditions. Quantification shown was a result of at least eight independent experiments.

that are important for their regulation under both resting and activated conditions (Tong et al., 2005). Recently, microarray analysis identified additional ESS1-containing transcripts that were also regulated in T cells in response to immune activation (Ip et al., 2007). Interestingly, this approach also identified several genes that undergo signal-induced alternative splicing that do not contain an ESS1, suggesting new categories of regulatory cis-acting elements.

Following the identification and characterization of ESS1 as the main regulatory element of exon 4 splicing, further studies were conducted to identify the proteins that bind this sequence and repress splicing under resting conditions. Several biochemical approaches identified a complex of hnRNPs, namely hnRNP L, hnRNP E2 and hnRNP I/PTB, which bind specifically to ESS1 (Rothrock et

al., 2005). Importantly, hnRNP L binding was dependent upon the presence of the wildtype ESS1 element (K. Lynch, data not shown), suggesting that L was a critical component within this complex. However, the function of the ESS1-binding proteins and the mechanism by which their association resulted in exon 4 repression remained unknown.

The data presented in this thesis demonstrates the function as well as the mechanism by which the ESS1-binding proteins, hnRNP L in particular, act to regulate CD45 exon 4 splicing. First, an *in vitro* splicing system using JSL1 nuclear extract was developed to provide a means to test the functionality of the proteins identified as binding to ESS1 (Rothrock et al., 2005). Importantly, *in vitro* splicing of minigenes containing exon 4 also demonstrates the same signal-induced splicing pattern seen *in vivo*, so the system is applicable to understanding splicing regulatory events under both conditions. Both *in vitro* and *in vivo* functional analyses showed that hnRNP L is the main component controlling ESS1-dependent basal exon repression, while PTB showed no activity and hnRNP E2 causes general splicing inhibition at a high level of expression (Rothrock et al., 2005).

Next, the mechanism by which the ESS1 element and its cognate binding proteins function to repress the use of exon 4 was addressed. Surprisingly, the ESS1 did not block spliceosome assembly at the earliest step in the pathway, as most previously characterized silencers have been shown to function, rather the

stall in assembly occurred at an unusual step (House and Lynch, 2006). Careful analysis of this stalled complex identified it as a U1 and U2 snRNP dependent A-like exon-defined complex (or AEC) (House and Lynch, 2006). Formation of the stalled AEC is required for normal exon regulation under resting conditions (House and Lynch, 2006). This inhibition represents a new mechanism for splicing regulation, and suggests the importance of an AEC intermediate along the spliceosome assembly pathway.

The AEC intermediate represents a very poorly understood transition point along the assembly pathway during which critical processes such as exon pairing and tri-snRNP recruitment occur. As such, purification and characterization of the AEC will provide insight into fundamental aspects of the splicing reaction. Toward this end, a purification scheme was designed for the isolation and enrichment of the AEC. Preliminary analysis of RNA-RNA and RNA-protein interactions within the stalled complex suggest that aberrant contacts between the spliceosome and the ESS1-containing pre-mRNA contribute to AEC formation and stabilization. While a detailed characterization of the stalled complex remains to be solved, the mechanism by which ESS1 and hnRNP L function to regulate CD45 exon 4 have been identified.

CHAPTER TWO

HnRNP L Represses Exon Inclusion by Binding the Signal-Responsive Splicing Regulatory Element of CD45

Rothrock, C.R., House, A.E., and Lynch, K.W. Embo J., 2005

Introduction

During pre-mRNA processing, excision of non-coding intron sequence and ligation of exonic coding sequence is directed by sequence specific splice sites at the exon and intron boundaries. Splicing is catalyzed by the spliceosome, a large complex of small nuclear ribonucleoproteins (snRNPs) U1, U2, U4, U5, and U6 and associated proteins, which assemble on pre-mRNA in a precise and coordinated manner. In higher eukaryotes, pre-mRNA splicing is further under the control of positive and negative regulatory elements, located in exon or intron sequence. These regulatory elements help determine if a particular exon is included in mature mRNA, by either promoting or preventing spliceosome assembly on the exon. Depending on their physical location and activity, these elements are called intronic or exonic splicing enhancers or silencers.

Numerous studies regarding exonic splicing enhancers (ESEs) have led to the conclusion that these motifs are present in most mammalian exons and promote exon inclusion primarily by serving as binding sites for the SR family of splicing activator proteins (Blencowe, 2000; Schaal and Maniatis, 1999b). In contrast to ESEs, exonic splicing silencers (ESS) have been less well studied,

although recent estimates suggest these sequences are likely to be as abundant and important as ESEs (Fairbrother and Chasin, 2000; Fu, 2004; Wang et al., 2004). Specifically, ESS motifs are thought to play a critical role in repressing the use of pseudo-exons and controlling the efficiency of alternative exon inclusion (Fu, 2004; Zhang and Chasin, 2004). Most ESSs that have been studied are known to function by binding to members of the heterogeneous nuclear ribonucleoprotein (hnRNP) family (Black, 2003; Zheng, 2004). Several members of this family have been shown to have sequence-specific effects on numerous steps in RNA processing and function, including alternative splicing (Dreyfuss et al., 2002; Krecic and Swanson, 1999).

The human CD45 gene encodes a hematopoietic-specific transmembrane protein tyrosine phosphatase. Three of the exons (exons 4, 5 and 6) that encode a portion of the extracellular domain of the CD45 protein are alternatively spliced. These variable exons are excluded from a portion of the transcripts that are generated in resting cells and from the majority of the transcripts that are expressed in activated cells (Lynch and Weiss, 2000; Trowbridge and Thomas, 1994). The extent of inclusion of these variable exons has been shown to alter CD45 homodimerization and consequently to modulate the threshold for T cell activation (Xu and Weiss, 2002). Thus, identifying the factors responsible for silencing the CD45 variable exons is of significant importance to understanding the finely-tuned control of the immune system. Previously, a 60 nucleotide ESS

within CD45 variable exon 4 was identified that is responsible for the partial repression of exon 4 in resting cells (Lynch and Weiss, 2001). It was further demonstrated that this silencer element, termed ESS1, is necessary and sufficient for the regulated increase in skipping of CD45 exon 4 that is observed upon cell stimulation (Rothrock et al., 2003). Therefore, ESS1 is the primary determinant of CD45 exon 4 inclusion, and ESS1 may be classified as a "regulated ESS" as its activity is augmented in response to extracellular signals.

This chapter describes the identification of three hnRNP proteins (hnRNP L, PTB and hnRNP E2) that specifically associate with ESS1. Notably, the binding of one of these proteins, hnRNP L, is markedly decreased by mutations that abolish both the basal and stimulated activity of ESS1. In addition, hnRNP L represses exon usage in an ESS1-dependent manner *in vitro* and *in vivo*. HnRNP E2 also can repress exon usage when present at high levels *in vitro*, however this protein is normally much less abundant in nuclear extract than hnRNP L. Therefore, hnRNP L is the primary protein responsible for exonic silencing mediated by ESS1, although the activity of hnRNP L is perhaps facilitated by the presence of other proteins such as hnRNP E2.

Results

Mutations that disrupt ESS1 function inhibit exon silencing complex association.

The three variable exons of the human CD45 gene are partially repressed in resting T lymphocytes and more completely repressed upon T cell activation

A. globin

glo-ESS

glo-mESS

globin glo-ESS glo-mESS

- + - + - + PMA

72 73 4 1.2 80 78 % 3 exon product

B.

ESS1 UCCACUUUCAAGUGACCCCCUUACCUACUCACACCACUGCAUUCUCACCCGCAAGCACCUU

mESS1 UCCACUUUCAAGUGACCCCCUUACCUACUCACACCACUGGAUUCUCACCCGGAAGUACCUU

E14 GUCUGGAACAUGACUGUCUCCAUGACAUCAGAUAAUAGUAUGCAUGUCAAGUGUAGGCCU
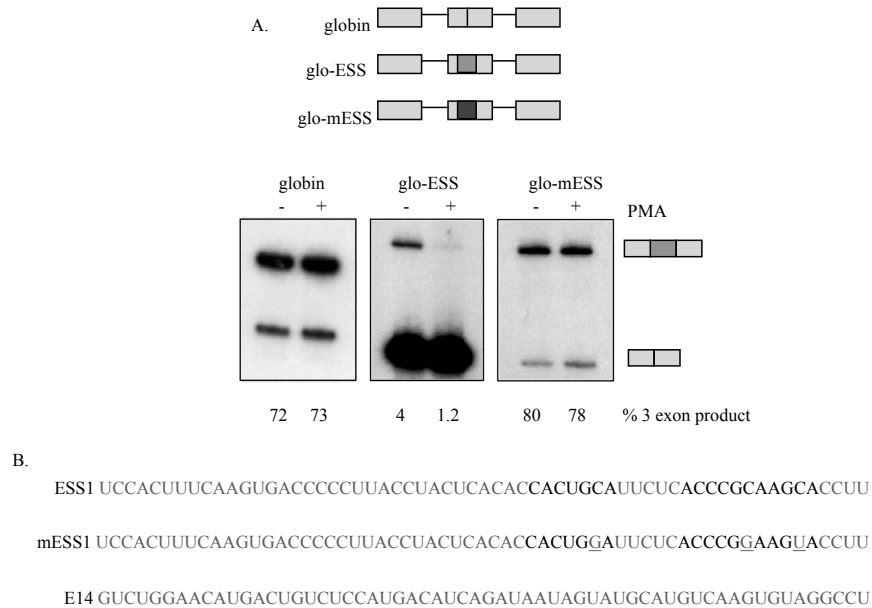
Figure 2-1. ESS1 is necessary and sufficient for both basal and activation-induced regulation of exon 4. (**A**) RT-PCR analysis of the splicing of three minigenes stably expressed in JSL1 cells under resting (-PMA) or activated (+PMA) conditions. These minigenes consist of introns and exons from the human B-globin gene, and either no insertion (globin) or insertion of wildtype (grey box, glo-ESS1) or mutant (black box, glo-mESS) version of the ESS1 sequence. Quantification of the central exon (% 3 exon) was achieved by averaging results from at least four independent clones and two independent experiments. Standard deviation for the averages shown is <10% in each case. (**B**) Sequence of the WT ESS1 RNA, functionally mutant ESS1 (mESS), and nonspecific (E14) RNAs used in all the experiments in this study. Bold nucleotides designate the ARS consensus motif. Mutations in the mESS relative to ESS1 are within the ARS motif and are indicated by plain text underlined.

(Lynch and Weiss, 2000). The 60 nucleotide ESS1 sequence is necessary and

sufficient for both basal and activation-induced exonic silencing, and contains a

core motif referred to as the "ARS consensus," that is also found within variable

exons 5 and 6 (Lynch and Weiss, 2001; Rothrock et al., 2003). As shown

previously (Rothrock et al., 2003), insertion of ESS1 into a heterologous exon

reduces the inclusion of that exon, as revealed by RT-PCR analysis of minigene-

derived mRNA expressed in unstimulated cells (Figure 2-1A, globin vs. glo-ESS

–PMA). Moreover, the presence of the ESS1 element is sufficient to confer

further exon repression upon phorbol ester treatment of cells (Figure 2-1A, glo-ESS –PMA vs. +PMA). Importantly, both the basal and induced activity of ESS1 are completely abolished by the presence of three point mutations within the conserved ARS motif, demonstrating that this sequence is critical for exon silencing (Figure 2-1B). Interestingly, the ARS motif does not match any of the predicted constitutive ESS motifs identified by others (Zhang and Chasin, 2004; Wang et al., 2004), nor does ESS1 contain any matches to functional silencers in either the FAS-hex3 (http://genes.mit.edu/fas-ess/) or the PESS (http://cubweb. biology.columbia.edu/pesx) ESS databases.

The vast majority of splicing enhancer and silencer sequences function as binding sites for regulatory proteins (Black, 2003). To determine if potential *trans*-acting factors stably interact with the ESS1 sequence, binding reactions were performed with ESS1 RNA and nuclear extracts prepared from JSL1 cells, a cell line that faithfully recapitulates all aspects of CD45 splicing in peripheral human T cells. Native RNA mobility shift assays showed that two slower-migrating complexes were only visible upon incubation of ^{32}P-labeled ESS1 RNA with nuclear extract derived from unstimulated JSL1 cells (C.R.R., data not shown)(Rothrock et al., 2005). Specificity of the complex was confirmed by performing competition native gel shift assays with various unlabeled RNAs. Assembly of a complex on the wild type ESS1 RNA probe is almost completely abolished by addition of unlabeled ESS1 RNA. Importantly, competition with the

mESS RNA that contains the three mutations that abolish function *in vivo* is much less efficient in disrupting the silencer complex, and competition with a non-specific RNA (E14) has no affect on complex formation (C.R.R., data not shown)(Rothrock et al., 2005). Therefore, a complex specifically associates with the functional form of ESS1. This native gel shift analysis, as well as all other binding assays described in this study, were also conducted with nuclear extract prepared from stimulated JSL1 cells; however, no difference in complex formation or associated proteins was observed (data not shown), suggesting that the increase in ESS1-mediated repression upon stimulation is not due simply to a conspicuous change in protein binding. Therefore, in this study we have focused on characterizing the proteins involved in the activity of ESS1 under unstimulated conditions as a critical first step toward understanding the interplay between basal and induced exon silencing via ESS1.

The specificity of the native gel complex suggests that the binding of *trans*-acting factors to ESS1 is functionally relevant. However, to more directly confirm the functional role of *trans*-acting factors in ESS1-mediated exon silencing, exogenous ESS1 RNA was added to an *in vitro* splicing assay. Splicing of a standard CD45 exon 4 minigene in nuclear extract derived from resting JSL1 cells shows a low level of exon 4 inclusion or "three exon product" (Figure 2-2A, WT -comp RNA), consistent with the partial repression of exon 4 previously observed in resting cells (Lynch and Weiss, 2001). Addition of exogenous ESS1

RNA to the splicing reaction greatly alleviates exon 4 silencing, up to a 10-fold increase in 3 exon product (Figure 2-2A). Significantly, no effect on exon 4 inclusion is observed upon addition of either the mutant ESS1 (mESS) or non-specific RNA (Figure 2-2A). To determine the specificity of ESS addition,
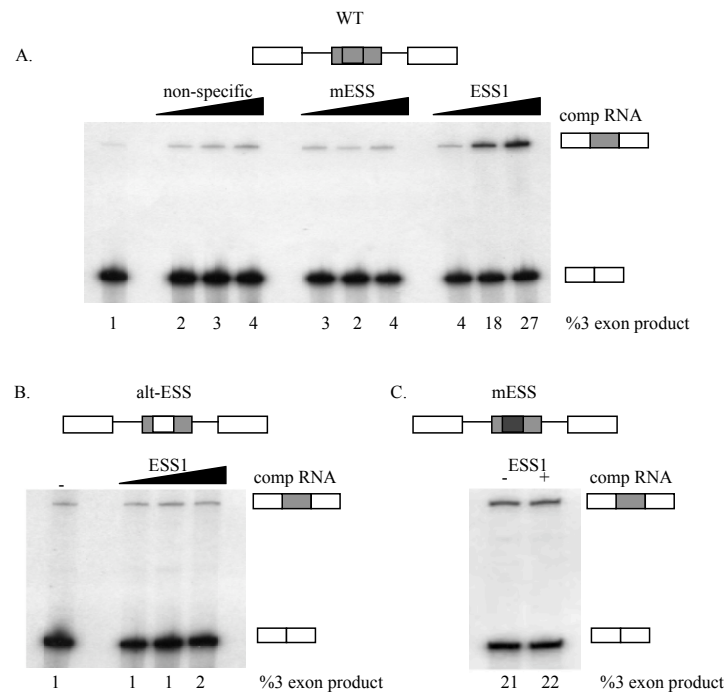
Figure 2-2. An exon repression complex specifically associates with ESS1 and functions to repress splicing. (**A**) Approximately 1 fmol unlabeled, capped RNA derived from a minigene containing wildtype CD45 variable exon 4, flanked by constitutive exons 3 and 7, was incubated in nuclear extract from unstimulated JSL1 cells in the presence or absence of exogenous competitor RNA. The resulting spliced products were then assayed by RT-PCR, as done for RNA derived from cells. Quantification of the % 3-exon product is the average of at least four experiments with a standard deviation of <20% for all values given. (**B**) RNA derived from a CD45 exon 4 minigene in which the ESS1 has been deleted and replaced with heterologous sequence was spliced in the same assay as used for (A). (**C**) *In vitro* splicing as in panel B of RNA derived from a CD45 exon 4 minigene in which the ESS1 has been mutated to the mESS sequence shown in Figure 2-1C.

exogenous ESS1 RNA was titrated into an *in vitro* splicing reaction using a minigene in which the ESS1 element has been removed and replaced with heterologous sequence from CD45 exon 14 that binds hnRNP A1 and A2 (alt-

ESS)(Figure 2-2B). The heterologous sequence used in alt-ESS has inherent silencer activity and represses three exon splicing in JSL1 cells (Rothrock et al., 2003). However, the silencer activity in the alt-ESS construct is clearly distinct from that of ESS1 in that repression is not stringently observed in all JSL1 extract preparations (see Figure 2-4) and is not active in 293 cells (see Figure 2-6). Importantly, this heterologous silencer activity is unaffected by the presence of competitor ESS1 sequence (Figure 2-2C). Additionally, ESS1 RNA does not increase inclusion of an exon that contains the functionally-dead element (Figure 2-2C). Taken together, the specificity of complex binding and functional competition strongly indicate that ESS1 mediates splicing silencing by recruiting *trans*-acting factors to the repressed exon.

HnRNPs L, E2 and PTB specifically associate with ESS1

To identify the protein components of the ESS1-specific silencing complex an RNA affinity approach was employed. Wild type ESS1 RNA, mutant ESS RNA, or non-specific RNA containing a 5' terminal biotin group were individually incubated in JSL1 nuclear extracts and RNA-associated proteins were analyzed by SDS-PAGE and silver stain (C.R.R., Figure 2-3A). Comparison of the proteins precipitated with ESS1 RNA versus non-specific RNA reveals several bands that associate specifically with ESS1 (indicated by arrows in Figure 2-3A). Each of the ESS1-specific bands was excised from the

A.

ESS1 mESS E14

116 kD

97 kD

hnRNP-L

PTB

66 kD

hnRNP-E

45 kD

C.

PTB E2 L

ESS1

GCA…..GCAAGCA

PTB E2

mESS1

GgA….. GgAAGtA
*   *   *

B.

ESS1 UCCACUUUCAAGUGACCCCUUACCUACUCACACCACUGCAUUCUCACCCGCAAGCACCUU

------   ----   ------ -----   -----
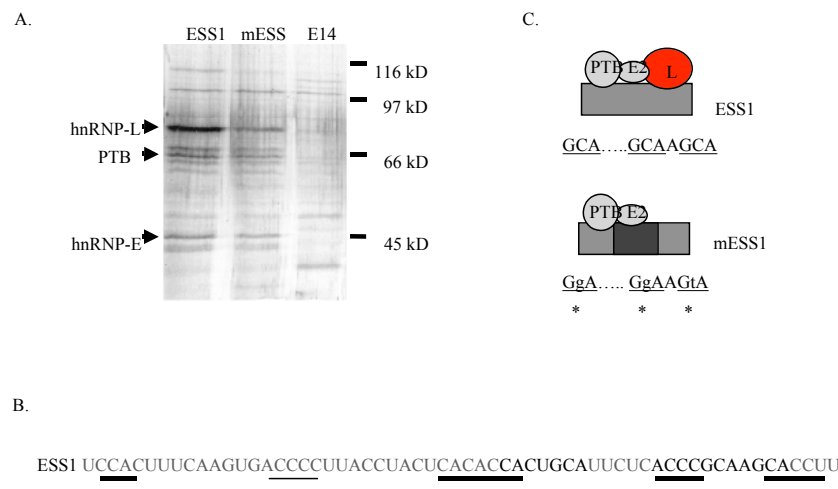
Figure 2-3. HnRNPs L, E2, and PTB identified as ESS1 binding proteins. (A) RNA affinity purification of proteins associated with ESS1 RNA. Silver stained SDS-PAGE gel of proteins isolated from JSL1 nuclear extract by virtue of association with chemically synthesized, 5'-biotinylated ESS1, mESS, and E14 RNAs. (B) Schematic figure showing that mutations in the ESS1 that abolish repressive function specifically inhibit the binding of hnRNP L. Biochemical analysis of protein binding was performed by C.R.R. (C) Sequence of ESS1 with predicted high-affinity binding sites indicated for hnRNP L (bold lines), PTB (dashed lines), and hnRNP E (plain lines).

gel and analyzed by mass spectrometry. Multiple peptides corresponding to hnRNP L, hnRNP-I (PTB) and hnRNP E2 were identified for each band as indicated (C.R.R., Figure 2-3A).

The ability of hnRNP L, PTB and E2 to bind to the ESS1 regulatory sequence of CD45 exon 4 was also independently confirmed using UV cross-linking and immuno-precipitation assays, western blot analysis of the ESS or mESS-affinity purified proteins and antibody-induced super-shift of the RNA mobility shift assays (C.R.R., data not shown)(Rothrock et al., 2005). Thus, although we cannot fully rule out the presence or importance of other proteins, RNA-affinity purification clearly identifies the hnRNP family members L, E2 and

PTB as primary proteins associated with the ESS1 regulated exonic silencer. Previous studies have identified high affinity binding sites for hnRNP L, PTB and hnRNP E2 as ACAC, UCUC and Poly(C) respectively (Chan and Black, 1997a, b; Hui et al., 2005; Leffers et al., 1995). Although the specificity of RNA-binding proteins can be highly context dependent (Lynch and Maniatis, 1996), the presence of predicted binding motifs for hnRNPs L, PTB and E2 within ESS1 (shown in Figure 2-3B) is consistent with our identification of these three hnRNPs as major ESS1-binding proteins.

HnRNP L binding to ESS1 is specifically inhibited by mutations that disrupt silencing

To more explicitly correlate the binding of hnRNP L, PTB and E2 with the function of ESS1, UV cross-linking assays were used to determine how the binding of these proteins is individually affected by the mutations that disrupt ESS1 function. Competition with the unlabelled ESS1, mESS or E14 RNAs demonstrated that hnRNP L is able to discriminate between functional and non-functional ESS1, consistent with the preliminary suggestion of specificity from the RNA-affinity experiments and with the observation that at least some of the mutations in mESS fall within putative hnRNP L binding sites (C.R.R., Figure 2-3C). In contrast, PTB and E2 are not altered by mutations that disrupt exonic silencing (C.R.R., Figure 2-3C).

UV cross-linking competition experiments using recombinant GST-tagged hnRNP L, PTB purified from Sf9 cells and recombinant MBP-hnRNP E2 purified from bacteria again demonstrated that mutations disrupting ESS1 silencer activity specifically inhibit the binding of hnRNP L binding but not PTB (C.R.R., data not shown). Therefore, the binding specificity of hnRNP L observed in nuclear extract is an inherent feature of hnRNP L and is not induced by cooperative interactions with other accessory protein(s). Thus, the association of PTB and hnRNP E2 with ESS1, while demonstrating specificity with respect to the E14 sequence, does not correlate with the exonic silencer activity of this regulatory element.

Recombinant hnRNP L induces ESS1-dependent exon silencing in vitro

The correlation of sequence requirements for the binding of hnRNP L *in vitro,* and the function of ESS1 *in vivo,* suggests that the exonic silencing activity of ESS1 is mediated predominantly by the association of hnRNP L. To test this prediction, the *in vitro* splicing assay was used to determine the functional effect of hnRNP-L, PTB and E2 on repression of CD45 exon 4. Titration of purified recombinant hnRNP L into *in vitro* splicing reactions using the standard wildtype CD45 exon 4 minigene results in a dose-dependent decrease in exon 4 inclusion (Figure 2-4A and 2-4D). Importantly, this activity of hnRNP L is dependent on the presence of the ESS1 sequence within the repressed exon, since only the
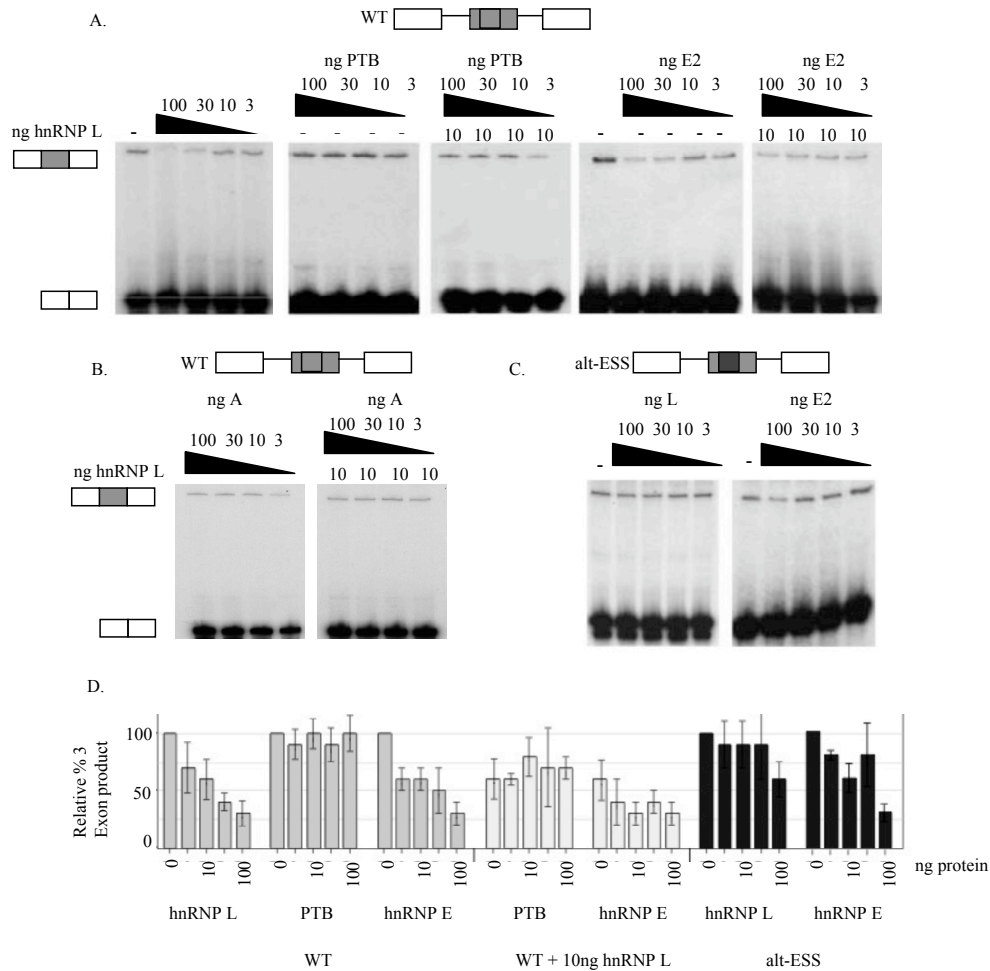
Figure 2-4. HnRNP L induces exon repression in *in vitro* splicing assays. (**A**) *In vitro* splicing assays using the WT CD45 exon 4 minigene as described in Figure 2-2. Splicing reactions contained either nuclear extract along (-) or supplemented with purified recombinant GST-hnRNP L, GST-PTB, and/or MBP-hnRNP E2, as indicated. Quantification of replicate experiments is given in panel D. (**B**) *In vitro* splicing as in panel A but reactions are supplemented with purified recombinant hnRNP A1 in the absence or presence of GST-hnRNP L. (**C**) *In vitro* splicing as in panel A, but using the ΔESS splicing substrate that lacks the ESS1 regulatory sequence. Quantification of replicate experiments is given in panel D. (**D**) Graphical representation of the three-exon product from at least four independent experiments, identical to those shown in panels A and C, and similar experiments as in panel B. Numbers are given as % of 3-exon product as compared to NE alone (set at 100%).

highest concentration of hnRNP L shows even a modest silencing effect on the alt-ESS substrate (Figure 2-4C and 2-4D). Addition of an unrelated hnRNP, hnRNP A1, also does not alter the splicing of exon 4 either on its own or in the

presence of low levels of additional recombinant hnRNP L (Figure 2-4B) suggesting that repression caused upon the addition of hnRNP L is specific and not due to the general phenomenon of hnRNP repression. By contrast, addition of purified, recombinant PTB has no effect on exon 4 splicing, either on its own or in the presence of low levels of additional recombinant hnRNP L (Figure 2-4A and 2-4D). As recombinant PTB is capable of binding to ESS1 (C.R.R., data not shown), we conclude that while PTB associates with exon 4, it does not act to repress the exon *in vitro*.

Addition of recombinant hnRNP E2 into *in vitro* splicing reactions does result in repression of exon 4 inclusion and shows a roughly additive silencing effect when added in conjunction with hnRNP L (Figure 2-4A and 2-4D). The ability of hnRNP E2 to repress splicing *in vitro* was initially surprising given that the mESS sequence is not sufficient to mediate repression despite the fact that hnRNP E2 binds efficiently to this mutant element. However, comparison of the relative abundance of both hnRNP L and hnRNP E2 in nuclear extract suggests that hnRNP L is present in approximately a 30-fold molar excess over hnRNP E2 (300 fmol versus 10 fmol per mg total protein based on comparison to known quantities of recombinant protein, data not shown). Therefore, the standard concentration of hnRNP E2 in the nucleus may not be sufficient to mediate exon repression when the binding of hnRNP L is decreased. Moreover, recombinant hnRNP E2 also partially represses the exon 4 variant lacking the ESS1 motif

(Figure 2-4C and 2-4D). Thus, hnRNP E2-mediated exon repression *in vitro* may be due to mechanisms separate from its ESS1 binding activity.

Depletion of hnRNP L relieves exon repression in vitro and in vivo

As a further test of the function of hnRNP L, we asked whether this protein could complement an ESS1-depleted extract. As shown in Figure 2-4, ESS1 repressing activity can be functionally depleted by the addition of exogenous ESS1 RNA into the *in vitro* splicing assays. Importantly, in such a
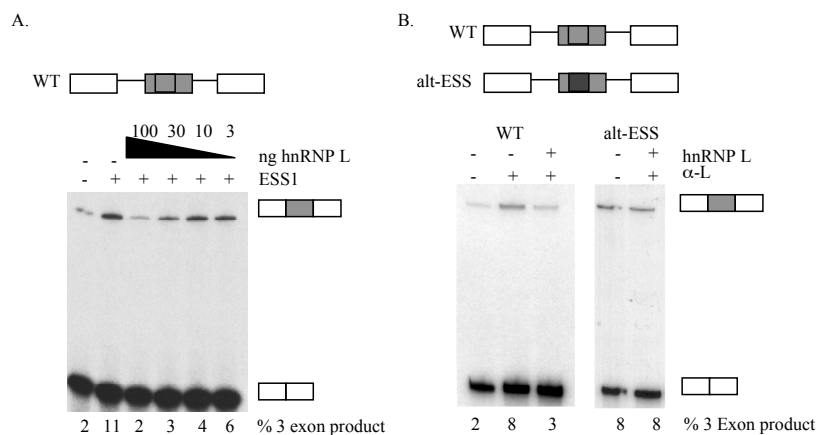
Figure 2-5. Depletion of hnRNP L *in vitro* leads to increased inclusion of an ESS1-containing exon. (**A**) *In vitro* splicing assays lacking (-ESS) or containing (+ESS) exogenous ESS1 RNA similar to experiments shown in Figure 2-, in which purified recombinant GST-hnRNP L is also added to splicing reactions at the concentrations indicated. Quantification is from at least four independent experiments, with a standard deviation of <20% of value. (**B**) *In vitro* splicing assays in the presence (+) or absence (-) of 2ul 4D11 antibody and/or 100 ng recombinant GST-hnRNP L. Quantification is derived from at least two independent experiments with standard deviation <10% of value.

functionally-depleted background, a robust rescue of exonic repression is observed upon the addition of recombinant hnRNP L, but not PTB (Figure 2-5A; data not shown). Blocking of hnRNP L by addition of anti-hnRNP L antibody to the *in vitro* splicing reactions also relieves repression of exon 4, and is reversed

by supplementing the reactions with recombinant hnRNP L (Figure 2-5B). In

contrast, no change in the inclusion of exon 4 was observed upon addition of

antibody specific for hnRNP A1 (data not shown), and the anti-hnRNP L antibody

has no effect on the splicing of an exon lacking ESS1 (Figure 2-5B). It should

also be noted that exon repression was significantly alleviated upon the addition

of a 5'-biotin labeled CA-dinucleotide repeat oligonucleotide (Figure 2-6A)(Hui

et al., 2005; Hui et al., 2003). Western blot analysis of extracts depleted of factors

Figure 2-6. Functional depletion of CA-element binding proteins does not alleviate ESS1-dependent exon repression *in vitro*. (**A**) RT-PCR analysis of *in vitro* splicing reactions using the WT minigene performed in the absence (-) or presence (+) of increasing amounts of exogenous ESS1 competitor or a 5' end labeled biotin-CA oligonucleotide, $(CA)_{20}$. (**B**) Western blot analysis of hnRNP L protein levels in untreated, mock- or $(CA)_{20}$-treated JSL1 nuclear extract. (**C**) RT-PCR analysis of *in vitro* splicing reactions using either the WT or the alt-ESS minigene performed in JSL1 nuclear extracts that were mock-treated or $(CA)_{20}$-treated to remove CA-element binding proteins, including hnRNP L. (**D**) UV cross-linking analysis of proteins to ^{32}P-labeled ESS1 RNA in either mock-treated or $(CA)_{20}$-treated JSL1 nuclear extract. HnRNP L migrates around 75kD and is marked using an arrow.

that bind the CA oligonucleotide showed nearly total depletion of hnRNP L (Figure2-6B). Surprisingly, splicing of the WT minigene in CA-depleted nuclear extract showed high levels of exon repression despite the efficient removal of hnRNP L (Figure 2-6C). UV cross-linking analysis of proteins bound to ESS1 in the CA-depleted extracts demonstrated that in the absence of hnRNP L, another protein can bind the silencer element and presumably function to repress use of exon 4 (Figure 2-6D), suggesting functional redundancy exists in this pathway and may play a role in regulation.

While the above experiments demonstrate a role of hnRNP L in ESS1-mediated silencing *in vitro*, the *in vivo* function of hnRNP L in ESS1-mediated exon silencing remained unclear. Due to the high level of hnRNP L expression in the JSL1 cell line and the fact that these cells do not support RNAi, we have been unable to modulate hnRNP L expression levels in the JSL1 cells. While other cell lines do not support activation-induced alternative splicing of CD45, and may differ from JSL1 cells in the relative expression of hnRNP L and other splicing regulatory factors, we have found that the 293 cell line does recapitulate the splicing pattern of the CD45 exon 4 minigene observed resting JSL1 cells. HnRNP L is highly abundant in 293 cells; however, using a pool of siRNAs against hnRNP L we were able to achieve about a 50% decrease in hnRNP L protein levels (Figure 2-7). Strikingly, this 50% reduction in hnRNP L is sufficient to induce a significant increase in exon 4 inclusion from a co-

WT   alt-ESS

G   L   G   L   siRNA

| 38 | 59 | 89 | 91 | % 3 exon product |

α-hnRNP L

α-Erk1/2

G   L   G   L   siRNA
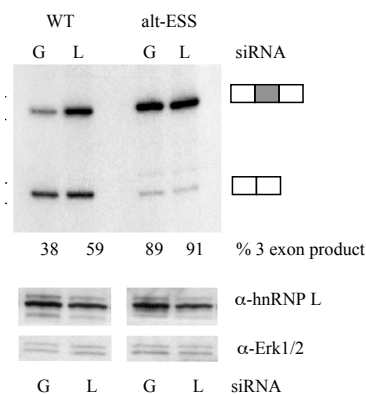
Figure 2-7. Depletion of hnRNP L *in vivo* results in increased inclusion of an ESS1- containing exon. RT-PCR analysis of WT or ΔESS minigene-derived RNA harvested from 293 cells transiently co-transfected with a minigene encoding vector and siRNAs against either GFP (G) or hnRNP L (L). Quantification of three-exon product is derived from four independent transfections with standard deviation <5%. Western blot analysis of hnRNP L, or Erk1/2 as internal control, protein levels from corresponding transfections was performed. The average reduction of hnRNP L protein in transfections with hnRNP L siRNAs versus GFP siRNAsx was 50±10%.

transfected WT minigene (38% +/- 4% to 59% +/- 5%), consistent with decreased activity of the ESS1 silencer. In contrast, parallel transfections with the alt-ESS minigene show no effect of hnRNP L depletion (Figure 2-7). These data strongly suggest that hnRNP L is required for ESS1-dependent exon silencing *in vivo* as well as *in vitro*.

Discussion

Previously the 60nt ESS1 sequence in human CD45 exon 4 was identified as a regulated exonic splicing silencer that is necessary and sufficient both for basal exon repression and for increased exon repression in response to PMA treatment (Lynch and Weiss, 2001; Rothrock et al. 2003). Here three hnRNPs, L, PTB and E2, were identified as the primary proteins that bind to the ESS1 regulated exonic splicing silencer. Several lines of evidence indicate that hnRNP L is the predominant protein through which the function of ESS1 is mediated. First, hnRNP L is the most prominent ESS1-binding protein as assayed by both

RNA-affinity purification and UV cross-linking. Secondly, hnRNP L is the only one of the ESS1-binding proteins whose affinity is decreased by the introduction of mutations that disrupt both the basal and inducible activities of ESS1 (Figure 2-3). Finally, we have shown that modulating the levels of hnRNP L, both *in vitro* and *in vivo*, specifically alters the splicing of an ESS1-containing exon (Figures 2-5 and 2-6).

In contrast to hnRNP L, PTB and hnRNP E2 bind with indistinguishable affinity to ESS1 and the functionally-inactive mutant mESS (Figure 2-4). Therefore, the level of association of these proteins in cells with mESS, and by analogy ESS1, must not be sufficient to mediate exonic silencing. The inability of hnRNP E2 or PTB to functionally compensate for hnRNP L may be due, at least in part, to the fact that the binding of both of these proteins to ESS1 in nuclear extract is much less pronounced than that of hnRNP L. Indeed, when we increased the concentration of hnRNP E2 in *in vitro* splicing assays this protein was able to promote exonic silencing, although this effect was not strictly dependent on the presence of the ESS1 element (Figure 2-4). Therefore, while there is no evidence for a functional role of PTB in ESS1 activity, it cannot be ruled out that hnRNP E2 might contribute in some way to the overall exonic silencing.

Interestingly, hnRNP L, PTB and hnRNP E2 have previously been shown to interact with one another by both yeast two-hybrid and GST pull-down

experiments (Kim et al., 2000). Using UV crosslinking assays with recombinant hnRNP L, PTB and E2 we do not detect any evidence for cooperative binding of these proteins to ESS1 (data not shown). However, interaction between these proteins may occur once bound to the RNA and may increase the overall stability of the ESS1-bound regulatory complex and/or be important for mediating exon repression. Further mapping of the precise sites of association of hnRNP E2 and PTB within the ESS1 element will be required to better understand the potential contribution of these proteins to the overall activity of this silencer.

PTB has been shown to bind exonic splicing silencers in several genes, and to be essential for the silencing activity of many of these regulatory sequences (Wagner and Garcia-Blanco, 2001). However, neither hnRNP L nor hnRNP E2 have been previously implicated in ESS function. To our knowledge, hnRNP E2 has, in fact, never been shown to influence pre-mRNA splicing. However, hnRNP-L has recently been shown to bind to a CA-rich element within an intron of the eNOS gene and stimulate its removal (Hui et al., 2003). Other splicing regulatory proteins have been shown to have dual function to promote the removal of introns or skipping of exons depending whether they are bound within the intron or exon respectively (Dredge et al., 2005). Thus, although the mechanisms by which hnRNP L stimulates either intron removal or exon repression have yet to be elucidated, these activities may be related to one another

and may reflect a general ability of hnRNP L to mark RNA sequences for removal by the splicing machinery.

Previously it was shown that the ARS core motif from ESS1 is also present in the other CD45 variable exons and in several signal-regulated exons from other genes (Rothrock et al., 2003). Interestingly, in a parallel studies to those described here for exon 4, we have found that hnRNP L binds to the minimal ARS-containing silencing sequences from CD45 variable exons 5 and 6, and this binding of hnRNP L is abrogated by mutations within the ARS core of these exons (Tong et al., 2005). Therefore, it is possible that hnRNP L may influence the splicing of all of the CD45 variable exons, or even ARS-containing exons from other genes. Similarly, recent studies from the Bindereif group has found that hnRNP L binds to CA-rich <u>intronic</u> enhancer and silencer elements in three other genes in addition to eNOS (Hui et al., 2005). Taken together these studies suggest that hnRNP L may play a broad role as a master splicing regulatory protein that controls the isoform expression of a large number of genes.

In conclusion, hnRNP L, PTB and hnRNP E2 are the primary ESS1 binding proteins. Further, hnRNP L is the key regulatory protein within the complex that is responsible for mediating ESS1-dependent exon silencing under resting conditions. These studies not only broaden the known functions of hnRNP L by implicating it in ESS binding and function, but also lay a critical

foundation for future studies aimed at understanding the mechanism and regulation of ESS1-dependent silencing activity and the control of CD45 splicing.

CHAPTER THREE

An Exonic Splicing Silencer Represses Spliceosome Assembly After ATP-dependent Exon Recognition

House, A.E. and Lynch, K.W., Nat Struct Mol Biol, 2006.

Introduction

Virtually all mammalian pre-mRNA transcripts are spliced, through the removal of intronic sequence and the ligation of exonic sequence, to generate a mature protein-coding mRNA transcript. This splicing reaction is catalyzed by a complex, macromolecular machine known as the spliceosome, that is comprised of five snRNAs and several hundred associated proteins (Jurica and Moore, 2003). Each snRNA (U1, U2, U4, U5, U6) forms the core of a specific snRNP component and promotes formation of the spliceosome through base-pairing interactions with the splice site sequences within the pre-mRNA template and/or with other snRNAs (Black, 2003). Importantly, the mature, catalytic spliceosome (complex C) is not a pre-formed enzyme, but rather assembles on the pre-mRNA in a step-wise and highly dynamic manner. *In vitro* studies have identified several distinct intermediates along this assembly pathway (E-A-B)(Black, 2003; Matlin et al., 2005).

Isolation of the distinct E, A and B intermediate complexes along the spliceosome assembly pathway has allowed for the study of specific steps in the splicing process such as exon recognition, selection of splice sites and catalysis

(Black, 2003; Matlin et al., 2005). However, such studies do not preclude the existence of other spliceosome assembly intermediates, and do not provide details on critical transitions in spliceosome assembly such as the transition from spliceosomal subunits interacting across an exon (i.e. exon-recognition) to the eventual cross-intron (i.e. exon-pairing) interaction that is required for catalysis (Matlin et al., 2005). In particular, E, A and B complexes have primarily been analyzed and defined in studies utilizing simple two-exon/single-intron constructs, such that the spliceosomal components can only assemble across the intron. However, a number of studies have shown that at least the U1 and U2AF subunits of the spliceosomal E complex can interact across a single exon as part of an exon-definition complex that is essential for high-fidelity splice site recognition (Berget, 1995; Reed, 2000). Likewise, the U1 and U2 containing A-complex is defined only as a cross-intron complex, a view which is supported by at least one study that demonstrated stable pairing of exons concurrent with A complex formation (Lim and Hertel, 2004). Nevertheless, in experiments in which two exons are artificially separated from one another, a U1- and U2-containing complex can form on an isolated exon and then "pair" with an exogenous exon to result in a catalytically active spliceosome (Chiara and Reed, 1995). Therefore it is possible for the U1 and U2 snRNPs to first interact across a single exon before pairing with spliceosomal components on flanking exons, perhaps indicating that a U1 and U2-containing (i.e. A-like) exon-definition

complex may be able to form on natural substrates as part of the spliceosome assembly pathway (Black, 2003; Matlin et al., 2005).

While spliceosome assembly and catalysis occurs with high fidelity, it is also subject to intricate regulation. Indeed, regulated inclusion or exclusion of exons, by the process of alternative splicing, is predicted to be a primary mechanism for regulating gene expression (Black, 2003). In particular, exonic splicing enhancers (ESEs) and splicing silencers (ESSs) act to promote or inhibit recognition of a regulated exon by the spliceosome through the activity of associated regulatory proteins. Previous studies of the mechanism of exon repression by the ESS-class of sequences have shown that regulation typically occurs during the initial ATP-independent recognition of splice sites by U2AF or the U1 snRNP (Izquierdo et al., 2005; Matlin et al., 2005; Sharma et al., 2005; Wagner and Garcia-Blanco, 2001; Zhu et al., 2001). However, the inherently dynamic nature of the spliceosome suggests the potential for biologically relevant regulation of splicing at any of the intermediates along the spliceosome assembly pathway.

The CD45 gene is an excellent model system for understanding the mechanism and regulation of alternative splicing events. Previous analysis of cis-acting elements that govern the regulation of exon 4 splicing identified an exonic silencer element (ESS1) that is required for exon repression (Lynch and Weiss, 2001; Rothrock et al., 2003). Moreover, at least three heterogeneousribonucleo-

proteins (hnRNPs) bind specifically to a core sequence within ESS1 and at least one of these, hnRNP L, functions to repress exon splicing (Chapter 2)(Rothrock et al., 2005). However, the mechanism by which hnRNP L and the ESS1-binding proteins function to repress splicing remained unclear.

This chapter describes the identification of a spliceosomal complex that forms efficiently on ESS1-repressed substrates that resembles A complex (dependent on U1, U2 and ATP), however subsequent spliceosome assembly is blocked. Characterization of the sequence requirements for the ESS1-stalled spliceosomal complex show that it is dependent on the integrity of both the 5' and 3' splice sites at the boundaries of the regulated exon, but is not dependent on the presence of upstream or downstream flanking splice sites. Moreover, formation of this specific stalled complex is required for exon regulation. Together these data demonstrate that ESS-mediated exon repression can occur after the ATP-dependent recognition of an exon by U1 and U2, and suggest that the interaction of these two snRNPs across an exon can be regulated so as to prevent pairing with neighboring exons and/or stable recruitment of the tri-snRNP.

Results

The CD45 ESS1 stalls spliceosome assembly at an unusual step

Previously it was demonstrated that a 60 nucleotide exonic splicing silencer sequence (ESS1) is necessary and sufficient for the skipping of the CD45 variable exon 4 both *in vivo* and *in vitro* (Rothrock et al., 2003; Rothrock et al.,
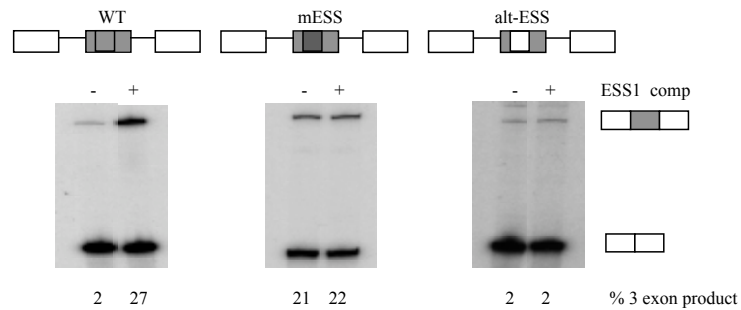
Figure 3-1. ESS1 represses splicing of CD45 exon 4 *in vitro*. RNA derived from CD45 minigenes, containing regulated exon 4 with WT, mESS1 or alt-ESS sequence flanked by constitutive exons 3 and 7, was incubated in JSL1 nuclear extract in the absence (-) or presence (+) of exogenous competitor (comp) ESS1 RNA for 110 min, and products analyzed by RT-PCR. The accuracy of all spliced products was confirmed by cloning and sequencing. % 3-exon is the percentage of three-exon products.

2005). *In vitro* splicing reactions using a minigene containing the wildtype exon 4 sequence flanked by the CD45 constitutive exons 3 and 7 (Figure 3-1, WT), show a low level of exon 4 inclusion or "three-exon product". However, upon addition of exogenous ESS1 RNA there is a marked increase in the level of exon inclusion (Figure 3-1, - vs. + ESS1), consistent with the exogenous ESS1 titrating functionally important ESS1-binding proteins away from the pre-mRNA substrate, thereby alleviating repression. As expected from previous studies (Rothrock et al., 2005), the ability of exogenous ESS1 to promote exon inclusion is dependent on the regulated exon containing a functional ESS1 element. Splicing of the mESS1 minigene, which contains point mutations within ESS1 that abolish silencing activity (Rothrock et al., 2003), results in an increased basal level of exon inclusion that cannot be further enhanced by addition of competitor ESS1 RNA (Figure 3-1, mESS1). Similarly, the addition of ESS1 competitor has no effect on the splicing of a minigene in which the entire ESS1 element is

removed and replaced with a heterologous sequence from CD45 exon 14 that binds hnRNP A1 and A2 (alt-ESS) and contains unrelated silencing activity in some contexts (Figure 3-1)(Rothrock et al., 2003; Rothrock et al., 2005). The alt-ESS and mESS1 sequences also have no ability to competitively alter the splicing of the WT RNA substrate (Rothrock et al., 2005). Taken together, these studies show that when ESS1 is bound by its cognate repressor proteins, it functions to inhibit splicing by preventing use of exon 4 by the spliceosome.

As an initial step toward understanding the mechanism of exon repression, the step in spliceosome assembly that is blocked by ESS1 was determined. First, the 5' splice site of the first exon (CD45 exon 3) in the WT minigene was inactivated so that splicing and spliceosome assembly occur only on the downstream intron (WTΔE3). This construct thus allows us to observe spliceosome assembly and catalysis only with regards to the regulated exon 4, without complications from the exon 3-7 splicing pathway that occurs upon exon 4 repression in the WT construct. Splicing of the WTΔE3 minigene shows ESS1-dependent regulation, in that exon 4 remains predominantly unspliced (repressed) in the absence of competitor RNA but is efficiently spliced to the downstream exon (de-repressed) in the presence of exogenous ESS1 competitor RNA (Figure 3-2A, top, and Figure 3-11). It should be noted that there is some degradation of the RNA after 2 hours of incubation in extract under both repressed and de-repressed conditions. While this instability is not unusual in extract, and is

independent of the regulation we are studying, the splicing reaction is terminated

just prior to 2 hours to minimize degradation.
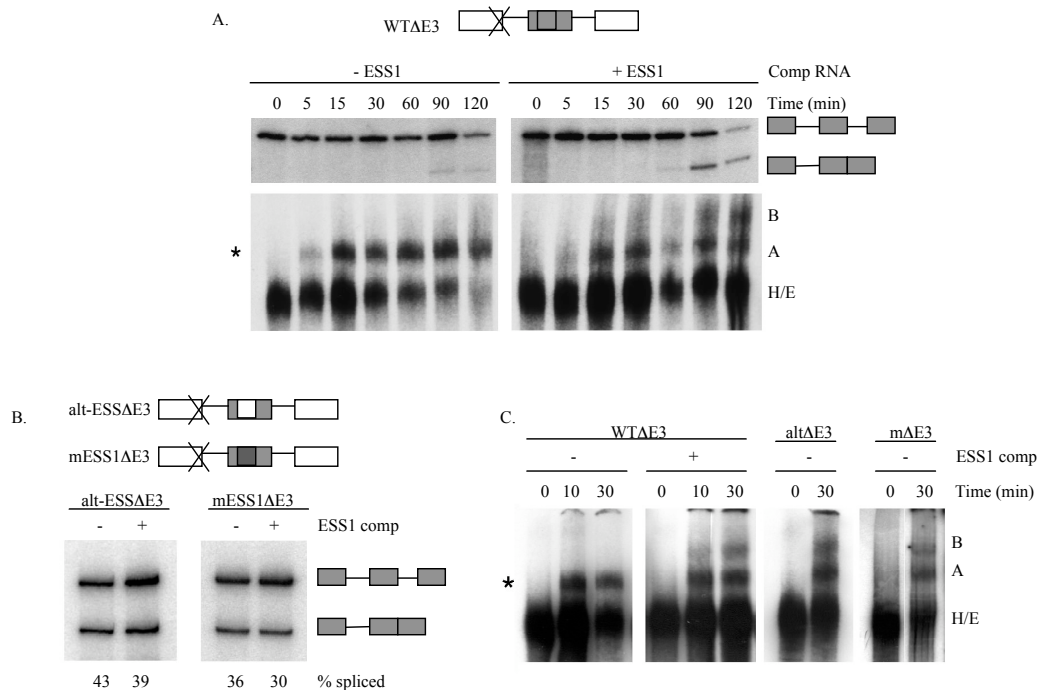
Figure 3-2. ESS1 represses splicing by stalling spliceosome assembly at an unusual step. (**A**) Top, RNA derived from the WTΔE3 minigene was spliced as in Figure 3-1. For quantification, see Figure 3-11. Bottom, ^{32}P-labeled WTΔE3 RNA was incubated in JSL1 nuclear extract under splicing conditions in the absence (-) or presence (+) of exogenous ESS1 competitor RNA, and resulting spliceosome complexes were resolved on a non-denaturing polyacrylamide gel. Co-migrating H and E complexes (H/E), A and B complexes and the stalled complex (asterisk) are labeled. In (A), B complex in the presence of ESS is more diffuse at 15-60 minutes than in (C), because we held these reactions on ice with heparin for the remainder of the extended time course before loading. (**B**) Splicing of RNA derived from alt-ESSΔE3 (altΔE3) and mESS1ΔE3 (mΔE3) minigenes. Splicing reactions for these and all subsequent experiments were terminated at 110 minutes. (**C**) Spliceosome assembly gels as in (A) using ^{32}P-labeled versions of the RNAs shown.

To identify the step in the splicing of exon 4 that is blocked by ESS1,

spliceosome assembly on WTΔE3 was examined in parallel with the *in vitro*

splicing reactions. Resolution of splicing reactions by native gel electrophoresis

results in a well-defined pattern of shifts corresponding to the known sequential

complexes along the assembly pathway (Konarska and Sharp, 1986). As shown

in Figure 3-2 and Figure 3-11, spliceosome assembly on WTΔE3 progresses efficiently under de-repressed (+ESS1) conditions as A and B complex are readily detected after a 15-30 minute incubation with nuclear extract. The catalytic C complex cannot be resolved on these gels given the large size of the template pre-mRNA, however, it must also form efficiently given the fact that up to 50% of WTΔE3 pre-mRNA is converted to spliced product under these de-repressed conditions. Remarkably, under repressed conditions a complex migrating at the same position as the pre-spliceosomal A complex forms as rapidly and efficiently as in de-repressed conditions (denoted by *), however no B complex is observed (Figure 3-2A, bottom -ESS1). Even after a two hour incubation, at which point the stalled A-like complex (*) is significantly accumulated on the WTΔE3 substrate, little or no B complex is observed (Figure 3-2A, bottom).
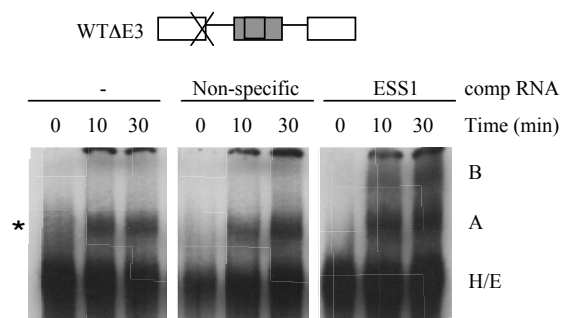
Figure 3-3. Block in assembly is specifically alleviated by ESS1 competition. ^{32}P-labeled WTΔE3 RNA was incubated in JSL1 nuclear extract under splicing conditions in the absence (-) or presence (+) of exogenous non-specific or ESS1 competitor RNAs.

To further determine whether the block that was observed in spliceosome assembly on WTΔE3 is specifically due to ESS1-mediated repression, the ΔE3 mutation was engineered into the mESS1 and alt-ESS substrates. The splicing of both of these constructs is not influenced by the addition of exogenous ESS1 RNA and, in this context, the alt-ESS no longer functions as a silencer (Figure 3-2B). Notably, for both of the alt-ESSΔE3 and mESS1ΔE3 substrates, efficient progression to B complex in the absence of ESS1 RNA was observed (Figure 3-2C, see below for confirmation of B complex assignment). Moreover, use of a non-specific competitor RNA does not allow progression to B complex on the

WTΔE3 substrate (Figure 3-3). Together, these data demonstrate that the lack of B complex formation on WTΔE3 is indeed dependent on the ESS1 repressor activity. Importantly,
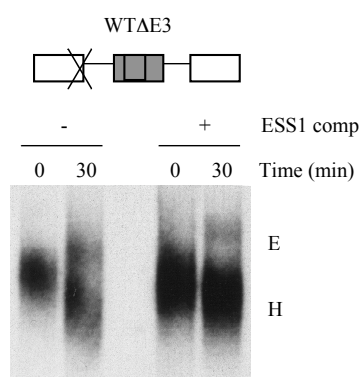
Figure 3-4. Spliceosome assembly prior to A complex is not inhibited by ESS1. ^{32}P-labeled WTΔE3 RNA was incubated as in Figure 3-3, but the resulting spliceosome complexes were resolved by native agarose gel electrophoresis to separate the H and E complexes.

the spliceosome assembly reactions with the WTΔE3 substrate were also resolved on native agarose gels to separate H and E complexes (Das and Reed, 1999), and

no difference was observed in the efficiency of E complex formation either in the absence or presence of ESS1 competitor (Figure 3-4). Finally, RT-PCR analysis of *in vitro* splicing also recapitulates the ESS1-dependent signal-induced splicing pattern seen *in vivo* (Figure 3-5A). Interestingly, a stalled intermediate complex formed at the same transition along the spliceosome assembly pathway under activated conditions (Figure 3-5B). This study, however, is focused on understanding the mechanism of basal repression, as this provides a critical insight into the overall regulation of CD45.
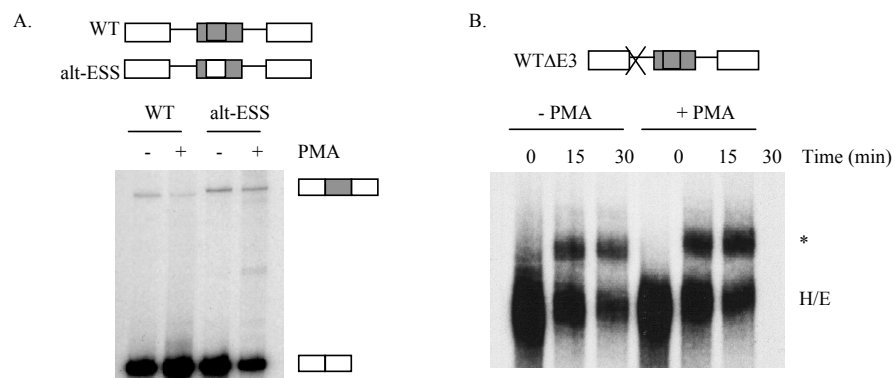
Figure 3-5. The stall in spliceosome assembly occurs at the same transition under both resting and activated conditions. (**A**) RT-PCR analysis of *in vitro* splicing using the WT and alt-ESS minigene incubated in JSL1 NE from resting (- PMA) or activated (+ PMA) conditions. (**B**) ^{32}P-labeled WTΔE3 RNA was incubated in JSL1 NE under resting (- PMA) or activated (+ PMA) conditions.

Although the ESS1-dependent stalled complex migrates at a position consistent with it being an A, or A-like, complex (Konarska and Sharp, 1986, 1987), the dependence on ATP and the requirements for individual snRNPs were determined to more rigorously characterize the complex. The canonical A

complex is defined as the ATP-dependent association of the U1 snRNP with the

5' splice site on the upstream exon and the U2 snRNP bound at the 3' splice site

branch point sequence of the downstream exon in a cross-intron configuration,
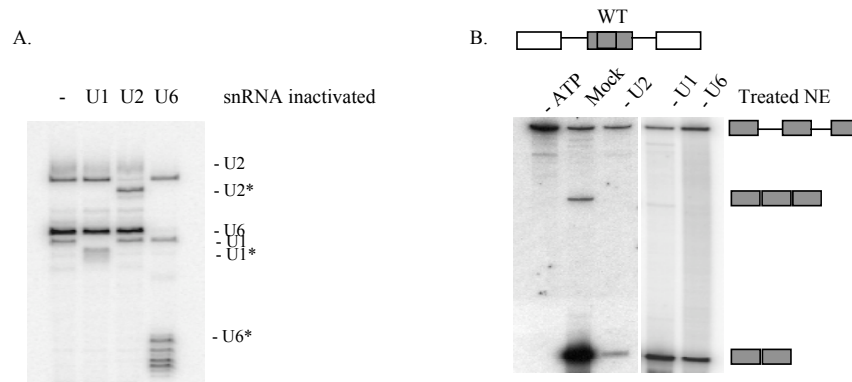
Figure 3-6. Inactivation of spliceosomal snRNP components. (**A**) JSL1 nuclear extract was incubated with exogenous RNase H and an oligonucleotide complementary to the regions of either U1, U2, or U6 snRNA that are required for spliceosome assembly. Primer extension of each snRNA showed specific and robust cleavage of the target (>90%). (**B**) RT-PCR analysis of *in vitro* splicing using unlabeled, capped RNA derived from the WT minigene showed snRNA inactivated extracts had a reduced ability to catalyze pre-mRNA splicing.

whereas a canonical exon-definition complex does not involve the ATP-

dependent association of the U2 snRNA (Black, 2003). To determine the

dependency of the stalled complex on specific snRNPs, oligo-directed RNase H

mediated cleavage of the U1, U2 or U6 snRNA was used to remove the region of

the snRNAs required for binding the pre-mRNA (Figure 3-6A)(Black et al., 1985;

Black and Steitz, 1986). Primer extension of each spliceosomal snRNA shows

that cleavage was specific and that greater than 90% of the target snRNA was

inactivated, consistent with the diminished ability of the depleted extracts to

catalyze pre-mRNA splicing (Figure 3-6B). Significantly, in the absence of the

U1 or U2 snRNPs, formation of the stalled complex is dramatically reduced relative to mock-depleted extract, while inactivation of U6 snRNP has no effect (Figure 3-7A and 3-7C). Formation of A complex also has a strict requirement for ATP, making this the first ATP-dependent step in the assembly pathway. Depletion of ATP from the assembly reactions completely abolishes formation of the stalled complex (Figure 3-7B and 3-7C). Taken together, the requirement of ATP, U1 and U2 snRNA for the robust formation of the ESS1-stalled complex demonstrates that this complex has the primary hallmarks of an A-like complex.
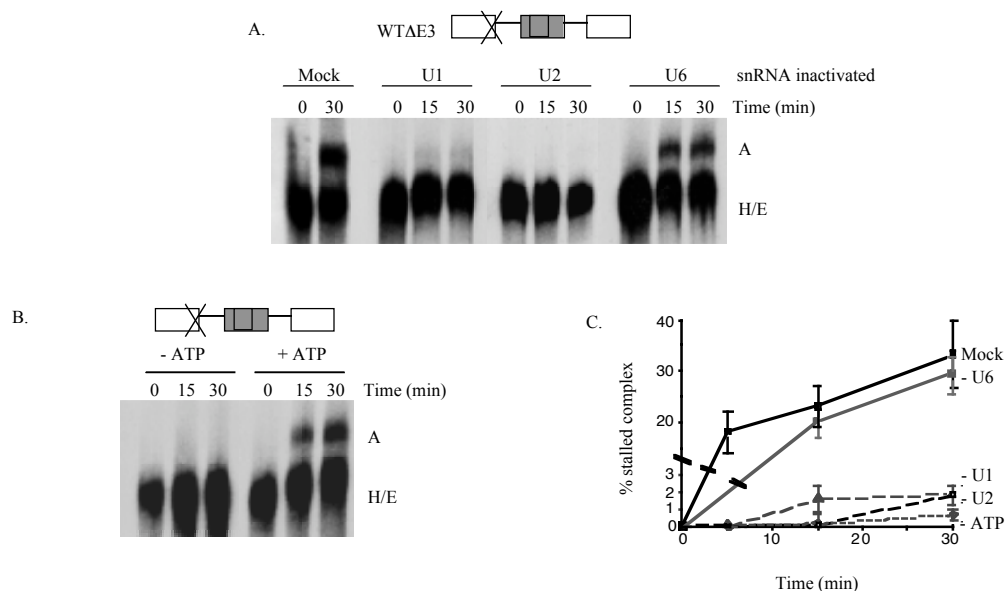
Figure 3-7. Stalled complex has the hallmarks of a canonical A complex. (**A**) The stalled complex is dependent on U1 and U2 snRNAs. ^{32}P-labeled WTΔE3 RNA was incubated with either mock –treated or snRNP-inactivated JSL1 nuclear extract (-U1, -U2, or -U6) under conditions otherwise favorable to spliceosome assembly, and complexes were resolved as in Figure 3-2A. (**B**) The stalled complex is dependent on ATP. ^{32}P-labeled WTΔE3 RNA was incubated in JSL1 nuclear extract depleted of ATP under conditions in which both ATP and phosphocreatine were absent from the assembly reaction (-ATP) and compared to reactions containing ATP (+ATP). (**C**) Summary of results from assembly reactions as in A and B. Percentage of stalled complex relative to total spliceosome complexes was calculated using densitometry. Each value is an average from four to six independent experiments; error bars indicate s.d.

As shown in Figure 3-2 and Figure 3-3, a slow migrating complex does not form on the WTΔE3 substrate under repressed conditions. Initially, this slow-migrating complex was assigned as the tri-snRNP containing B complex based on its typical migration consistent with previous studies (Konarska and Sharp, 1986).
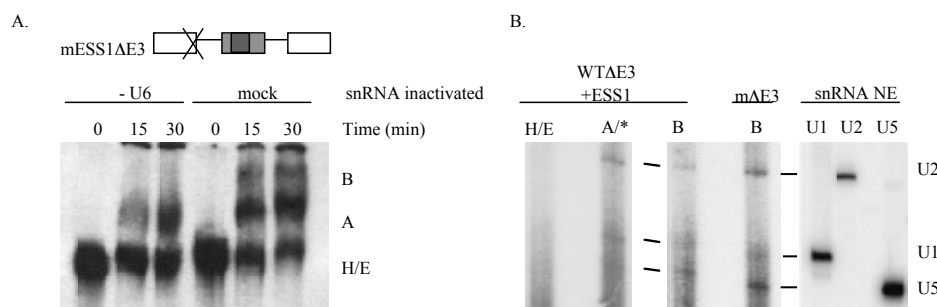
Figure 3-8. Complex assigned as B complex has hallmarks of tri-snRNP association. (A) Spliceosome assembly reactions as in Figure 3-2A, using the mESS1ΔE3 RNA, which efficiently assembles an apparent B complex. Reactions were done in mock-depleted or U6 depleted JSL1 nuclear extracts as in Figure 3-6A. (B) Primer extension analysis of RNA eluted from complexes assembled on either WTΔE3 under derepressed conditions (+ ESS1) or on mESSΔE3 RNA. Indicated complexes were excised from non-denaturing gels and RNA was extracted and analyzed with primers specific for U1, U2 and U5 snRNAs (pooled). Assignment of products is based on reactions done with individual primers using total RNA from nuclear extract (NE lanes).

To further confirm this assignment of B complex, the requirement for the U6 snRNA in the formation of this complex was tested. Depletion of the U6 snRNA abolishes the slow-migrating complex on the mESSΔE3 construct, which otherwise forms this complex robustly under mock conditions (Figure 3-8A). To determine if U5 snRNA was also recruited to this slower-migrating complex, the complexes formed on mESSΔE3 and WTΔE3 under de-repressed conditions (+ESS) were cut from assembly gels, the RNA was eluted and the sample was assayed for the presence of the U1, U2 and U5 snRNAs by primer extension. As shown in Figure 3-8B, in the A or stalled complex from WTΔE3 the primarily

signal detected was the U1 and U2 snRNAs, consistent with the studies shown in Figure 3-7. While a low level of U5 snRNA was detected in the "A/*" complex, the amount of U5 snRNA signal was significantly enriched in the "B" complex formed on both mESSΔE3 and WTΔE3+ESS, with a corresponding decrease in U1 signal (Figure 3-8B), consistent with the assignment of this complex. Taken together, the experiments shown in Figures 3-2 through 3-8 strongly argue that the ESS1 blocks spliceosome assembly in the transition from an A, or A-like, complex to the tri-snRNP associated B complex. Importantly, such a ESS-mediated block is past the stage at which the vast majority of splicing regulation has been shown to occur (Izquierdo et al., 2005; Sharma et al., 2005; Wagner and Garcia-Blanco, 2001; Zhu et al., 2001), and suggests a new mechanism for exon silencing.

The stalled complex is suggestive of an exon-defined A complex

Since there is little precedent for an ESS functioning to repress exon inclusion after the first ATP-dependent step in splicing, it is important to better understand the step at which the ESS1 stalls spliceosome assembly. Traditionally A complex has been thought of as being "intron-defined", that is comprising of an upstream U1 snRNP interacting with a downstream U2 snRNP across the intervening intron. However, *in vitro* trans-splicing studies have shown that an A-like complex, containing the U1 and U2 snRNPs, can form across an isolated

exon in an exon-defined manner (Chiara and Reed, 1995). To determine if the ESS1-dependent block in splicing prior to B complex formation was specific for the intron downstream of exon 4 (i.e. the only usable intron in the WTΔE3 construct), or was a more generalized block of exon 4 itself, a version of the WT construct was generated in which the 3' splice site branch-point sequence of the downstream exon 7 was inactivated (WTΔE7), so that assembly and splicing can now occur only on the upstream intron. As observed for the WTΔE3 construct (Figure 3-2), splicing of the WTΔE7 was also inhibited under normal conditions, and this inhibition was alleviated upon addition of competitor ESS1 RNA **(**Figure 3-9A**)**. Strikingly, the WTΔE7 pre-mRNA shows an ESS1-dependent block at the
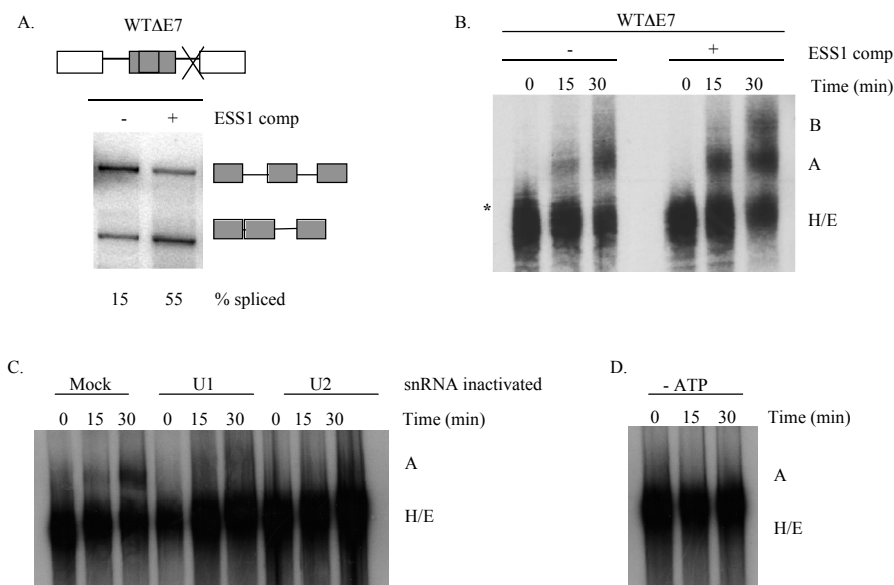
Figure 3-9. Formation of the stalled complex is not an intron-specific event. (**A**) *In vitro* splicing of RNA derived from the WTΔE7 minigene, in which only the upstream intron is functional. Splicing was done in the absence (-) and presence (+) of exogenous competitor (comp) ESS1 RNA and quantified as in Figure 3-11. (**B**) Spliceosome assembly on a ^{32}P-labeled RNA derived from the WTΔE7 minigene shows a stall in spliceosome assembly at the transition that is blocked on the WTΔE3 minigene. (**C**) Assembly reactions using ^{32}P -WTΔE7 RNA were performed in mock-treated or snRNP inactivated JSL1 nuclear extracts. (**D**) Spliceosome assembly using the ^{32}P-WTΔE7 RNA under reaction conditions lacking ATP as in Figure 3-6.

same stage of spliceosome assembly observed in the WTΔE3 minigene (Figure 3-9B). Consistent with the data shown for WTΔE3, efficient formation of the stalled complex on WTΔE7 also requires the presence of ATP, U1 snRNP, and U2 snRNP in the assembly reaction (Figure 3-9C and 3-9D). Since ESS1-mediated repression of spliceosome assembly occurs on both the upstream (WTΔE7) and the downstream (WTΔE3) introns in the same manner, it suggests that the exon containing the ESS1 sequence is itself the unit of regulation. In other words, these data indicate that the ESS1-dependent stalled complex is an A-like complex in which the U1 and U2 snRNPs bound to the exon 4 splice sites interact across the repressed exon. Since such a complex is clearly distinct from either a canonical E or A complex, this ESS-dependent stalled complex shall be referred to as an AEC for A-like Exon-definition Complex.

To provide further evidence that the ESS1-stalled complex is an AEC, the possibility of forming a complex with the characteristics of the stalled complex on exon 4 in the absence of introns was examined (i.e. no possibility of intron definition). Therefore, a minigene was designed with both the upstream exon 3 splice site and the downstream exon 7 splice site inactivated (ΔE3E7) so that assembly can only occur across the regulated exon (Figure 3-10A). Importantly, a complex with mobility identical to the ESS1-dependent stalled complex was detected using the ΔE3E7 (Figure 3-10B). This complex on ΔE3E7 requires ATP,
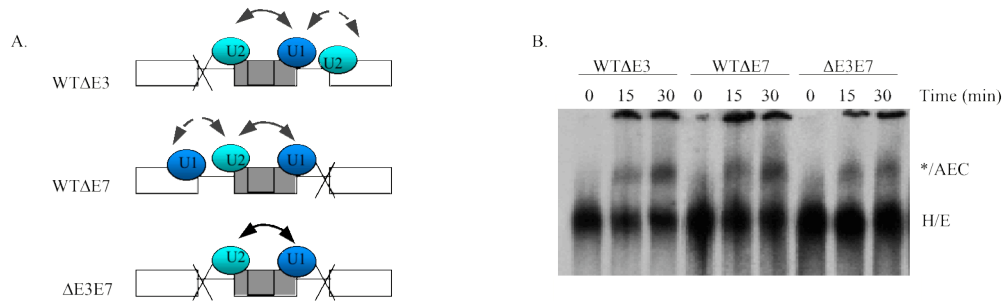
Figure 3-10. ESS1-dependent formation of the stalled complex does not require either flanking splice site. (**A**) Schematic representation of the spliceosome intermediates that may form on each tested pre-mRNA substrate. Both WTΔE3 and WTΔE7 RNAs are able to form both exon- and intron-defined A-like complexes, while ΔE3E7 RNA is only able to form the exon-defined A-like complex. (**B**) Spliceosome assembly of ^{32}P-labeled RNAs derived from the WTΔE3, WTΔE7 or ΔE3E7 minigenes in the absence or presence of exogenous ESS1 competitor RNA.

U1 and U2 snRNAs for formation, whereas depletion of U6 has little to no effect (Figure 3-11A and 3-11C). To show that recognition of the splice sites by U1 and U2 snRNAs is also required for the ΔE3E7 complex, as predicted for an AEC, pre-mRNAs corresponding to the ΔE3E7 substrate were generated that contained additional modifications to weaken either the U1 binding site at the 5' splice site of exon 4 (Δ5' ΔE3E7), or the U2 snRNP binding site at the 3' splice site branch point sequence of exon 4 (ΔBPS ΔE3E7). Disruption of either functional splice site significantly inhibits complex formation, dropping the efficiency to less than half that of the wildtype (Figure 3-11B and 3-11C). Taken together, the characterization of the complex on the ΔE3E7 minigene and comparison of this to the ESS1-dependent stalled complex, strongly indicate that ESS1 functions by stalling spliceosome assembly at an AEC intermediate.

AEC formation is required for ESS1-dependent exon repression
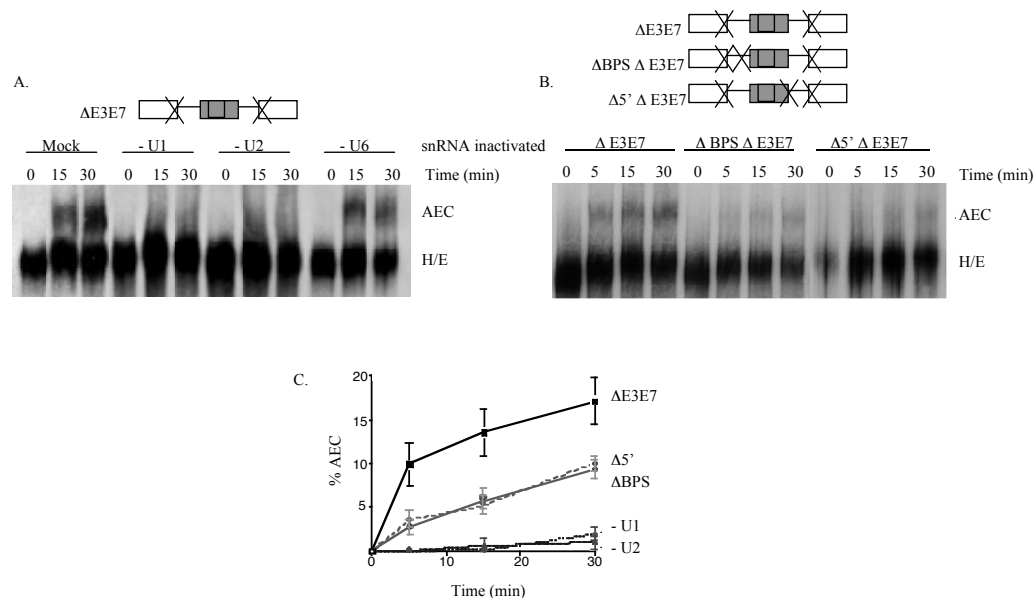
Figure 3-11. Stalled complex has the hallmarks of an A-like complex assembled across an exon. (**A**) Assembly on ^{32}P-labeled RNA derived from the ΔE3E7 minigene, under mock-treated or snRNP-inactivated conditions as in Figure 3-6A. (**B**) Spliceosome assembly on ^{32}P-labaled RNA derived from ΔE3E7 minigenes containing the indicated additional mutations. (**C**) Summary of efficiency of AEC formation in assembly reactions lacking U1, U2 or the binding sites for these snRNAs, as in A and B. ΔE3E7 is a mock-treated positive control. Percentage of stalled AEC complex relative to total spliceosome complexes was calculated using densitometry. Each value is an average of four to six independent experiments; error bars indicate s.d.

If the formation of a stalled AEC complex is indeed the mechanism by which ESS1 represses exon inclusion then inhibiting formation of the AEC should circumvent ESS1 mediated splicing repression. Since both the 5' and 3' splice sites are important for AEC formation (Figure 3-11), the requirement for cross-exon interactions in ESS1-dependent splicing regulation was examined. Quantification of the splicing of WTΔE3 (as shown in Figure 3-2) shows only ~4% splicing to exon 4 under repressed conditions, but a 6-8 fold increase in splicing efficiency upon addition of exogenous ESS1 competitor to de-repress exon 4 (Figure 3-12A). Strikingly, parallel reactions with constructs containing
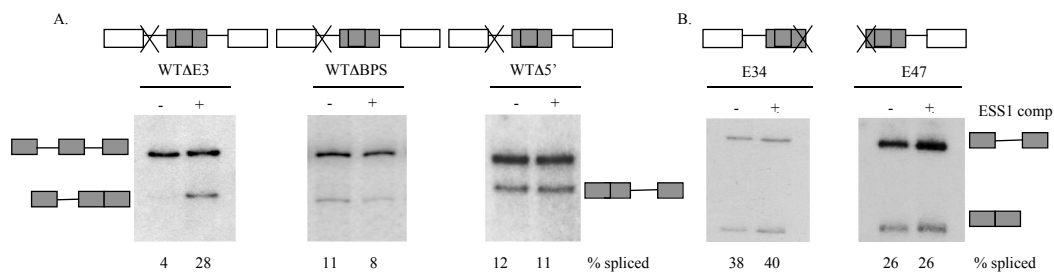
Figure 3-12. Formation of an AEC is required for ESS1-dependent repression of splicing. (**A**) RT-PCR analysis of *in vitro* splicing with three-exon wildtype (WTΔE3) or splice site mutant (WTΔBPS, WTΔ5') minigenes. RNA derived from minigenes was incubated under splicing conditions in the absence (-) or presence (+) of exogenous ESS1 competitor (comp) RNA, as in Figure 3-1. Percentage of spliced product was determined by phosphorimaging and represents the average of at least four independent experiments. s.d. for all splicing quantifications is <10% of the average value shown. (**B**) RT-PCR analysis of *in vitro* splicing with single-intron constructs. RNA derived from with the E34 or E46 minigene was spliced and analyzed as in A.

mutations in the splice sites surrounding exon 4 (Figure 3-12A, WTΔBPS or WTΔ5') show no significant increase in splicing upon addition of exogenous ESS1 RNA, suggesting that ESS1 is not a functional repressor of constructs in which the formation of the AEC complex is inhibited. However, analysis of the WTΔBPS or WTΔ5' constructs is complicated by the fact that in a significant portion of the RNA the flanking exons are spliced directly together due to the weakening of the middle exon 4 (data not shown). To circumvent this problem, single-intron exon 4 constructs were also analyzed, in which only intron-defined spliceosome assembly can occur and no alternate splicing pattern is possible (Figure 3-12B). Importantly, neither of the single-intron E34 or E47 substrates show any ESS1-mediated repression, since addition of exogenous ESS1 competitor has no effect on splicing efficiency (Figure 3-12B). Taken together, the requirement for the 5' and 3' splice sites of exon 4, both for the efficient formation of the AEC stalled complex and the regulation of splicing, indicates

that the formation of an AEC exon-definition complex is essential for ESS1-mediated exon repression.

HnRNP L is sufficient to induce an AEC stall in spliceosome assembly

Previously it was shown that a complex of hnRNP proteins, including hnRNPs L, E2 and PTB, bind to the ESS1 silencer element (Rothrock et al., 2005). Of these proteins, hnRNP L is the primary functional component responsible for mediating ESS1-dependent exon silencing; whereas hnRNP E2 augments the repressive activity of hnRNP L while PTB has no apparent effect on the inclusion of CD45 exon 4 (Rothrock et al., 2005). These data suggest that hnRNP L and/or hnRNP E2 are likely to be critically involved in the formation of the AEC; thus stalling spliceosome assembly and forcing exon skipping. Consistent with our previous studies (Rothrock et al., 2005), and due to the high level of hnRNP L in nuclear extract, immunodepletion of hnRNP L is less efficient at relieving exon repression than is addition of exogenous ESS1 competitor, and is not sufficient to relieve the block at the AEC (data not shown). Moreover, upon efficient de-repression of the AEC block by addition of ESS1 competitor, the addition of recombinant protein was not sufficient to reverse the effect of the competitor. However, upon partial relief of the AEC stall by reduced concentrations of ESS1, some B complex formation was observed. Under these more sensitized conditions, addition of the highest concentration of recombinant
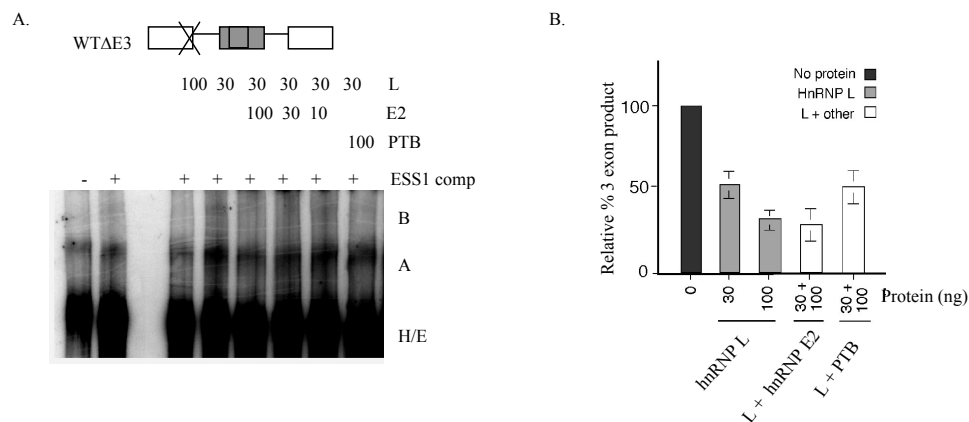
Figure 3-13. Proteins that cause ESS1-dependent exon skipping inhibit B complex formation. (**A**) Spliceosome assembly of ^{32}P-labeled WTΔE3 RNA in the absence (-) of presence (+) of 2.5 pmol exogenous competitor (comp) ESS1 RNA and purified recombinant hnRNP proteins as indicated. A/AEC, co-migrating A and AEC complexes. (**B**) Summary of two to four experiments in which purified recombinant hnRNP L proteins were added to a derepressed *in vitro* splicing reaction, in which inclusion of exon 4 has been stimulated by addition of exogenous ESS1 RNA. Error bars indicate s.d. percent exon 4 inclusion (3-exon product) is normalized to the amount of inclusion observed in the presence of ESS1 competitor but in the absence of additional recombinant protein.

hnRNP L (100 ng) is sufficient to inhibit B complex formation and restore the

AEC block on the WTΔE3 construct (Figure 3-13A). Spliceosome assembly on

WTΔE3 is also blocked at lower concentrations of hnRNP L when supplemented

with increasing concentrations of hnRNP E2 (Figure 3-13A). In contrast, addition

of PTB has no ability to restore the block at AEC, either alone (data not shown) or

in combination with low levels of hnRNP L (Figure 3-13A). The ability, or lack

thereof, of hnRNP L, E2 and PTB to stall spliceosome assembly at the AEC step

is entirely consistent with the effect of these proteins in repressing exon 4

inclusion as assayed by splicing (Figure 3-13B). Finally, none of these proteins

alter spliceosome assembly on the mESS1ΔE3 constructs (data not shown),

consistent with the ESS1-dependence of both hnRNP L function and AEC

repression. These results confirm the critical role of hnRNP L in the repression of CD45 exon 4 and demonstrate that this protein functions by helping to stall spliceosome assembly prior to B complex formation.

Discussion

Spliceosome assembly has thus far been described to pass through three intermediates (E-A-B) during formation of the final catalytic C complex. Previous studies aimed at understanding the role of splicing regulatory sequences in modulating spliceosome assembly have predominantly shown that regulation of spliceosome assembly and splice site choice occurs prior to ATP utilization through inhibiting the formation of an early (E) exon-definition complex or by preventing the ATP-dependent association of U2 during A complex formation (Black, 2003; Matlin et al., 2005), with only a very few studies suggesting other mechanisms of regulation (Giles and Beemon, 2005; Lallena et al., 2002; Zhu et al., 2003). Importantly, in this study the ESS1 silencer element of CD45 exon 4 was shown to repress splicing after formation of an ATP, U1 and U2-dependent exon-definition complex, and prevents this repressed exon from progressing into a B complex. Such a block in the transition from an A or A-like (AEC) complex to B complex formation provides a new mechanism for the function of exonic splicing silencers.
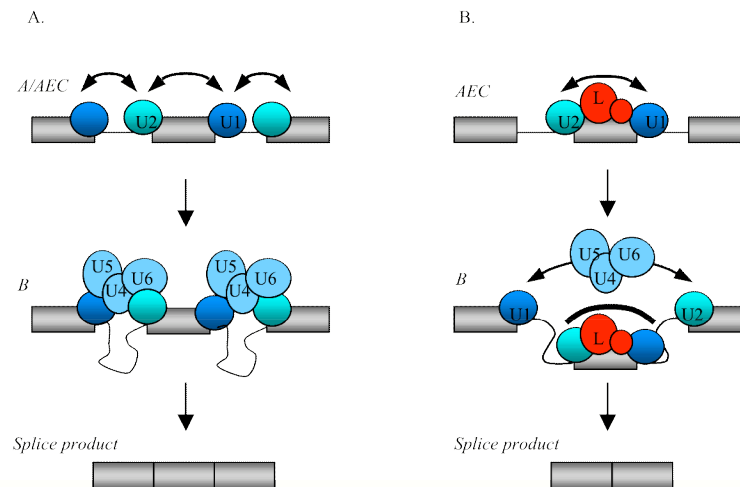
Figure 3-14. Model for ESS1 function in hyper-stabilizing an AEC. Under normal splicing conditions (**A**), U1 and U2 snRNPs associate with the pre-mRNA, perhaps initially interacting across the exon in an AEC-like complex but ultimately forming an intron-defined A complex (A/AEC). The tri-snRNP is then recruited to each intron in a canonical B complex, resulting in the removal of each intron and the inclusion of all exons in the final product. However, in the presence of ESS1 and its binding proteins (hnRNP L and E2, and possibly others, (**B**)), the U1 and U2 snRNPs form a stable AEC. This stable AEC probably prevents the U1 and U2 snRNPs bound to the ESS1-containing exon from interacting across the introns with snRNPs bound to the flanking exons. Thus, the flanking snRNPs instead pair with each other, sequestering the ESS1-containing exon into an effective intron that is skipped from the final product.

Figure 3-14 shows a model for ESS1 function based on our data presented here. We propose that on a permissive (un-repressed) exon, U1 and U2 bind to the flanking splice sites, perhaps first making contact across the exon in an AEC, but ultimately interacting across the introns with snRNPs bound to the flanking exons (Figure 3-14A, "A/AEC"). The U5/U4•U6 tri-snRNP is then recruited to each intron resulting in accurate joining of all three exons (Figure 3-14A, "B"). In contrast, in the presence of the ESS1 sequence, the hnRNP proteins bound to the ESS1 (HnRNP L, E2 and perhaps others) likely interact strongly with the U1 and U2 snRNPs to form a ternary complex across the exon that is more favorable than the competing cross-intron conformations of U1 and/or U2 snRNPs (Figure

3-14B, "AEC"). Thus the flanking snRNPs pair with one another, thereby omitting the ESS1 containing exon from the final product (Figure 3-14B, "B"). This model is consistent with the fact that both of the exon 4 splice sites need to be functional to achieve ESS1-dependent stalling of spliceosome assembly and repression of exon 4 inclusion. Loss of either U1, U2 or the hnRNPs from the AEC complex in Figure 3-14 would destabilize this inactive conformation and allow the remaining snRNPs to interact across the introns. Future proteomic and structural characterization of the stalled AEC will therefore not only reveal further insight into the mechanism by which the ESS1 functions, but will also provide a valuable tool to better understand the poorly characterized transition in the developing spliceosome from exon-definition to exon-pairing and tri-snRNP recruitment.

Most of the biochemical analysis of splicing regulation that has been done to date involves the use of two-exon/single-intron constructs. Such substrates greatly simplify analysis, and have allowed detailed characterization of some regulatory mechanisms such as those that involve direct enhancement or inhibition of splice site binding by U1 or U2AF35 (Forch et al., 2002; Valcarcel et al., 1993; Zhu et al., 2001; Zuo and Maniatis, 1996). However, more complex splicing regulatory mechanisms, such as those described here for CD45 exon 4, are not observed in such minimal systems (as in Figure 3-11B) and may therefore have been missed in previous studies. Indeed, given the dynamic and multi-

component nature of spliceosome assembly, and the abundance and complexity of mammalian alternative splicing, the likelihood that splice site choice can be regulated by only a few mechanisms seems low. From the studies herein a model is proposed in which other ESSs may function by blocking B complex formation, as described for the CD45 ESS1, and also that as the understanding of splicing regulation and the ability to analyze complex substrates increases, examples of regulation occurring at all points of spliceosome assembly are likely to be uncovered.

CHAPTER FOUR

Characterization of the AEC Intermediate Complex

Introduction

The mammalian spliceosome, which catalyzes intron removal, is comprised of ~ 300 proteins and 5 snRNAs, each of which are contained within a protein-RNA particle or "snRNP" (Jurica and Moore, 2003). The final enzymatic complex is assembled *de novo* on each intron through a step-wise series of key interactions between the snRNP components and the splice sites within the pre-mRNA substrate. The inherent dynamic nature of the assembly process results in significant heterogeneity of this enzymatic machine, consequently limiting the feasibility of structural and biochemical characterization of the spliceosome. While some of the assembly intermediates (E-A-B-C) have been trapped and characterized by electron microscopy and/or mass spectrometry, the transitions between these intermediates are very poorly understood (Jurica and Moore, 2002). In particular, when and how during spliceosome assembly does the transition occur from the snRNPs interacting across the exon to interacting across the intron remain major unanswered questions.

Recently, we identified a splicing silencer sequence within CD45 regulated exon 4 (ESS1), which binds a complex of hnRNP proteins that function to repress exon splicing (Chapter Two)(Rothrock et al., 2005). Namely, the ESS1

binding proteins act to stall spliceosome assembly after the formation of an ATP-, U1-, and U2-snRNP dependent A-like exon-definition complex (AEC) on the repressed exon, such that recruitment of U4•U6/U5 tri-snRNP is blocked and the exon cannot be used by the splicing machinery (Chapter 3)(House and Lynch, 2006)). This mechanism of splicing repression is novel in that previous examples of spliceosome regulation have almost exclusively been shown to inhibit the earliest stages of assembly by blocking exon definition. Therefore, characterization of the AEC stalled intermediate complex will provide significant insight into a unique mechanism of splicing repression, and increase our understanding of the conformational transitions that are required for exon pairing within the growing spliceosome complex. This chapter describes the biochemical purification and preliminary characterization of the naturally-occurring stalled AEC intermediate complex.

Results

AEC is hyper-stabilized relative to the canonical A complex

Several lines of evidence suggested that the AEC intermediate is a remarkably stable complex, and that perhaps this inherent stability is important in understanding how this complex functions to promote splicing repression. The initial identification of the AEC showed that the stalled complex formed on WTΔE3 was stable out to 2 hours under standard spliceosome assembly conditions (Chapter 3, Figure 3-2A). Additionally, "on pathway" spliceosome

assembly assays were performed to determine if once formed the AEC was capable of being de-repressed and chased into a functional spliceosome. Initially, assembly on the WTΔE3 minigene was allowed under repressed conditions. Subsequently, the reaction conditions were switched to de-repressed conditions, by the addition of excess ESS1 competitor to the assembly reaction already in progress, and the resultant complexes were resolved by native gel electrophoresis. Interestingly, when assembly was initiated under repressed conditions the spliceosome could not progress beyond the AEC (data not shown). This data correlates with parallel *in vitro* splicing assay results, in which splicing of the WT minigene showed no increase in exon inclusion upon the delayed addition of ESS1 competitor to initially repressed reaction conditions (data not shown). The simplest interpretation of this data is that the stalled AEC intermediate is a highly stable complex, and once formed on the repressed exon it cannot easily be remodeled to allow inclusion. Alternatively, it is also possible that the AEC is not an "on pathway" intermediate in the process of functional spliceosome assembly; however, these two models cannot be distinguished based on our current understanding of the AEC.

To more directly assess hyper-stability of the stalled complex, we analyzed the ability of both the repressed AEC as well as the permissive A complex to remain intact under varying salt concentrations. Assembly of the AEC was assayed using the WTΔE3 minigene under standard conditions and
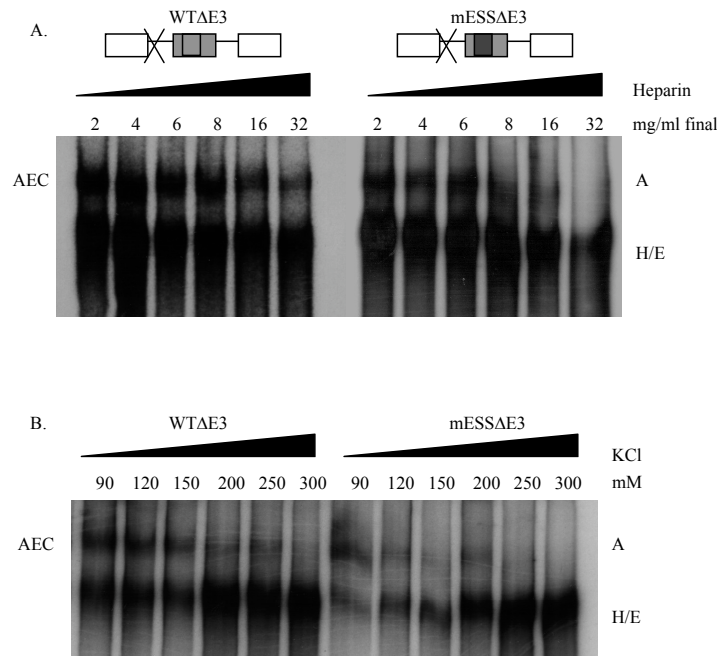
Figure 4-1. The stalled AEC intermediate is hyper-stabilized relative to the canonical A complex. (A) Spliceosome assembly on ^{32}P-labeled RNA derived from the WTΔE3 or mESS1ΔE3 minigenes incubated in normal or U6 snRNA inactivated JSL1 nuclear extract to allow formation of the AEC or canonical A complex, respectively. Following assembly, reactions were treated with increasing levels of heparin salt and then resolved on a native polyacrylamide gel. (B) Spliceosome assembly analysis as in (A), but the reactions were treated with increasing levels of potassium chloride (KCl).

lacking excess ESS1 competitor. Assembly of the permissive canonical permissive A complex was assayed using the mESSΔE3 minigene incubated in nuclear extract that was inactivated for tri-snRNP to prevent progression of the A complex into B/C complexes. Following assembly, both the AEC and the A complex samples were treated with increasing concentrations of heparin ranging from 2 to 32 mg/ml final. While the majority of the canonical A complex was disassembled at heparin concentrations at or above 16 mg/ml, the repressed AEC remained intact and appreciable amounts of the stalled complex were detected at

even the highest levels of heparin tested (32 mg/ml)(Figure 4-1A). An analogous experiment in which KCl concentrations were manipulated showed a similar trend, that is the canonical A complex was more sensitive to increasing salt then the repressed AEC (Figure 4-1B). The ability of the AEC to remain intact under stringent conditions suggests that the AEC is in fact hyper-stabilized, and this feature of the complex likely reflects the underlying mechanism of exon repression.

Altered U1 snRNA contacts at the 5'ss region within the AEC

While the previous experiments demonstrated that the AEC intermediate is hyper-stabilized, the reason for this inherent strength of the stalled complex remained unclear. As an initial step towards characterizing the spliceosome intermediates, psoralen UV cross-linking followed by primer extension was performed to map contacts between the pre-mRNA and the spliceosomal snRNA components. First, we generated a minigene in which the 5'ss sequence was altered to contain an ideal binding site for the U1 snRNA (UpΔE3, GTAAGTA). The UpΔE3 minigene served as a control to confirm our ability to detect U1-pre-mRNA interactions with this assay. As expected, *in vitro* splicing of UpΔE3 demonstrated that there was an increase in the basal level of exon inclusion as well as the loss of activation induced exon repression (Figure 4-2A), suggesting that increasing the strength of the 5'ss is sufficient to override the ESS1-mediated exon repression via the AEC. Psoralen cross-linking and primer extension
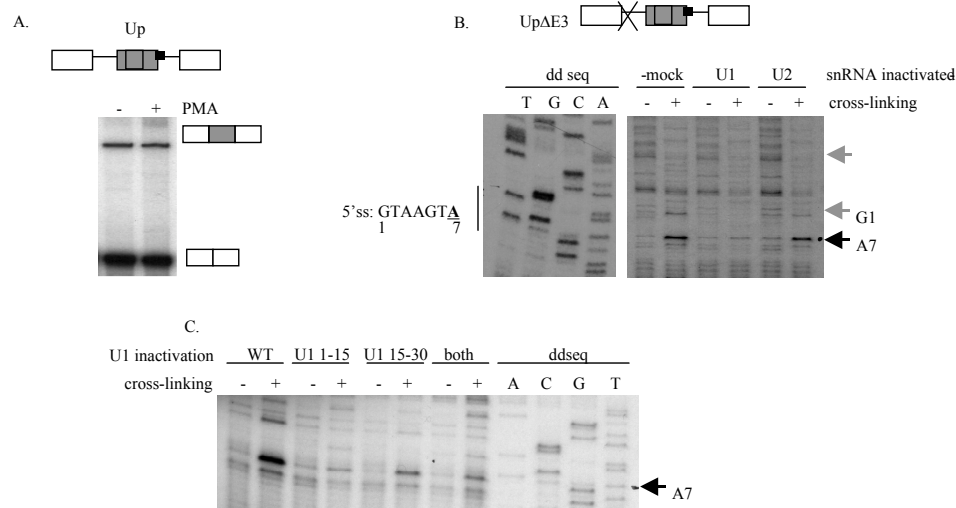
Figure 4-2. U1 snRNA makes functional contacts with pre-mRNA assembled into a canonical A complex. (A) RT-PCR analysis of *in vitro* splicing using RNA derived from the Up minigene. Point mutations were created in the 5'ss sequence of CD45 exon 4 to generate an ideal U1 snRNA consensus binding site, thereby alleviating ESS1-mediated repression. **(B)** Primer extension analysis of RNA-RNA cross-links between the spliceosomal snRNA and the UpΔE3 pre-mRNA. Following spliceosome assembly on the UpΔE3 RNA using mock-treated, U1 or U2 inactivated JSL1 nuclear extract, reactions were incubated in the absence (-) or presence (+) of psoralen and exposed to long wave UV light. ^{32}P- labeled oligonucleotides complementary to sequence downstream of the UpΔE3 5'ss were used in reverse transcription (RT) reactions to map cross-links. Dideoxynucleotide sequencing of UpΔE3 RNA was performed using the same oligos. Black arrows indicate a cross-link occurring at nucleotide position A7 that is specific to the complex formed on the de-repressed UpΔE3 RNA. Grey arrows indicate cross-links specific to the repressed WTΔE3 RNA (see Figure 4-3). **(C)** Primer extension analysis of psoralen and UV-induced cross-links as in (B), but UpΔE3 RNA was incubated in JSL1 nuclear extract inactivated for U1 by targeting distinct regions of the snRNA for cleavage.

mapping of contacts at the 5'ss of UpΔE3 showed one strong band, both UV- and psoralen-dependent, that was mapped to nucleotide position A7 (Figure 4-2B, black arrow). Work from another group showed U1 cross-linked to position A7 on a different exon, and suggested that the strong band we mapped to A7 on UpΔE3 is U1 (Sharma et al., 2005).

To confirm that the cross-linked species was due to interactions with the spliceosome rather than secondary structure within the pre-mRNA itself, we used RNase H mediated oligo targeting to inactivate specific either the U1 or U2 snRNAs. Importantly, inactivation of U1, but not U2, resulted in a loss of the

band (Figure 4-2B and 4-2C, black arrow). Typically, the U1 snRNA was inactivated by cleaving the first 15 nucleotides at the 5' end of the sequence (Black et al., 1985). However, it has also been shown that regions of the U1 snRNA outside of the first 15 nucleotides play a role in splicing, specifically nucleotides 15-30 from the 5' end of the snRNA (Seiwert and Steitz, 1993). Cross-linking and mapping analysis in extracts U1 snRNA inactivated with the U1 15-30 oligonucleotide showed a weak but still detectable crosslink band at A7 within the UpΔE3 5'ss (Figure 4-2C, black arrow).

Next, we wanted to look at how the U1 snRNA interacts with the inherently weak 5'ss of exon 4 within the stalled AEC. Toward this end, we used the standard WTΔE3 minigene to map RNA-RNA base-pairing interactions. Interestingly, the predominant cross-linked species does not map at position A7 (grey arrow) but rather to position G1 (black arrow), which is immediately at the exon-intron boundary (Figure 4-3A). Surprisingly, in U1 inactivated extracts there was no reduction in the G1 cross-linked species (Figure 4-3A). There were also additional cross-linked bands that mapped to nucleotide positions within the exon itself that occurred specifically with the WTΔE3 minigene (Figure 4-3A and 4-3B, top black arrow), and not with the UpΔE3 minigene (Figure 4-3B, top grey arrow). Mutation of a single nucleotide within the 5'ss sequence (C to T, WT$_{C \rightarrow T}$ΔE3) resulted in restoration of the typical U1 crosslink at A7 while maintaining the unusual cross-links within the exon specific to repressed
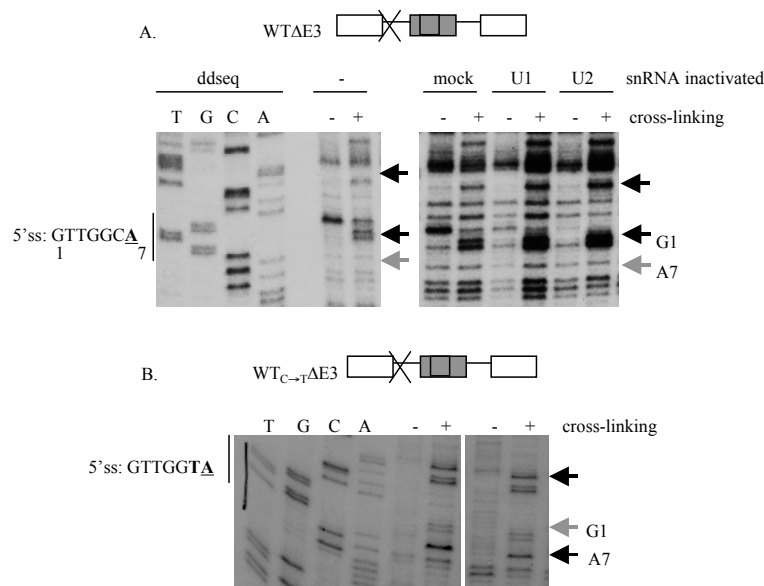
Figure 4-3. U1 snRNA makes aberrant contacts with ESS1-containing pre-mRNA assembled into a stalled AEC intermediate. (**A**) Primer extension analysis of psoralen and UV-induced RNA-RNA cross-links between the spliceosomal snRNA and the WTΔE3 pre-mRNA as in Figure 4-2. Dideoxynucleotide sequencing of WTΔE3 RNA provides a nucleotide ladder to map cross-links. Black arrows represent cross-links specific to the complex formed on the repressed WTΔE3 RNA, and include a contact at nucleotide position G1 within the 5'ss of exon 4. Grey arrows indicate cross-links specific to the de-repressed UpΔE3 RNA complex (see Figure 4-2B). (**B**) Primer extension of RNA-RNA cross-links occurring within the spliceosome intermediate complex formed on the WT$_{C \to T}$ΔE3 RNA as in Figure 4-2. The WT$_{C \to T}$ΔE3 minigene contains a single point mutation within the 5'ss sequence of CD45 exon 4 that enhances the ability of U1 snRNA to base-pair with this region of the pre-mRNA.

conditions (Figure 4-3B). The unusual cross-linked species specific to the repressed WTΔE3 construct suggest that U1 may make aberrant contacts within the AEC that could contribute to hyper-stabilization of the complex.

Differential accessibility of the PPT in the AEC versus canonical A complex

Based on the RNA cross-linking analysis of the AEC, it was clear that the spliceosome contacts the 5'ss region of the repressed exon in an unusual manner. As previous data have emphasized the importance of both the 5'ss and the 3'ss of exon 4 in splicing repression and AEC formation (Chapter 3, Figure 3-10B and 3-11)(House and Lynch, 2006), we reasoned that other regions outside of the 5'ss

exon-intron boundary might also be involved in forming atypical contacts with splicing machinery thereby contributing to the mechanism of repression. To address this possibility, we employed a nonbiased approach and analyzed the accessibility of various regions both at the 5'ss and the 3'ss of exon 4 under repressed and de-repressed conditions.

A panel of oligonucleotides were designed that were complementary to the exon-intron boundary at the 5'ss and regions out into the downstream intron as well as the branchpoint A, PPT and exon/intron boundary within the 3'ss (Figure 4-4A). Following spliceosome assembly on either the WTΔE3 or the alt-ESSΔE3 pre-mRNA, a specific oligonucleotide was then added to the reaction and the accessibility of the complementary region within the pre-mRNA template was assayed by sensitivity to RNase H cleavage. Of the 5'ss regions that were screened, only the sequence targeted by 16/5 showed differential accessibility between the repressed AEC (WT) and de-repressed canonical A complex (alt-ESS) (Figure 4-4A and 4-4B). Quantification of the percent pre-mRNA cleavage after incubation with 16/5 showed a small but reproducible difference between the AEC and the canonical A complex (WT 49% vs. alt-ESS 61% at 25 pmol/µl of oligonucleotide). The 16/5 oligo is complementary to the entire region of the WT substrate that was identified as making unique contacts with U1, that is at position G1 as well as nucleotides within the exon. Interestingly, there was no difference in accessibility upon probing with the 5/10 oligo which also covers the 5'ss G1

nucleotide, but does not encompass the sequence within the exon (Figure 4-4A and 4-4B).
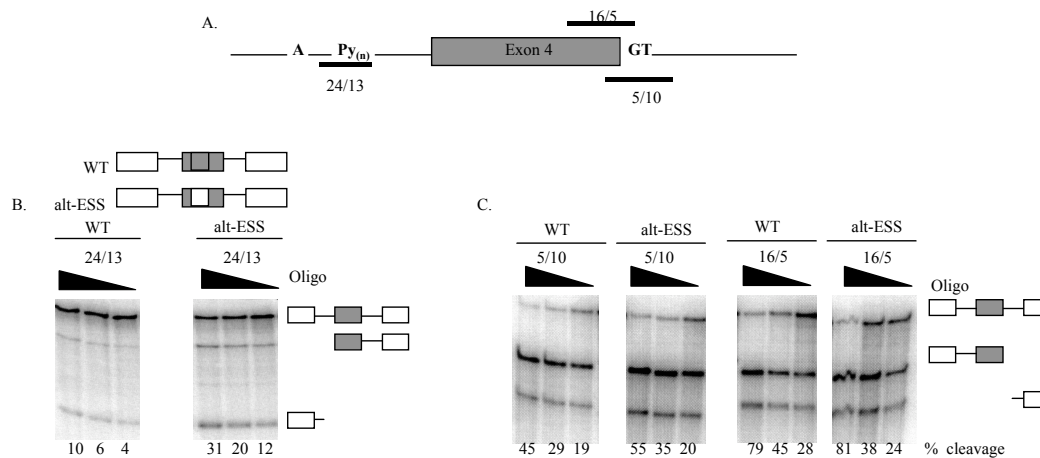
Figure 4-4. Differential accessibility of regions within the 5'ss and 3'ss of CD45 exon 4 under repressed versus derepressed conditions. (**A**) Schematic showing the names of and the regions flanking CD45 exon 4 that are targeted by the oligonucleotides used in the RNase H protection assay. For details see Chapter 6, Materials and Methods. (**B**) RNase H protection assay monitoring the accessibility of regions within the 5'ss of exon 4 when assembled into the stalled AEC or the permissive A intermediates. Spliceosome complexes were formed on ^{32}P-labeled RNA derived from the repressed WT or de-repressed alt-ESS minigenes incubated in JSL1 nuclear extract, and were treated with increasing amounts of the 16/5 or 5/10 oligonucleotides. Input concentrations of 25, 10 and 5 pmol/μl were used for 5/10. Input concentrations of 4, 2 and 1 pmol/μl were used for 16/5. Accessibility was measured as the percent cleavage of the full-length pre-mRNA template. (**C**) RNase H protection assay as in (B) except accessibility at the 3'ss was measured using the PPT oligonucleotide. Input concentrations of 25, 10 and 5 pmol/μl were used for 24/13.

Analysis of the 3'ss of exon 4 showed a dramatic difference in the accessibility of a specific region of the PPT between substrates packaged into spliceosome intermediate complexes under different conditions (Figure 4-4C). Several oligonucleotides were designed to cover 12-15 nucleotide sub-regions of the exon 4 PPT. Strikingly, probing with the 24/13 oligo showed a significant and ESS1-dependent difference in accessibility (Figure 4-4C). Quantification of the amount of cleavage determined that the alt-ESS pre-mRNA packaged into the canonical A complex was 3 times more accessible than the same region within the

WT pre-mRNA assembled into the AEC (31.1% alt-ESS vs. 9.8% WT at 25 pmol/µl of oligo). Interestingly, parallel assays using oligonucleotides that were complementary to portions of the PPT immediately adjacent to the 24/13 region did not show a difference in accessibility, suggesting that the change in accessibility observed with 24/13 is specific. Taken together, these studies confirm the importance of both the 5'ss and the 3'ss in AEC formation and suggest that perhaps the stalled AEC is a result of aberrant recruitment and/or association of spliceosomal proteins with the splice sites.

Purification of AEC and canonical A complex intermediates

In order to understand the underlying mechanism by which formation of the AEC blocks progression of the pre-spliceosome into a functional mature spliceosome, the stalled AEC was purified under native conditions to allow for further biochemical and structural characterization. Given that the stall in assembly at the AEC is a highly effective and naturally-occurring event, accumulation and trapping of the intermediate was not a problem (Chapter 3, Figure 3-2A and 3-6C)(House and Lynch, 2006). We chose to isolate the native AEC using a purification scheme modified from that initially described by the Reed lab (Das et al., 2000; Zhou et al., 2002) and later employed by Jurica and Moore for isolation the C complex for biochemical analysis (Figure 4-5)(Jurica, 2005; Jurica et al., 2002; Jurica and Moore, 2002). This method relies on the insertion of viral coat MS2 protein binding sites into the pre-mRNA template, and
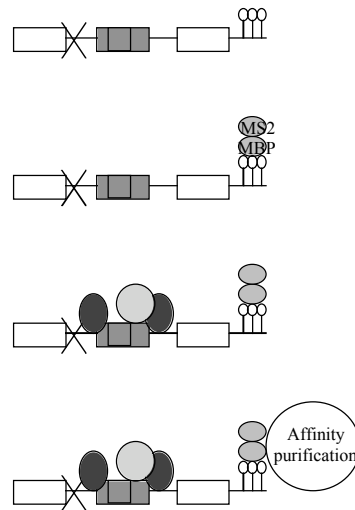
Modified from M. Jurica, 2002.

Figure 4-5. Purification scheme for isolation and enrichment of the stalled AEC intermediate complex. MSΔE3 and alt-MSΔE3 minigenes were generated based on the WTΔE3 and alt-ESSΔE3 minigenes, respectively, containing three copies of the MS2 viral coat protein binding site at the 3' end of the RNA. ^{32}P-labeled RNA is pre-bound to the MS2-MBP fusion protein before incubating with JSL1 nuclear extract to allow spliceosome assembly. Following complex formation, the assembly reactions are passed twice over an amylose resin column and washed extensively. Finally, spliceosome intermediate complexes are eluted from the column under native conditions using maltose. For proteomic analysis, samples are treated with RNase A and TCA. For structural analysis, samples are eluted in a smaller volume to improve the effective concentration of the sample.

using the MS2 protein fused to maltose binding protein (MS2-MBP) as an affinity tag. The MS2 protein binds with high affinity to its cognate hairpin binding sites, and will also bind to amylose resin. The complex can then be eluted under native conditions by using maltose. A difference between our purification scheme and those used by other groups is the lack of a size exclusion step (Jurica, 2005; Jurica et al., 2002; Jurica et al., 2004)(S. Sharma, personal communication). Due to the large size of our pre-mRNA substrate, common methods such as size exclusion chromatography or glycerol gradient fractionation were not amenable for isolation our complex (data not shown). However, as discussed below, the purity of the isolated AEC complex was sufficient for preliminary analysis.

First, we generated a version of our WT pre-mRNA template containing three MS2 hairpin sites at the very 3' end of the substrate (MSΔE3). Importantly, neither splicing regulation (data not shown) or regulation of spliceosome assembly was altered by the insertion of the three MS2 binding sites (Figure 4-6A, - MS2-MBP). Further, the normal block in assembly was not affected by pre-binding of the MS2-MBP fusion protein to the MSΔE3 substrate prior to spliceosome assembly (Figure 4-6A, + MS2-MBP). Native gel electrophoresis of the final eluted spliceosome intermediate demonstrated that the isolated complex migrated at approximately the same position as the input suggesting that we had isolated the AEC (Figure 4-6B). Similar experiments were performed using MS2-tagged versions of the alt-ESSΔE3 and mESSΔE3 minigenes (alt-MSΔE3 and mESS-MSΔE3 respectively) and demonstrated the ability to isolate the canonical A complex on these de-repressed constructs in extract treated to inactivate tri-snRNP (data not shown). For all observed pre-mRNA substrates, it was estimated that final recovery of the spliceosome intermediate complex was upwards of 30%, similar to that reported by other groups (Sharma, S., personal communication). Silver stain analysis of protein samples from various points along the purification scheme confirmed our ability to recover reasonable amounts of material, roughly estimated around 200-500 ng of protein total (data not shown). To further confirm the identity of the purified complex, the presence of individual snRNAs was assayed by primer extension analysis. Complexes purified using the MSΔE3
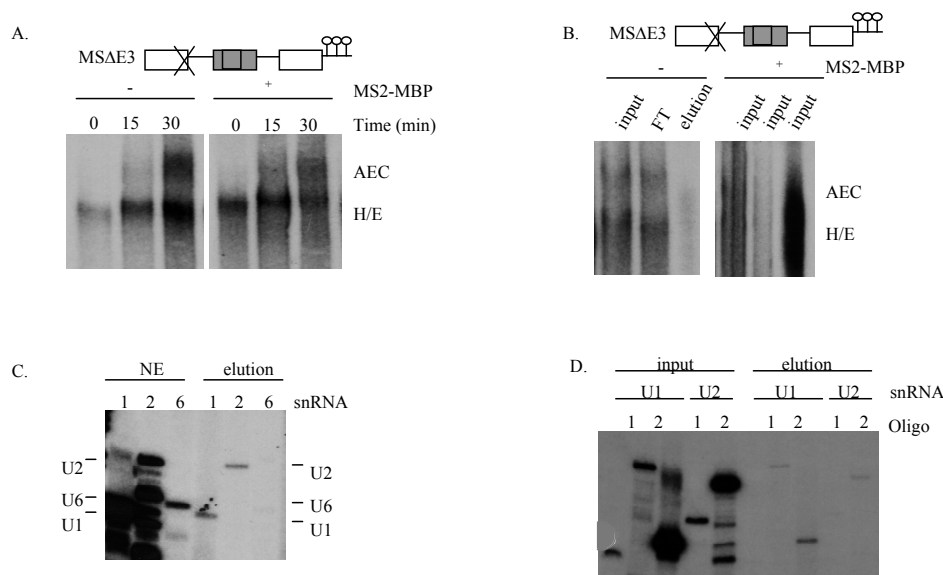
Figure 4-6. Initial biochemical and structural characterization of the purified stalled AEC. (**A**) The introduction of MS2 binding sites and association with the MS2-MBP fusion protein does not disrupt the ESS1-mediated stall in spliceosome assembly. MSΔE3 was incubated in JSL1 nuclear extract in the absence (-) or presence (+) of the MS2-MBP fusion protein, and in both conditions assembly was stalled at the AEC. (**B**) Co-migration of the purified AEC complex with input samples containing the AEC in standard spliceosome assembly reactions. Elution of spliceosome intermediate complexes requires pre-binding of the MS2-MBP fusion protein to the MSΔE3 RNA (- vs. +MS2-MBP). (**C**) Primer extension analysis of the spliceosomal snRNPs present in the purified spliceosome intermediate complex. ^{32}P-labeled oligonucleotides complementary to the U1, U2 and U6 snRNAs were used to identify the snRNA components in the purified sample and confirmed the isolation of a complex bearing the hallmarks of the stalled AEC (U1 and U2, but no U6). (**D**) Primer extension using a panel of oligonucleotides complementary to different regions within the U1 and U2 snRNAs. ^{32}P-labeled oligonucleotides were used to test the ability to detect signal when priming various regions within the snRNA sequence. Those amenable to this assay were then used to map features of the secondary structure of U1 and U2 (data not shown).

substrate contained both the U1 and the U2 snRNAs, but not the U6 snRNA, indicative of an AEC intermediate (Figure 4-6C). In contrast, samples that were isolated using the alt-MSΔE3 substrate incubated in tri-snRNP inactivated extracts contained only U1 and U2 snRNAs, while the U6 snRNA was detected in samples purified from untreated extract (data not shown). Taken together, the co-migration of the purified spliceosome intermediate with the AEC input sample

and the presence of both U1 and U2, but not U6, suggest the successful purification of the AEC intermediate.

Structural and proteomic analysis of the AEC

Initial studies suggested that the binding of hnRNP L to ESS1, as well as the aberrant association of the U1 and/or U2 snRNPs, were required for both the formation and hyper-stabilization of the AEC (Chapter 3)(House and Lynch, 2006). However, the purified sample of the AEC intermediate provides a much cleaner system in which to study the structural features of the stalled complex. As we were able to use primer extension to identify snRNA components present in the purified complexes (Figure 4-6C), it followed that primer extension would be a suitable approach to map higher order structure within snRNAs that might contribute to aberrant snRNP association with the pre-mRNA. Initial screening of a panel of oligonucleotides complementary to various regions within the U1 and the U2 snRNA sequences confirmed the ability to detect a signal (Figure 4-6D). Eluted intermediate spliceosome complexes were treated with psoralen, cross-links between the snRNA and the pre-mRNA were induced by UV light, and these contacts were mapped using primers directed against either the U1 or the U2 snRNA. However, no signal was detected for any of the cross-linked purified complex samples, suggesting that perhaps following additional treatment and RNA extraction the final signal is below the detectable threshold (data not shown).

Previous work demonstrated the altered accessibility of the wildtype versus mutant pre-mRNA substrates and suggested that perhaps the two distinct pre-spliceosome complexes differed in protein arrangement and/or protein composition (Figure 4-4). Toward this end, the protein composition of both the purified stalled complex was analyzed using mass spectrometry. Importantly, initial analysis identified core spliceosomal proteins, as well as several regulatory

Classification	Protein Name
hnRNP protein	hnRNPA2/B1
	hnRNP M
	hnRNP A0
	hnRNP 2H9B
	hnRNP A3
	hnRNP C1/C2
	hnRNP AB
	hnRNP H1
	hnRNP U
SR protein	Splicing factor, arginine/serine-rich 3 (SRp20)
	Splicing factor, arginine/serine-rich 1 (SF2/ASF)
	Transformer-2-beta isoform 3
	Splicing factor, arginine/serine-rich 7 (9G8)
Spliceosomal protein	Splicing coactivator subunit SRm300
Other proteins	Dead box, X isoform (DBX); DEAD box protein 3 (DDX3X); Helicase-like protein 2 (HLP-2)
	RNA binding motif protein 3
	KHSRP; FUSE binding protein 2
	SIAHBP1; PUF60
	ELAV-like 1; HuR
	Growth regulated nuclear 68 protein/DEAD box polypeptide 5
Unknown proteins	Hypothetical protein KIAA0670

Figure 4-7. Initial identification of the purified stalled AEC protein composition. Mass spectrometry analysis of proteins present in the stalled AEC intermediate. An eluted sample containing the purified stalled AEC, formed on the MSΔE3 substrate, was treated with RNase A and TCA, prior to submitting the sample in batch. Several spliceosomal proteins as well as hnRNP and SR proteins were identified.

hnRNPs and SR proteins. So then, the above result suggests that the purification method is amenable to this type of experimental approach, and that the final sample is likely the complex of interest (Figure 4-7). However, the canonical A complex intermediate formed on the MSE3 template under de-repressed conditions will also need to be submitted for mass spectrometry analysis.

Additionally, the differential recruitment of specific proteins to the purified complexes was analyzed by western blot. As the 3'ss PPT was previously identified as a region with a dramatic difference in accessibility between the AEC and the A complex (Figure 4-4), spliceosome factors known to associate with this region of the pre-mRNA at early stages in assembly, specifically SF-1 and U2AF65, were likely candidates for differential recruitment. However, earlier work also demonstrated the importance of both the ESS1 and the 5'ss, as well as the 3'ss, in the mechanism of repression (Chapter 3)(House and Lynch, 2006). As such, the presence of proteins known to associate with these
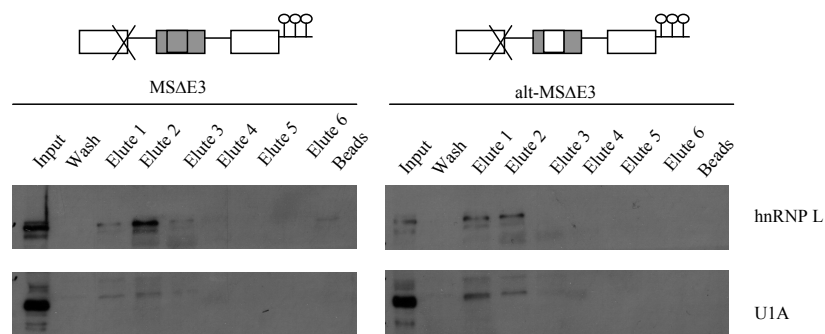
Figure 4-8. Initial proteomic characterization of the purified stalled AEC. Western blot analysis of several candidate proteins known to interact with the pre-mRNA at the 3'ss PPT or 5'ss during pre-spliceosome assembly. Purified stalled AEC (MSΔE3 or canonical A complex (alt-MSΔE3) were treated with RNase A and TCA, prior to resolving on denaturing SDS-PAGE gels. The presence of ESS-1 binding proteins, such as hnRNP L, was tested.

sequences, hnRNP L and U1A respectively, were also examined (data not shown). Western blot of both factors showed no apparent difference in the levels of protein present in the AEC versus the canonical A complex (Figure 4-8).

Finally, electron microscopy pilot experiments were attempted in order to gain insight into the overall structure of the stalled intermediate. Briefly, eluted AEC complexes were imaged on a thin carbon supports in negative stain. We were unable to confirm the presence of the AEC using this particular technique, suggesting that the sample was either not concentrated enough or that staining and imaging conditions were not ideal for this particular RNA complex (data not shown).

Discussion

The ESS-1 dependent splicing repression is mediated by the formation of the AEC intermediate thereby causing an efficient block in spliceosome assembly. The idea that the AEC might be hyper-stabilized originated from "commitment" spliceosome assembly assays, which demonstrated that if assembly was initiated under repressive conditions that the growing spliceosome could not recover and progress into a functional enzyme once repression was alleviated. The inability to chase the repressed AEC into a functional spliceosome by addition of excess ESS1 competitor suggests that perhaps hnRNP L, or other ESS1-binding proteins, are buried within the AEC preventing their removal. Alternatively, once the U1 and U2 snRNPs have been recruited to the

repressed exon perhaps they are positioned in such a way to prevent their rearranging into a functional complex. Certainly, the presence of aberrant contacts between the U1 snRNA and the pre-mRNA template suggest that the U1 snRNP is improperly recruited to or positioned at the 5'ss of the repressed exon (Figure 4-4A). However, the psoralen cross-linking analysis was limited by the lack of helical RNA structure between the U1 snRNA and the wildtype 5'ss sequence. As a result of weak base-pairing interactions, the ability of psoralen to induce RNA-RNA cross-links was compromised. Our attempts to partially restore base-pairing between U1 and the pre-mRNA ($WT_{C \to T} \Delta E3$) recovered the ability to detect the canonical U1 contact. While this was effective in improving psoralen function, the ultimate effect of this modification on splicing regulation is unclear as the inherent weakness of the 5'ss is critical for the mechanism of regulation (Chapter 3). Finally, failure to confirm that the cross-linked species present at the 5'ss within the AEC was due to binding of the U1 snRNA suggests that other regions of U1, aside from that known to directly bind the pre-mRNA 5'ss, may make abnormal contacts with the pre-mRNA within the stalled AEC and play a role in stabilizing the nonfunctional intermediate.

Previous work demonstrated that both the 5'ss and the 3'ss of exon 4 were required for regulation via AEC formation (Chapter 3)(House and Lynch, 2006), but the exact role of these regions in the underlying mechanism of repression remained unclear. By comparing the accessibility at the 5'ss or the 3'ss of pre-

mRNAs that either contained or lacked ESS1, we identified several differences in the overall arrangements of the AEC versus the canonical A complex. Overall, pre-mRNA packaged into the AEC was less accessible to RNase-mediated cleavage than templates assembled into the permissive A complex. This trend of increased protection of the RNA within the AEC is most evident when comparing accessibility within the 3'ss PPT, where this region is dramatically less accessible on the WT substrate compared to the alt-ESS substrate (Figure 4-5C). In particular, the clear difference in interactions occurring at the 3'ss PPT correlates with our previous studies demonstrating the absolute requirement for both the wildtype 3'ss sequence and U2 snRNP binding in order to assemble the AEC intermediate (Chapter 3)(House and Lynch, 2006). The inaccessibility of the PPT when packaged into the AEC suggests that perhaps a spliceosomal factor normally associated with the 3'ss during pre-spliceosome assembly such that it cannot be released from the growing spliceosome and assembly is stalled prior to tri-snRNP recruitment.

In order to better understand the mechanism of repression and the stall in assembly, we developed a purification scheme to isolate the AEC under native conditions. Once purified away from contaminating free snRNPs or other spliceosome complexes, characterization of both the protein and the RNA structure of the stalled complex were attempted. It should be noted that purified AEC preparations were contaminated with E complex (Figure 4-6B). However,

likely the repressive factors, such as hnRNP L, that are required for AEC formation are already bound to the pre-mRNA as early as E complex formation, suggesting that a mixed population of repressed pre-spliceosome complexes will not affect characterization. Identification of both the U1 and the U2 snRNAs, but not the U6 snRNA, from samples purified using the MSΔE3 template, suggested the isolation of the AEC (Figure 4-6C). While the input signal was sufficient to detect individual snRNAs, following psoralen and UV treatment the samples no signal indicating snRNA secondary structure was detected. However, this problem may easily be addressed by increasing the input into the purification reaction to enhance the final recovery providing a sufficient boost in material to assay using this experimental approach. The isolated complexes used for mapping the intramolecular snRNA contacts were purified under conditions using one third of the input material used by other groups in similar experiments (Sharma, S., personal communication). Alternatively, optimization of psoralen treatment and/or primer extension protocol may be required for each snRNA, as secondary structure will differ at distinct regions within the snRNA templates, and this is known to affect the ability of psoralen to induce RNA-RNA cross-links.

Importantly, proteomic analyses of the purified stalled complex, both by western blot and mass spectrometry, confirmed our ability to recover enough material to assay for possible altered protein recruitment and/or composition between the distinct intermediate complexes. However, mass spectrometry

analysis of spliceosome complexes performed by other groups using similar purification schemes typically identifies on the order of a hundred proteins, as opposed to our results of less than 30 factors, suggesting that while recovery is on the order of the total protein required for mass spectrometry, the overall yield must be improved for efficient analysis (Figure 4-7)(Behzadnia et al., 2007; Deckert et al., 2006).

While no obvious distinction in protein composition was detected by western, it is possible that the differences between the AEC and the A complex are subtle. That is, rather than the presence versus absence of a particular factor, the orientation of a protein with respect to the pre-mRNA might differ between the two complexes. Initially, the presence of hnRNP L in the permissive A complex purified samples was surprising; however, it seems likely that the association of hnRNP L is independent of regulatory sequence elements, like ESS1, as hnRNPs are known to non-specifically coat pre-mRNA transcripts. Further, U1A has been shown to bind PSF (Lutz et al., 1998), a known component of the ESS-1 protein complex under activated conditions (Melton et al., 2007). Perhaps then the orientation of U1A is altered in the AEC, due to binding PSF, thereby contributing to repression. Additionally, a number of additional factors beyond those we screened are known to associate with the pre-mRNA 3'ss region and influence assembly, including SAP155 and hSlu7 (Chua and Reed, 1999; Gozani et al., 1998), suggesting a potential role in regulating splicing by

mediating AEC formation. Further proteomic analysis of native complexes isolated by this purification method may yield critical insight into how the AEC forms and why once it has the pre-spliceosome cannot progress beyond this stage of assembly.

CHAPTER FIVE

Conclusion

While ESS1-dependent regulation of the signal-responsive alternative splicing of CD45 exon 4 is well documented, the mechanism by which this element functions to promote exon repression has been unclear. In Chapter 2, I report the development of an *in vitro* splicing system that faithfully recapitulates the splicing regulation seen *in vivo*. I have focused on understanding the mechanism of exon repression under resting conditions, as a critical first step toward an overall understanding of the relationship between basal and activated exon skipping. Using this *in vitro* system, I show that a complex of hnRNP proteins, namely hnRNP L, PTB and hnRNP E2, which specifically bind to the ESS1 element, act to promote exon repression (Rothrock et al., 2005). In particular, hnRNP L is the main functional component of the ESS1-associated protein complex (Rothrock et al., 2005).

In Chapter 3, I show that the ESS1 element and its cognate binding proteins, specifically hnRNP L, cause exon skipping by stalling spliceosome assembly at an unusual step. Formation of the stalled complex requires ATP as well as both the U1 and U2 snRNPs, suggestive of an A-like exon-defined complex (AEC) (Figure 5-1)(House and Lynch, 2006). This inhibition represents a novel mechanism of splicing regulation, and suggests that the formation of an

121
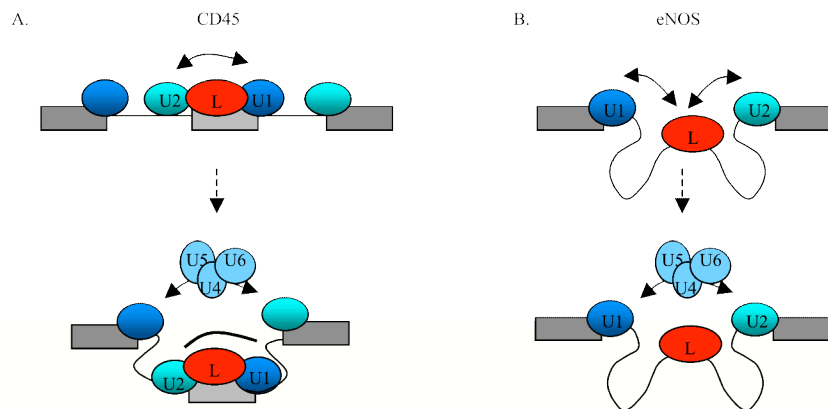
Figure 5-1. Mechanisms of hnRNP L mediated splicing regulation. (**A**) CD45 variable exon 4 contains the ESS1 silencer, that when bound by hnRNP L results in exon repression via the formation of a U1, U2 and ATP-dependent exon recognition complex (AEC). The simplest model for the activity of hnRNP L is that it interacts with the adjacent U1 and U2 snRNPs, holding them in an aberrant and hyper-stabilized conformation, thus preventing cross-intron pairing with the spliceosome components required for tri-snRNP recruitment. (**B**) Binding of hnRNP L to a CA-rich element within an intron of the eNOS transcript promotes intron removal and exon ligation. In this context, hnRNP L would be predicted to facilitate cross-intron pairing of the U1 and U2 snRNPs thereby promoting formation of a canonical A complex that proceeds efficiently to the catalytic complex.

AEC intermediate is an important transition along the spliceosome assembly pathway. In Chapter 4, I present preliminary data regarding the structure and proteomic characterization of the stalled AEC intermediate. These initial studies suggest that altered RNA-RNA and/or RNA-protein contacts within the AEC contribute to hyper-stabilization and the resultant exon repression. As the AEC intermediate occurs at a very poorly understood point in spliceosome assembly, characterization of the stalled complex will provide valuable insight into fundamental processes of the splicing reaction.

Implications of mechanistic diversity

The spliceosome itself is highly dynamic and flexible, assembling *de novo* on each substrate. It follows, then, that both the assembly and activity of this

machine can be modulated to achieve the differential splicing patterns within a single gene. Importantly, the recognition of the intron substrate by spliceosome components, and assembly of these components to form a catalytic spliceosome, occurs through a network of highly combinatorial molecular interactions. As previously discussed, many, if not all, of these interactions are subject to regulation (see Chapter 1), suggesting the potential for regulation at any number of as yet unidentified transitions required for building a spliceosome. It should also be noted that, additional issues such as speed of transcriptional elongation and co-transcriptional recruitment of splicing factors have also been shown to influence the kinetics of spliceosome assembly and thus splice site choice (Bentley, 2005; Kornblihtt, 2006).

Given the extreme diversity of regulatory mechanisms one might wonder why nature has bothered to develop so many different routes to the same ultimate goal of controlling exon inclusion. One possibility is that the most efficient mechanism for the regulation of any given gene is dependent on the specific rate-limiting step in spliceosome assembly and catalysis for that particular gene. Recent global analyses of splicing have shown that knock-down of proteins thought to be core components of the spliceosome results in the expected large defects in splicing of some genes, but has little to no effect on the splicing of other substrates (Clark et al., 2002; Park et al., 2004; Pleiss et al., 2007). The interpretation of these results is that pre-mRNA substrates differ in their requirement for even central

spliceosomal proteins due to redundancy of splicing signals or differences in affinity of substrate-spliceosome interactions. Therefore, by analogy, it is predicted that exons differ widely in their susceptibility to modulation of exon definition, exon pairing or catalysis. In particular, those exons that need to be included under most conditions are likely to have particularly strong splice sites (i.e. high affinity for U2AF or snRNPs), such that only later steps in assembly are available for regulation. Moreover, exonic sequences have to conform to coding constraints, while introns often harbor transcription regulatory sequences or small non-coding RNAs. Thus, sequences that determine alternative splicing regulation are not unlimited in their location and identity, but rather have to accommodate other evolutionary constraints.

Mechanisms to balance splicing fidelity and splicing regulation

Overall, the spliceosome assembly process can be viewed as a series of checkpoints that allows the splicing machinery to sample different choices and then adjust splicing decisions according to the local dictates and cellular requirements. Already a two-state model, similar to that for ribosomal decoding, is widely accepted as explaining how the spliceosome uses one active site to accommodate the two distinct transesterification reactions (Konarska and Query, 2005; Moore and Sharp, 1993; Steitz and Steitz, 1993). Moreover, modulation of the equilibrium between the two states may explain how inherent properties of the pre-mRNA template or outside regulatory factors can affect splicing fidelity.

Further, a kinetic proofreading model was proposed to explain progress of a pre-mRNA template through the splicing reaction (Burgess and Guthrie, 1993a, b).

Both of these models were proposed based on studies that examined splicing catalysis. However, a proofreading model might also be applied to explain the balance between splicing fidelity and splicing regulation during the process of spliceosome assembly. In the case of CD45 exon 4, formation of the AEC, as opposed to the canonical A complex, is required for splicing regulation. Analysis of variable exon 4 splicing in the context of a minigene shows that the exon is skipped in roughly 50% of total splice product generated under resting conditions, suggesting that the decision to commit to a stalled AEC or form a permissive A complex is a balance of positive and negative factors. Following activation, exon 4 is now skipped in upwards of 80% of the splice product, suggesting a shift in the equilibrium driven by factors that promote repression. Taken together, the flexibility and control of spliceosome assembly, rather than being just a property of assembling such a large machine, may ultimately provide for the extent of alternative splicing that is now recognized to be so pervasive in complex organisms.

Future experiments

While I have identified both the function and the mechanism of ESS1 binding proteins in mediating CD45 exon 4 splicing repression, many questions

remain regarding the nature of the stalled AEC intermediate complex. First, further evaluation of the AEC should be performed to identify the specific mechanisms allowing for hyper-stabilization of the complex. This information may provide valuable insight into both the AEC-mediate splicing regulation of CD45 exon 4, but also poorly understood processes such as tri-snRNP recruitment and exon pairing. While initial studies identified aberrant RNA-RNA contacts using psoralen cross-linking, there are limitations this type of analysis when using psoralen as a modifying reagent that can be circumvented by employing other experimental approaches. For example, hydroxyl-radical probing has been successfully employed to identify the spatial organization in early spliceosome complexes by mapping the localization of U2 relative to U1 and the pre-mRNA (Donmez et al., 2007). While this technique requires the synthesis of chemically-modified snRNA components, a similar approach, known as selective 2' hydroxyl acylation analyzed by primer extension (SHAPE), also provides insight into RNA secondary structure without needing to generate synthetic RNA templates (Wilkinson et al., 2006). Preliminary experiments were performed using SHAPE to study the structure of the U1 and U2 snRNAs within the purified AEC (data not shown). With improved purification yield of the spliceosome intermediates, SHAPE analysis is likely to provide valuable information regarding changes in snRNA secondary structure that may occur between the canonical A complex and the repressed AEC.

As mentioned previously, further characterization of the spliceosome intermediates is likely to require an improved overall yield in the purified complexes. While scaling up the total input did improve the final yield, there are additional steps that may be included in the current purification scheme to improve recovery. Glycerol gradient centrifugation has been successfully employed by a number of different groups in the study of spliceosome structure and composition. Experiments were performed using glycerol gradients to isolate the stalled AEC from E complex (data not shown); however, gradients were never utilized as a purification tool for isolating the AEC away from free snRNPs, unbound MS2-MBP, etc. Perhaps the use of glycerol gradient centrifugation following spliceosome assembly, and prior to applying the sample to the amylose column, might serve to improve overall isolation of the AEC. Alternatively, an affinity step in the purification scheme might also improve recovery. One attractive approach is to utilize one of our existing cell lines, which expresses a myc-tagged version of hnRNP L. Some fraction of the stalled AEC intermediate formed under spliceosome assembly conditions in nuclear extract from this cell line would contain myc-tagged hnRNP L protein, and these complexes could then be isolated by a immuno-purification step using an anti-myc antibody.

In addition, while hnRNP L is the main functional component mediating ESS1-dependent exon silencing, it was shown that other hnRNPs can also bind the variable exon and perhaps repress inclusion. As such, these additional

hnRNPs may provide critical protein-protein and/or protein-RNA contacts that function to promote exon skipping by contributing to hyper-stabilization of the AEC. For example, hnRNP E2 was shown to repress exon inclusion, although in an ESS1-independent manner (Rothrock et al., 2005). Interesting, the addition of hnRNP E2 augmented the inhibition of spliceosome assembly, suggesting that hnRNP E2 may play an important role in stabilizing the AEC, but perhaps requires hnRNP L to direct specificity (House and Lynch, 2006). Analysis of hnRNP E2 function *in vivo*, using knockdown and over-expression studies, may improve our understanding of its role in regulation.

Additionally, hnRNP K has been shown to bind to the ESS1 element under both basal and activated conditions (Melton et al., 2007). HnRNP K is a unique hnRNP family member, as it doesn't contain the canonical RRM RNA binding motif, but rather a KH domain. Strikingly, preliminary data using morpholino knockdown of hnRNP K protein levels in JSL1 cells show an increase in exon inclusion, suggesting that it may function to repress splicing (L. Motta-Mena and K.W. Lynch, UTSWMC). Further, hnRNP K is estimated to be 56 kD, approximately the size of the protein that binds and represses exon 4 splicing under conditions where hnRNP L is limiting (Figure 2-6). So then, one model is that hnRNP K may function in a redundant pathway to ensure the proper regulation of CD45 splicing.

Alternatively, given the difference between hnRNP L and hnRNP K in domain structure, perhaps hnRNP K functions independent of hnRNP L, and is a critical component of the wildtype ESS1 silencing complex. Work by another group has shown that hnRNP K binds to an ISE, and that U1 snRNP binding under these conditions correlates with intron removal (Expert-Bezancon et al., 2002). By analogy to hnRNP L, perhaps hnRNP K functions in a position-dependent manner, such that in binding an ISE within β-tropomyosin it promotes splicing of exon 6A via canonical U1 recruitment, whereas binding within CD45 exon 4 results in aberrant U1 recruitment and exon repression. While the exact role of hnRNP K remains unclear, further analysis using the *in vitro* splicing system may provide additional insight into its function.

My work has predominately focused on the mechanism of splicing regulation under resting conditions. Initial experiments have already shown that the mechanism responsible for increased exon repression upon activation appears to be similar, suggesting a model in which the same transition in spliceosome assembly is inhibited, but with increased strength allowing for the increase in exon skipping. Further analysis of the stalled AEC intermediate that forms under activated conditions may offer insight into the exact mechanisms providing for the increase in splicing repression. It is known that PSF binds to the ESS1 element following activation thereby enhancing exon skipping (Melton et al., 2007). Additionally, work by other groups has shown that PSF can exist in

complexes with core splicing machinery, suggesting a possible role for this in mediating spliceosome assembly (Kameoka et al., 2004; Peng et al., 2002; Peng et al., 2006). Perhaps then, the recruitment of PSF to the ESS1 hnRNP complex results in additional protein-protein and/or protein-RNA interactions that in this context ultimately result in the exaggerated hyper-stabilization of the stalled AEC complex. Taking advantage of the current purification scheme, biochemical and proteomic characterization of the isolated AEC intermediate from stimulated JSL1 NE, similar to that done for the AEC formed under resting conditions, should provide information as to why the stalled complex that forms under activated conditions generates a more effective block in assembly and splicing.

Conclusion

In conclusion, I show that the signal-responsive alternative splicing regulation of CD45 exon 4 can be recapitulated *in vitro* using nuclear extract from JSL1 cells under resting and activated conditions. This in vitro system provided the framework to demonstrate the function of the ESS1 binding proteins, particularly hnRNP L, in mediating splicing regulation, and to identify that the mechanism of exon repression occurs via AEC formation. Future characterization of the stalled AEC intermediate will provide insight into both the mechanism of CD45 splicing regulation, as well as fundamental splicing processes.

CHAPTER SIX

Materials and Methods

Plasmids and RNAs.

The Glo minigene was engineered from the three exon Dup175 construct (Xie and Black, 2001) as described previously (Rothrock et al., 2005). The Glo-ESS, Glo-mESS, pSPT7-ESS, pSPT7-mESS and pSPT7-E14 minigenes were engineered as described previously (Rothrock et al., 2005). The WT, mESS1 and alt-ESS pre-mRNAs used for *in vitro* splicing were generated from the CD1 and CD14 minigenes (Rothrock et al., 2003) as previously described (Rothrock et al., 2005). PCR mutagenesis was used to introduce point mutations into specific splice sites in order to generate the minigene constructs used for both spliceosome assembly and splicing analysis. Minigenes in which the U1 binding site of exon 3 was inactivated (designated ΔE3) contain mutations altering the wildtype 5' splice site from CTG/GTAAGA to CTA/TCAATA. Minigenes in which the U2 binding site of exon 7 was inactivated (designated ΔE7) contain mutations altering the wildtype 3' splice site branch point sequence from AAT…ACGAATTAA to AGT… GCGAGTT AG. ΔE3E7 contains both the 5' splice site exon 3 and the 3' splice site exon 7 mutations within the same minigene. Minigenes in which the U1 binding site of exon 4 was inactivated (designated Δ5') contain mutations altering the wildtype 5' splice site from CAG/GTTGG to CAA/TCTTG.

Minigenes in which the U2 binding site of exon 4 was inactivated (designated ΔBPS) contain mutations altering the wildtype 3' splice site branch point from GATTCACATATTTAT to GGTTCGCGTGTTTGT. All CD45 three exon minigenes were *in vitro* transcribed using T7 RNA polymerase (Promega) as previously described (Rothrock et al., 2005). The single-intron constructs (E34 and E47) were *in vitro* transcribed using SP6 RNA polymerase (Promega). E34 was linearized such that transcription stops at the end of exon 4 resulting in no 5' splice site. E47 was constructed such that transcription begins 5 nucleotides into the start of exon 4 resulting in no 3' splice site.

Biotinylated ESS, mESS and E14 RNAs for affinity purification were chemically synthesized by Dharmacon. The biotinylated CA-dinucleotide RNA (CA_{20}) oligonucleotide consists of 20 CA-dinucleotide repeats and was chemically synthesized by Dharmacon.

RT-PCR assay.

RT-PCR and analysis of minigenes expressed *in vivo* were done as described previously (Rothrock et al., 2003).

In vitro **Splicing.**

Approximately 1 fmol of unlabeled RNA substrate was incubated in JSL1 nuclear extract under splicing conditions as follows (final concentrations): 30% JSL1 nuclear extract, 3.2 mM $MgCl_2$, 20 mM CP, 1mM ATP, 3% PVA, 1 mM DTT, 0.25 units RNasin (Promega), 90 mM KCl, 10 mM Tris pH 7.5, 0.1 mM

EDTA, 7% glycerol, and other proteins as indicated in the figures. Under de-repressed conditions, 5 pmol of exogenous ESS1 competitor RNA (Dharmacon) was added to splicing reactions. For competition studies, the indicated amount of CA_{20}, ESS, mESS, E14 or antibody was added to the splicing reactions immediately prior to addition of unlabeled substrate. Reactions were incubated for 2 hours at 30°C. The RNA was then recovered from the reactions by proteinase K (Roche) treatment, phenol-chloroform extraction and ethanol precipitation. The 'three-exon' CD45 constructs were assayed using the primers within CD45 exon 3 and exon 7, respectively:

> T7Mlu: 5' – GGGAGCTTGGTACCACGCGTCGACC - 3'

> E7R1: 5' - CAGCGCTTCCAGAAGGGCTCAGAGTGG - 3'

The 'single-intron' constructs E34 and E47 were assayed by RT-PCR using primers as described:

> pGEMmlu-F: 5' - GAATACTCAAGCTATGCATCCAACGC - 3'

> 34-R: 5' - TATCGATCTAGCATTATCCAAAGAGTCC - 3'

> 47-R: 5' - TATCGATAAGCTTGGATCTGT CGACG - 3'

RNA Affinity Purification.

Analysis of proteins bound to ESS1, mESS, and E14 (non-specific) RNAs was performed by C.R.R. as described in (Rothrock et al., 2005).

Analysis of proteins associated with the CA-dinucleotide sequence was performed by A.E.H. Approximately 40 µl of streptavadin agarose beads was

incubated with 1nmol/µl of 5' biotin labeled CA oligonucleotide with 200 µl GFB100 added to increase mixing volume. Reactions were incubated end-over-end for 5 hours at 4ºC. Then 150 µl of JSL1 NE was added to the CA$_{20}$-coupled beads and the reaction incubated end-over-end for 1 hour at 30ºC. The nuclear extract was then transferred to a new tube with another 40 µl of CA$_{20}$-coupled beads and incubated end-over-end for another hour at 30ºC. Total KCl concentration was brought to 600 mM with 2 M KCl. Reaction was incubated for 20 minutes at 4ºC. Supernatant was pulled and dialyzed against BC100 with 1mM DTT overnight at 4ºC (Pierce Mini-Dialysis units). Proteomic analysis was performed by either western blot (4D11, anti-hnRNP L) or by silver stain (BioRad kit).

UV Cross-linking.

Analysis of hnRNP L, PTB, and hnRNP E2 binding to wildtype of mutant versions of ESS1 was performed by C.R.R. as described in (Rothrock et al., 2005).

Analysis of hnRNP L binding under normal and depleted conditions was performed by A.E.H. JSL1 NE or purified recombinant hnRNP L was incubated with ^{32}P-labeled RNA (1 x 10^4 cpm/µl) under conditions as described in (Rothrock et al., 2005). Reactions were incubated at 30°C for 20 minutes, cross-linked using UV light (254 nm) for 20 minutes on ice, and digested with RNase T1 and RNase A (final concentration of 2 µg) for 20 minutes at 37°C. Reactions

were resuspended in 2X SDS loading buffer, denatured for 5 minutes at 95°C, analyzed under denaturing conditions on a 12% gel (Acrylamide/Bis 37.5:1, BioRad), and detected by autoradiography.

Western Blotting and Antibodies.

Western blotting was done as previously described (Lynch and Weiss, 2000). The antibodies for western blot analysis and splicing inhibition are as follows: anti-hnRNP L (4D11, Abcam), anti-PTB (anti-PTB 1758, kind gift of Dough Black), anti-hnRNP A1 (ImmuQuest), anti-U2AF65 (828, kind gift of Tom Maniatis), anti-SF1 (kind gift of Robin Reed), anti-U1A (kind gift of Mattgij), and anti-U2AF35 (827, kind gift of Tom Maniatis).

Recombinant proteins.

HnRNP L and PTB cDNAs were cloned into pFastBac (Invitrogen) and modified with an N-terminal GST tag. Expression plasmids were transformed into DH10Bac (Invitrogen) to generate recombinant bacmids, which were then transfected into SF9 cells using cellfectin (Invitrogen). Viral stocks were harvested, amplified and then used to infect SF9 cells for 60 hours to generate recombinant proteins. SF9 cells containing GST-hnRNP L or GST-PTB were lysed by repeated freeze-thaw cycles and recombinant proteins were purified with glutathione sepharose 4B resin (Amersham Biosciences) according to the manufacture's protocol.

Recombinant hnRNP E2 was expressed as a MBP fusion protein in E. coli. The expression plasmid pMALc2-PCBP2 was a kind gift of R. Andino and MBP-hnRNP E2 was expressed and purified as described previously (Gamarnik and Andino, 1997).

Recombinant MS2-MBP was expressed in E. coli. The expression plasmid was a kind gift of Josep Vilardell. MS2-MBP was expressed and purified as described previously (Jurica, 2005).

RNAi.

3×10^5 293 cells were plated in each well of a 6 well plate in 2 mls of high glucose DMEM. 24 hours after seeding, the cells were transfected with 5 ml Lipofectamine 2000 (Invitrogen), 0.5 mg WT or ΔESS minigene and 3 ml of a 200mM stock of either GFP duplex siRNA (Dharmacon) or the SMARTpool of siRNAs against hnRNP L (Dharmacon). 12 hours after transfection the lipid complexes were removed and replaced with fresh media. Cells were harvested for analysis of protein and RNA 48-60 hours after transfection.

Spliceosome Assembly.

Approximately 1 fmol of gel-purified uniformly ^{32}P-labeled RNA probe (1×10^5 cpm/μl) was incubated in JSL1 NE under splicing conditions in the absence or presence of exogenous competitor RNA (Dharmacon). For ATP-depleted reactions, ATP was depleted from nuclear extract by incubating at 25°C for 1 hr. RNase H inactivated extract was used in place of untreated nuclear extract to test

requirement for snRNPs in assembly (see below); however, all other reaction conditions were identical. Spliceosome complexes were analyzed using native polyacrylamide gel electrophoresis as described in (Konarska and Sharp, 1986) except that gels were run at 250 V/4 W for 7 hours to compensate for the large size of our pre-mRNA templates.

snRNA Inactivation.

For RNase H reactions, nuclear extract was incubated in a reaction containing (final concentrations): 30% JSL1 NE, 0.8 mM ATP, 20 mM CP, 4.4 mM $MgCl_2$, 30 units RNasin (Promega), 1 unit RNase H (Roche), 90 mM KCl in the presence or absence of 5 pmol oligonucleotide that is complementary to the target snRNA. The following oligonucleotides were used to target inactivation of the indicated snRNA: U1 and U2 were inactivated by 5'C and E15 respectively (Black et al., 1985), while U6f was used to inactivate U6 (Konforti and Konarska, 1994). Reactions were incubated at 30°C for 1 hour and RNA was extracted from 10 μl of the reaction for analysis by primer extension to determine the specificity and amount of inactivation (see below).

Primer Extension.

Primer extension analysis of snRNAs were performed using the RT steps from the RT-PCR assay (see above), except that a mixture of ^{32}P-radiolabeled primers each specific to an individual snRNA and at a final concentration of 1.5

ng/µl was used. Primers complementary to the 64-86 nt region of U1, 100-122 nt region of U2, the 33-58 nt region of U6, and the 55-75 nt region of U5 were used for extension. Products were analyzed on a denaturing 10% polyacrylamide gel and quantification done using a Typhoon Phosphoimager (Amersham Biosciences).

Primer extension mapping of psoralen cross-linking was performed as described above. Primers for mapping U1 contacts at the 5' splice site are as follows:

E45'ss-R1: 5' - CTGTAGAATTTTCTAAATGACATTCC - 3'

E45'ss-R2: 5' - GACAAGTTGTACTGATAACTGTAG - 3'

E45'ss-R3: 5' - CACATACTTAGAAACTGTGC - 3'

E4-5'ss-R: 5' - GAATTTTCTAAATGACATTTGG - 3'

E35'ss-R: 5' - GTAGTTAAATATATA AACTTTGCAACAAG - 3'

E4-5'ssR: 5' - GAATTTTCTAAATGACATTCCC - 3'

E4-5'ssR1: 5' - CTGTAGAATTTTCTAAATGACATTCC - 3'

Primer extension mapping of snRNA secondary structure within native spliceosome complexes was performed as described above, except that reaction volume size was doubled to compensate for diluted signal in the eluted spliceosome samples. Primers complementary to the designated nt region of each snRNA are as follows:

U1 64-75: 5' - CCGGAGTGCAAT - 3'

U1A 79-98: 5' - CCACTACCACAAATTATGC - 3'

U1 (I): 5' - CCTTCGTGATCA - 3'

U1 (III): 5' - CCCACATTTGG - 3'

U1 (IV): 5' - GGAAAGCGCGAACG - 3'

U2 79-98: 5' - CCATTTAATATATTGTCCTC - 3'

U2 (BPBS): 5' - GATAAGAACAG - 3'

U2 (IIb): 5' - GGATAGAGGACG - 3'

U2 (IV): 5' - GGAGGTACTGCAAT - 3'

U5 84-104: 5' - GGCAAGGCTCAAAAAATTGGGTTA - 3'

U6 90-104: 5'-AATATGGAACGCTTC-3'

Purification of Spliceosome Complexes.

Approximately 10 nM of ^{32}P-radiolabeled MS2 aptamer-tagged pre-mRNA template was pre-bound to 100 nM MS2-MBP fusion protein and then incubated in JSL1 or HeLa NE under spliceosome assembly conditions (see above), except as follows (final concentrations): 60% NE, 3.2 mM MgCl$_2$, 1 mM ATP, 20 mM CP, 0.25 units RNasin (Promega). Assembly reactions were carried out in a final volume of 500 μl, and typically six reactions were used per purification. After assembly, reactions were passed twice over a 1 ml amylose column. The column was washed with 20 column volumes of GFB100.

Spliceosome complexes were eluted with 30 mM maltose in GFB100 using 250 μl per elution sample.

Glycerol Gradients.

Spliceosome intermediate complexes were resolved on approximately 11 ml glycerol gradients (15-35%). Gradients were poured manually starting with the addition of 1.2 ml of the 35% glycerol stock to the very bottom of the tube (Beckman, ultra-clear) and then placing the tube at −80ºC until the surface was frozen, then repeating the process with each of the remaining stocks. Samples were layered on the surface of the gradient immediately prior to centrifugation. Gradients were spun at 29,000 rpm for 12 to 16 hours at 4ºC in a Beckman ultracentrifuge using the SW41 rotor. Fractions of 500 μl volume were collected starting at the top of the gradient. RNA was isolated by PCA extraction and ethanol precipitation. Migration of the sample was analyzed by tracking the ^{32}P-labeled pre-mRNA template in each collected fraction using polyacrylamide gel electrophoresis and autoradiography. U1, U2 and U6 snRNA levels indicative of distinct spliceosome intermediates was assayed by primer extension as described above. Spliceosome complexes from collected fractions were resolved by native gel analysis as described above.

Psoralen Cross-linking.

Approximately 100 fmol of capped, unlabeled RNA was incubated in JSL1 nuclear extract under splicing conditions, as previously described, except

reactions were 50 μl total volume and contained 60% NE. Samples were incubated at 30ºC, to allow for spliceosome assembly, and heparin treated (2 mg/ml final). Samples were placed on ice and psoralen (20 μg/mg final) was added. Samples were exposed to long wave (365 nm) UV light for 20 minutes while kept on ice. Following cross-linking, samples were treated with proteinase K (Roche), and RNA was isolated as previously described. Primer extension was used to map RNA-RNA cross-links (see above).

RNase H Protection assay.

^{32}P-labeled RNA probe (1 x 10^5 cpm/μl) was incubated in JSL nuclear extract under splicing conditions as described above. After incubation at 30ºC to allow for spliceosome assembly and minimal heparin treatment (2 mg/ml final), oligonucleotides complementary to sequences within the 5'ss or the 3'ss of exon 4 were added at the indicated concentrations. Samples were incubated at 30ºC for 15 minutes to allow endogenous RNase H-mediated cleavage. Addition of 1μl of exogenous RNase H (Roche) did not affect the cleavage efficiency; data presented herein relied on endogenous RNase H activity. Reactions were then proteinase K treated, and RNA was collected as previously described. RNA samples were resolved on a denaturing 5% polyacrylamide gel, and cleavage was assayed using phosphorimaging.

Mass Spectrometry.

Mass spectrometry was performed by the Protein technology Core at UT Southwestern Medical Center by digesting proteins in solution with procine trypsin. Tryptic peptides were dissolved and injected into reverse-phase HPLC/ion trap with a nanospray source, using a ThermoFinnigan LCQ Deca XP MS instrument and Xcalibur 1.3 software. MS/MS files were searched against NCBI-nr protein sequence databases, using Sonar database software (GenomicSolutions, Inc.).

APPENDIX A

In Vitro Splicing and RT-PCR

30% NE, 90 mM KCl are the standard conditions for JSL1 splicing system. Reactions are at a total volume of 12.5 μl.

Per reaction:
2.75 μl GFB100
 0.5 μl 80 mM MgCl$_2$, 0.5 M CP, 25 mM ATP
 0.5 μl BC850
 3.0 μl 13% PVA
 0.5 μl RNasin mix (.25 ddH$_2$0, 0.12 RNasin, 1 unit/μl, 0.12 DTT)
3.75 μl NE
 0.5 μl template RNA (1fmol/μl)

Incubate at 30°C for 2 hours. Add 175 μl proteinase K (PK) treatment mix, flick tubes several times to mix well and incubate for 15 minutes at 30°C.

PK treatment per reaction = 100 μl 2x PK buffer (see below), 71 μl ddH$_2$0, 2.5 μl proteinase K (@20mg/ml, activity 30 units/μl, see Roche), 1.5 μl glycogen.

Reactions can be placed on dry ice following PK treatment. PCA alcohol extract, ethanol precipitate and 70% ethanol wash. Resuspend the pellet in 10 μl ddH$_2$0. Store at -80°C, or continue on with the RT-PCR analysis.

Competition splicing assay

Per reaction:
2.25 μl GFB100
 0.5 μl 80 mM MgCl$_2$, 0.5 M CP, 25 mM ATP
 0.5 μl BC850
 3.0 μl PVA
 0.5 μl RNasin mix
3.75 μl NE
 0.5 μl competitor RNA
 0.5 μl template RNA (1 fmol/μl)

Order of addition is critical for successful and reproducible results. Always the NE first, then competitor RNA and finally pre-mRNA template.

Functional splicing assay
<u>Per reaction:</u>
0.75 μl GFB100
 0.5 μl 80 mM MgCl$_2$, 0.5 M CP, 25 mM ATP
 0.5 μl BC850
 3.0 μl PVA
 0.5 μl RNasin mix
3.75 μl NE
 2.0 μl protein
 0.5 μl template RNA (1 fmol/μl)

Again, order of addition is critical and is detailed in the per reaction mixture above. Due to variation between extract preps, the ability to see a change in splicing pattern requires NE in which exon inclusion is above 1-2%.

Functional splicing assay: competition background
<u>Per reaction:</u>
0.25 μl GFB100
 0.5 μl 80 mM MgCl$_2$, 0.5 M CP, 25 mM ATP
 0.5 μl BC850
2.75 μl PVA
 0.5 μl RNasin mix
3.75 μl NE
 0.5 μl competitor RNA
 2.0 μl protein
 0.5 μl template RNA (1 fmol/μl)

Order of addition is important to see derepression and subsequent re-repression by addition of hnRNP L. Addition of 5000 molar excess competitor ESS sequence per reaction (hand-transcribed RNA) results in 3 exon product change from 1-2% to 12-15%, which is still in the range to see re-repression upon addition of purified L. Although, the level of competitor will likely need to be optimized for each new NE batch and new purified hnRNP L batch.

RT-PCR Assay for *in vitro* splicing reactions

RT: 1 μl 5xHYB
    1 μl E7R1 (1ng/μl)

    Aliquot 2 μl per reaction and add 2 μl of *in vitro* splicing reaction.

RT-POL: 19.5 μl 1.25 x RT-PCR mix + dNTPs, pre-warmed to 43°C
      0.5 μl MMLV RT

    Add 20 μl of mix per reaction.

PCR: 1 μl E7R1 (5ng/μl)
    1 μl T7Mlu (2.5 ng/μl)
    1 μl ^{32}P-T7Mlu
   1.5 μl RT-PCR buffer
   0.2 μl Taq
  10.3 μl ddH$_2$0

Aliquot 15 μl of PCR mix into tubes. Add 5 μl from above RT/RT-POL steps.
    PCR program "Amy": 94°C 2 minutes
                  94°C 1 minute
                  65°C 1 minute
                  72°C 1.5 minutes
                  72°C 5 minutes, cycle 25 times
                   4°C hold

Add 15 μl formamide buffer to reactions. Store at -80°C or run out samples on a 5% PAG at 1200 V/30 mA for 30-35 minutes.

Expected splice products from CD2 template RNA with T7Mlu, E7R1:
    3 exon/347 = 368 bp
    2 exon/37　= 163 bp

Buffers (may be kept at room temperature or 4°C)

GFBx	BCx	2x PK buffer
20 mM Tris pH 7.5	20 mM Tris pH7.5	200 mM Tris pH7.5
0.2 mM EDTA	0.2 mM EDTA	25 mM EDTA
x mM KCl	x mM KCl	300 mM NaCl
	20% glycerol	2% SDS

APPENDIX B

Polyacrylamide Spliceosome Assembly Gel

This experiment can be done -/+ ESS competitor, -/+ PMA NE, etc. as determined by set up of splicing reaction. ATP-dependence analyzed by using NE that is ATP-depleted by incubation at room temp for 30-60 minutes (omit CP, ATP from splicing reaction in that condition).

1. Set up splicing reaction with ^{32}P-radiolabeled template RNA (1 x 10^5 cpm/μl).
    -   Make fresh each week as radiolysis of probe causes smeary lanes on gel.
    -   Also, probe made MUCH hotter than 1 x 10^5 cpm/μl and diluted back is not as clean, so I half the recipe for transcribing hot probe.

2. Immediately following addition of probe, incubate reactions at 30°C. Take a 0 minute time point prior to placing tubes at 30°C. Pull a 15 μl aliquot of the reaction, place and keep on ice. Add heparin to a final concentration of 5 ug/μl.

3. Pull 15 μl aliquots from reaction at time points of interest. Typically I look at 5, 15, 30 and 45 minutes following 30°C incubation. Transfer time point samples into a fresh eppendorf with heparin at a final concentration of 5 μg/μl. Keep all samples on ice until the final time point is taken.

4. Incubate all aliquots with heparin at 30°C for 5 minutes EXCEPT 0 minute time point which remains on ice until loaded on gel. Addition of heparin causes dissociation of H/E complex.

5. Load entire reaction directly onto spliceosome assembly gel without loading dye. Gel should be pre-run for 15 minutes at 250 V.

6. Run gel 7 hours at 250 V/4 W. Transfer to Whatman paper and dry at 80°C for 1-1.5 hours.

7. Image by autoradiography. Expose to BioMax film with intensifying screen for 30 minutes to 1 hour at -80°C, or overnight exposure on

BioMax without screen. Typically, images are crisper when an intensifying screen is NOT used.

Pouring Assembly Gel: 4% Acrylamide (80:1 bis-Acrylamide)

Mix in 250 ml flask:
- 6 ml 40% Acrylamide (80:1)
- 6 ml 10x Tris-Gly buffer
- 48 ml ddH$_2$O
- 600 μl 20% APS
- 60 μl TEMED

Mixture is enough for one gel with 1.5 mm spacers. Gel sets in approximately 15 minutes. Run in 0.5 x Tris-Gly buffer.

40% Acrylamide (80:1) is made from BioRad Acrylamide powder and BioRad bis powder. Store at 4ºC.

Tris-glycine buffer

500 mM Tris base
500 mM glycine

For 1L: 60.5 g Trizma
37.5 g glycine

bring to 1000 ml, adjust pH to 8.8 and filter thru KimWipe

APPENDIX C

Agarose Spliceosome Assembly Gel

The spliceosomal H and E complexes are visualized using native agarose gels (Das and Reed, 1999).

1.   For assembly of A, B, and C spliceosome complexes, pre-mRNAs were incubated under normal spliceosome assembly reaction containing a final concentration of 3.2 mM $MgCl_2$, 0.4 mM ATP, 20 mM creatine phosphate, 1U RNasin (Promega), and 30% JSL1 nuclear extract (see *in vitro* splicing protocol). Importantly, **no heparin is added** following assembly, as it causes dissociation of E complex.

> 2.75 μl   GFB100
> 0.5 μl   each of 80 mM $MgCl_2$, 0.5 M CP and 25 mM ATP
> 0.5 μl   BC850
> 3.0 μl   13% PVA
> 0.5 μl   RNasin mix (.25 dd$H_2$0, 0.12 RNasin, 1 unit/μl, 0.12 DTT)
> 3.75 μl   NE
> 0.5 μl   template RNA (1 x 10^5 cpm/μl)

2.   For assembly of the ATP-independent E complex, the nuclear extracts were depleted of ATP by pre-incubating them at room temperature (25ºC) for 30-60 minutes, and the reactions lacked ATP and phosphocreatine.

3.   For native agarose gel analysis 10 μL of each reaction was loaded on 1.5% agarose (Seakem GTG agarose) gels. Glycine loading buffer was added to the samples prior to loading. The gels (10 cm x 12 cm) were cast and run in 25 mM Tris-Gly buffer at 100 V for 5 hours at 4ºC. All gel running supplies including gel boxes, casting plates, combs, etc. were all treated with RNaseZap (Ambion) and rinsed thoroughly with water prior to use.

4.   The agarose gels were fixed in 10% acetic acid, 10% methanol for 30 minutes, and dried under a vacuum for 45 minutes without heat and then for an hour and a half at 65ºC.

5.   Spliceosome complexes were visualized using autoradiography

APPENDIX D

Affinity Purification of hnRNP L from JSL1 NE

Used to purify hnRNP L from our JSL1 NE. This protocol is a single day purification scheme. Known that this preparation of L is contaminated with YB-1 and PTB. Modified from Hui and Bienderief, NSMB 2003.

Pre-block buffer
4 mM Tris pH 7.5
.2 mM DTT
2 mM $MgCl_2$
20 mM KCl
0.002% TritonX-100
0.2 mg/ml tRNA
1 mg/ml BSA
0.2 mg/ml glycogen

Wash Buffer (400 mM KCl)
20 mM Tris pH 7.5
1 mM DTT
10 mM $MgCl_2$
400 mM KCl
0.01% TritonX-100

Wash Buffer (2M KCl)
20 mM Tris pH 7.5
1 mM DTT
10 mM $MgCl_2$
2M KCl
0.01% TritonX-100

Elution Buffer
6 M Urea
10 mM Tris pH 8.0
0.2 mM EDTA

5'- biotin-CA_{20} is kept at 500 pmol/μl stock, stored at -80°C (Dharmacon)

Depletion of L from NE
1. Pre-block beads (acrylamide, Pierce) for 1 hour at 4°C end-over-end: 80 μl 50% slurry/ condition.
2. Wash beads in 400 mM KCl wash buffer 3 times. Spin at 3500 rpm for 2-5 minutes at 4°C.
3. Couple beads to RNA by incubating 5 hours at 4°C end-over-end. Use 500 pmol bi-CA_{20}/ 20μl slurry. Add 200 μl GFB100 to facilitate mixing.
4. Incubate beads with nuclear extract for 1 hour at 30°C end-over-end. Use 300 μl NE/ 40 μl beads.
5. Transfer NE from step 4 into a new eppendorf tube with fresh CA_{20}-coupled beads. Incubate NE with new beads for 1 hour at 30°C e/o/e.

6. Bring total salt to 600 mM KCl. Incubate 20 minutes at 4°C end-over-end.
7. Dialyze against BC100 overnight at 4°C using Pierce mini-dialysis units.
8. Confirm depletion by Western blot analysis using 4D11 hnRNP-L antibody. Usually depletion of L is approximately 85-95%.

Elution of L from beads

1. Wash **total** beads from each condition in 2M KCl buffer 3 times. Spin at 3500 rpm for 2-5 minutes at 4°C.
2. Elute using 6 M urea buffer. Incubate on ice approximately 30 minutes, mixing occasionally. (For 300 μl NE depletion, elute in 60 μl buffer).
3. Dialyze against BC100 overnight at 4°C.

Track elution by Western blotting washes and elution fractions with 4D11.

APPENDIX E

RNase H Mediated Oligo-Directed snRNA Inactivation

Design an oligo complementary to specific snRNA target. Incubate oligo, RNase H and nuclear extract under slightly modified splicing conditions to inactivate target snRNA. Protocol modified from Black et al., Cell 1985.

Results in efficient inactivation of target U1, U2, or U6 snRNPs from JSL1 NE in batch.

1. Set up modified splicing reaction, as below. Total 12 μl volume. Salt at 90 mM, final NE at 30%. DO NOT ADD PVA. Oligo final concentration estimated at about 10-40 fold M excess of snRNA, according to Black et al.

    3.6 μl GFB100
     .5 μl 25 mM ATP
     .5 μl .5 M CP
     .7 μl 80 mM MgCl$_2$
     .5 μl BC850
     .5 μl RNasin mix
     1 μl RNase H (Roche, 1 unit/μl)
     1 μl 5pmol/μl oligo
   3.75 μl NE

2. Incubate at 30ºC for 1 hour.

3. Pull 10 μl for primer extension analysis. PK treat, 30ºC 10'. PCA extract, ethanol precipitate, 70% ethanol wash. Resuspend the pellet in 10 μl ddH$_2$0. RT and RT-POL with ^{32}P-kinased 1 ng primer for snRNA of interest. Run on 10% PAG at 1200 V for 40 minutes.

4. Snap freeze remainder of treated NE, store at −80ºC.

Primer extension oligos:

U1 5'- TCA GCA CAT CCG GAG TGC AAT GG -3'
U2 5'- CCT ATT CCA TCT CCC TGA TCC -3'

U4 5'- ACT ATA TTG CAA GTC GTC CG -3'
U5 5'- CAG AGT TGT TCC TCT CCA GGG -3'
U6 5'- CAT GCT AAT CTT CTC TGT ATC GTT CC-3'

RNase H inactivating oligos: (complementary RNA, nt)

U1 (5'C, nt 2-11) 5'-TTCAGGTAAGTACTCA-3'
U2 (E15, nt 1-15) 5'-AGGCCGAGAAGCGAT-3'
U6 (U6f, nt 33-48) 5'-TTC TCT GTA TCG TTC C-3'

5'C, E15 from Black et al., Cell 1985.
U6f from Konforti and Konarska, Genes & Development 1994.

APPENDIX F

Psoralen Cross-linking and Primer Extension Mapping

1. Set up 50 μl splicing reaction (*see below*) with 100 fmol/μl final of the RNA template. (I keep cold RNA stock at 50 fmol/μl).

2. Incubate reaction at 30°C in waterbath. For U1 binding, incubate for 60-90 minutes. Add heparin (Sigma Aldrich) to 20 μg/μl final.

3. Remove sample from waterbath, place on ice and add AMT psoralen to 20 μg/ml final. I add 2 μl psoralen at 500 μg/ml. Store stock and reaction stock at 4°C wrapped in foil because of light sensitivity. Transfer sample to U-bottom 96 well plate on ice. Crosslink using long wave UV light (365 nm) for 10 minutes on ice. (Works best if done in low light.)

4. Transfer sample to new eppendorf tube. PK treat by adding 175 μl PK mix to the reaction, incubate at 30°C for 15 minutes.

5. PCA extract, ethanol precipitate, 70% ethanol wash. Resuspend the pellet in 10 μl ddH$_2$O. Store at -80°C.

6. Set up RT and RT-POL reactions (as with standard lab RT-PCR protocol), but at double reaction volume (such that RT is 8 μl total and RT-POL is 40 μl total). Use ^{32}P-kinased primer (i.e. exon 4 5'ss with 5'R1 primer) at ~1.5 ng/μl.

7. PCA extract, ethanol precipitate, 70% ethanol wash. Resuspend the pellet in 10 μl formamide loading buffer. Run 5 μl sample on 10% PAG gel and run at 1200V for 35 minutes. Use ddseq ladder of RNA template as marker.

8. Image by autoradiography. With fresh ^{32}P primer, expose gel to film with intensifying screen for 2-4 hours.

Splicing reaction for psoralen xlinking:
Modified from standard *in vitro* splicing reaction, as follows:
  - NE at 60% final
  - PVA at 1% final
  - RNA template at 100 fmol input
  - Exclude RNasin from the reaction due to increased volume of NE.

Per reaction (50 μl total volume):
        6 μl GFB100
        2 μl MgCl$_2$
        2 μl CP
        2 μl ATP
        2 μl BC850
        4 μl PVA
       30 μl NE
        2 μl RNA

APPENDIX G

Reverse Transcription Dideoxy-sequencing

1.   Anneal
        10 ng RNA template
          4 μl ^{32}P-kinased primer (2 ng/μl)
        4.8 μl 5x AB
        bring reaction volume to 25 μl with ddH$_2$O

        90°C for 5 minutes, 42°C for 30 minutes, 4°C (program AMV RT in PCR block)

2.   RTase reaction
            4 μl 1x AB
            4 μl RT mix
            8 μl 1 mM dNTPs in 1x AB (+/- 400 μM ddNTP, 500 μM ddATP)
            4 μl annealed mix (above)

        42°C for 60 minutes (program AMV-POL in PCR block)

3.   PCA extract in 200 μl
4.   Ethanol precipitate in 500 μl, 20 μl 3 M NaOAc and 1 μl glycogen.
        Spin 13K 4ºC 10 minutes, 70% ethanol wash. Resuspend the pellet
        in 12 μl formamide loading buffer. Run 4-5 μl as ladder.

Buffers and Mixes:
(5x) AB: 200 μl 1M Tris pH 8.3
          40 μl 1M DTT
        560 μl ddH$_2$O

(5x) RT buffer: 100 μl 1M Tris pH 8.3   * or AMV buffer
                  20 μl 1M DTT
                  60 μl 1M MgOAc
                220 μl ddH$_2$O

RT mix: 8 μl ddH$_2$O
         3 μl (5x) RT buffer/AMV buffer
         4 μl AMV
         (this is enough for 3 reactions)

<u>ddNTP mixes (50 μl each):</u> 1 μl each dNTP (50 mM stocks)

4 μl ddC, ddG, ddT or 5 μl ddA (5 mM stocks)

10 μl 5x AB

Add ddH$_2$O to bring to 50 μl: dNTPs = 36 μl

ddA = 31 μl

ddC, G, T = 32 μl

APPENDIX H

Purifying MS2-MBP Affinity-tag adapter protein

The affinity-tag adapter protein is a recombinant MS2-MBP fusion expressed in *E. coli* (construct a gift from Josep Vilardell). This fusion places MBP N-terminal to MS2, and the MS2 portion carries a double mutation (V75Q and A81G) that prevents oligomerization as in LeCuyer, 1995. Single-step purification of MS2-MBP over an amylose column yields a single band on a Coomassie-stained gel (~55kD), but the A_{280}/A_{260} ratio (<1) reveals that a significant amount of bound nucleic acid remains as a contaminant. Heparin chromatography as a second purification step eliminates this contaminant.

Solutions:

1. *AB1*: 20 mM Tris, pH 7.5, 200 mM KCl, 1 mM EDTA. Make 500 ml by combining 10 ml of 1 M Tris, pH 7.5 stock solution, 50 ml of 2 M KCl stock solution, 1 ml of 0.5 M EDTA stock solution, and 439 ml of H_2O.

2. *AB2*: 20 mM Tris, pH 7.5, 20 mM KCl, 1 mM EDTA. Make 500 ml by combining 10 ml of 1M Tris, pH 7.5 stock solution, 5 ml of 2 M KCl stock solution, 1 ml of 0.5 M EDTA stock solution, and 484 ml of H_2O.

3. *ABE*: 20 mM Tris, pH 7.5, 20 mM KCl, 1 mM EDTA, 10 mM maltose. Make 100 ml by combining 2 ml of 1 M HEPES, pH 7.5 stock solution, 1 ml of 2 M KCl stock solution, 200 ml of 0.5 M EDTA stock solution, 2 ml of 0.5 M maltose and 74 ml of H_2O.

4. *PMSF*: 100 mM. To make 5 ml, dissolve 87.1 mg PMSF in 5 ml of ethanol. Store at 4°C.

5. *IPTG*: 1 M. To make 10 ml, dissolve 1.19 g of IPTG in 5 ml of H_2O. Store in 1 ml aliquots at −20°C.

6. *HB1*: 20 mM Tris, pH 7.5, 1 mM EDTA. Make 500 ml by combining 10 ml of 1 M Tris, pH 7.5 stock solution, 1 ml of 0.5 M EDTA stock solution, and 489 ml of H_2O.

7. *HB2*: 20 mM Tris, pH 7.5, 1 M KCl, 1 mM EDTA. Make 500 ml by combining 10 ml of 1 M Tris, pH 7.5 stock solution, 250 ml of 2 M KCl stock solution, 1 ml of 0.5 M EDTA stock solution, and 239 ml of H_2O.

Steps:

1. Inoculate a 10 ml culture of Luria broth (LB) with single bacterial colony of Rosetta DE3 cells transformed with a plasmid expressing MS2-MBP and grow overnight to saturation at 37°C with shaking. The next morning inoculate 500 ml of LB plus 2% glucose with 5 ml of the starter culture. Grow the cells at 37°C with shaking to an OD_{600} of ~0.5 and then induce expression of the protein by adding 1 ml of 1M IPTG . Continue to grow the cells for 2-3 hours and harvest by centrifugation at 6000 rpm for 10 minutes. Pour off the supernatant, freeze the cell pellet and store at –20°C.

2. Thaw and resuspend ~2.5 g of the cell pellet in 25 ml cold AB1 plus 500 ml PMSF. Break open the cells by sonication on ice. Centrifuge 30 minutes at 15,000 rpm at 4°C.

3. All the following steps of the purification are performed at 4°C. Load the supernatant on a ~5 ml amylose column equilibrated with AB1, and run by gravity flow. Reload the flowthru such that the sample is passed over the column twice. Wash the column with 40 ml of AB1, followed by 10 ml of AB2 to lower the salt concentration in preparation for heparin chromatography.

4. Elute the protein with 20 ml of ABE, taking 2 ml fractions. Run an aliquot of each collected fraction on a 12.5% protein gel and Coomassie stain. Pool the peak fractions, typically these are fractions number 2 through 5.

5. On an FPLC, equilibrate a 1 ml heparin column with a mixture of HB1 and HB2 to 20 mM KCl. Load the concentrate on the column and wash with 5 ml at 20 mM KCl.

6. Run a gradient from 20 to 400 mM KCl over 10 column volumes. The MS2-MBP protein elutes at ~60 mM KCl. Pool peak fractions and concentrate to in a Centricon-30. Add glycerol to 10% and freeze at –20°C in 100 ml aliquots.

7. Determine the protein concentration for MS2-MBP. An OD_{280} of 1 corresponds to 16.5 mM or 0.89 mg/ml.

APPENDIX I

Purification of Spliceosome Complexes

This method describes purification of the pre-spliceosomal A or AEC complexes assembled in nuclear extract on a uniformly ^{32}P labeled pre-mRNA that has 3 MS2 hairpins at the 3′ end (MS2Hind series of constructs). Assembly is typically carried out in a 500 μl reaction that contains the following. Six reactions are used per purification.

Reagent	Final Concentration	Volume to be added
Nuclear Extract (NE)	60%	300 μl
RNA ($2x10^4$cpm/μl)	10 nM	5 μl
MS2-MBP	100 nM (10 fold excess)	1 μl
80 mM MgCl$_2$	3.2 mM	20 μl
25 mM ATP	1 mM	20 μl
0.5 M CP	20 mM	20 μl
BC850		20 μl
RNasin mix	0.25 U	10 μl
ddH$_2$O		105 μl
		500 μl total volume

1. Pre-bind of MS2-MBP protein to RNA. Mix the RNA, MgCl$_2$, ATP, CP, BC850, and ddH$_2$0 in a separate 1.5 ml tube and incubate on ice for 30 minutes.
2. Add NE to the RNA/MS2-MBP complex. Mix well and incubate at 30°C for 60-90 minutes (if U6 snRNA depleted) or 35 minutes (untreated NE).
3. Pass the reaction twice through a 1 ml amylose column that is pre-equilibrated in buffer GFB100 containing 2.2 mM MgCl$_2$, 1mM DTT, 0.1 mM PMSF.
4. Wash the column with 20 column volumes of GFB100 with 2.2 mM MgCl$_2$, 1 mM DTT and 0.1 mM PMSF (approximately 20 ml).
5. Elute the bound complex in 250 μl of buffer GFB100 containing 2.2 mM MgCl$_2$, 1 mM DTT and 0.1 mM PMSF with a final concentration of 20 mM maltose.
6. Measure radioactivity in each 250 μl aliquot using dry scintillation ^{32}P counting.
7. Pool the fractions that contain the highest counts.

8. For proteomic analysis, digest the purified complex with RNase A (final 2 μg/μl) prior to adding TCA (final 10%) to precipitate protein.

For western blot analysis, resuspend in the protein pellet in 20 μl 5x SDS lysis buffer. Then add 5 μl 5x SDS sample buffer. Typically, loading 13 μl of the sample on a protein gel is sufficient to detect a signal using most antibodies.

APPENDIX J

Glycerol Density Gradient Centrifugation

1. Make 15-35% glycerol stocks using 10x GFB100, 50% glycerol and ddH$_2$0. Keep stocks at 4ºC. (See below.)

2. Begin to pour the gradient by starting with 35% stock and add 1.2ml of it to the very bottom of the centrifuge tube (Beckman or Seton, ultra-clear).

3. Place tube in the –80ºC until the layer of glycerol stock is frozen solid, providing a surface to add the next layer.

4. Next add 1.2 ml of 32.5% stock over the previous layer. For this, place the pipette tip immediately above the frozen existing layer and slowly dispense the content of the tip.

5. Repeat step 3-4 with the remaining stocks, adding each consecutive fraction to the tube. Gradients can either be used immediately (once thawed) or stored at –80ºC.

6. Load equal volumes of sample (up to 150 µl) over the gradient. (Make sure that your sample has less glycerol than 15% glycerol. PVA should be factored into calculation of % glycerol in reaction).

7. Centrifuge for 12-16 hours at 29,000 rpm at 4ºC in Beckman Ultracentrifuge using a SW41 rotor.

8. Collect 400 µl fractions starting from the very top of the gradient. To do this correctly, touch the side of the tube at the very top of the gradient with the end of the pipette tip and carefully take out 400 µl. Repeat.

Final % glycerol	10x GFB100 (ml)	50% glycerol (ml)	Water (ml)
15.0	1.0	3.0	6.0
17.5	1.0	3.5	5.5
20.0	1.0	4.0	5.0
22.5	1.0	4.5	4.5
25.0	1.0	5.0	4.0
27.5	1.0	5.5	3.5
30.0	1.0	6.0	3.0
32.5	1.0	6.5	2.5
35.0	1.0	7.0	2.0

BIBLIOGRAPHY

Behzadnia, N., Golas, M.M., Hartmuth, K., Sander, B., Kastner, B., Deckert, J., Dube, P., Will, C.L., Urlab, H., Stark, H*., et al.* (2007). Composition and three-dimensional EM structure of double affinity-purified, human prespliceosomal A complexes. Embo J *26*, 1737-1748.

Bentley, D.L. (2005). Rules of engagement: co-transcriptional recruitment of pre-mRNA processing factors. Curr Opin Cell Biol *17*, 251-256.

Berget, S.M. (1995). Exon recognition in vertebrate splicing. J Biol Chem *270*, 2411-2414.

Birkeland, M.L., Johnson, P., Trowbridge, I.S., and Pure, E. (1989). Changes in CD45 isoform expression accompany antigen-induced murine T cell activation. Proceedings of the National Academy of Science USA *86*, 6734-6738.

Black, D.L. (1995). Finding splice sites within a wilderness of RNA. RNA *1*, 763-771.

Black, D.L. (2003). Mechanisms of Alternative Pre-Messenger RNA Splicing. Annu Rev Biochem *72*, 291-336.

Black, D.L., Chabot, B., and Steitz, J.A. (1985). U2 as well as U1 small nuclear ribonucleoproteins are involved in premessenger RNA splicing. Cell *42*, 737-750.

Black, D.L., and Steitz, J.A. (1986). Pre-mRNA splicing in vitro requires intact U4/U6 small nuclear ribonucleoprotein. Cell *46*, 697-704.

Blanchette, M., and Chabot, B. (1999). Modulation of exon skipping by high-affinity hnRNP A1-binding sites and by intron elements that repress splice site utilization. Embo J *18*, 1939-1952.

Blencowe, B.J. (2000). Exonic splicing enhancers: mechanism of action, diversity and role in human genetic diseases. TIBS *25*, 106-110.

Blencowe, B.J. (2006). Alternative splicing: new insights from global analyses. Cell *126*, 37-47.

Blencowe, B.J., Issner, R., Nickerson, J.A., and Sharp, P.A. (1998). A coactivator of pre-mRNA splicing. Genes Dev *12*, 996-1009.

Buratti, E., Muro, A.F., Giombi, M., Gherbassi, D., Iaconcig, A., and Baralle, F.E. (2004). RNA folding affects the recruitment of SR proteins by mouse and human polypurinic enhancer elements in the fibronectin EDA exon. Mol Cell Biol *24*, 1387-1400.

Burgess, S.M., and Guthrie, C. (1993a). A mechanism to enhance mRNA splicing fidlity: the RNA-dependent ATPase Prp16 governs usage of a discard pathway for aberrant lariat intermediates. Cell *73*, 1377-1391.

Burgess, S.M., and Guthrie, C. (1993b). Beat the clock: paradigms for NTPases in the maintenance of biological fidelity. Trends Biochem Sci *18*, 381-384.

Byth, K.F., Conroy, L.A., Howlett, S., Smith, A.J.H., May, J., Alexander, D.R., and Holmes, N. (1996). CD45-Null transgenic mice reveal a positive regulatory role for CD45 in early thymocyte development, in the selection of CD4$^+$CD8$^+$ thymocytes, and in B cell maturation. J Exp Med *183*, 1707-1718.

Chan, R.C., and Black, D.L. (1997a). Conserved intron elements repress splicing of a neuron-specific c-src exon in vitro. Mol Cell Biol *17*, 2970.

Chan, R.C., and Black, D.L. (1997b). The polypyrimidine tract binding protein binds upstream of neural cell-specific c-src exon N1 to repress the splicing of the intron downstream. Mol Cell Biol *17*, 4667-4676.

Chiara, M.D., and Reed, R. (1995). A two-step mechanism for 5' and 3' splice-site pairing. Nature *375*, 510-513.

Chua, K., and Reed, R. (1999). The RNA splicing factor hSlu7 is required for correct 3' splice-cite choice. Nature *402*, 207-210.

Clark, T.A., Sugnet, C.W., and Ares, M., Jr. (2002). Genomewide analysis of mRNA processing in yeast using splicing-specific microarrays. Science *296*, 907-910.

Coulter, L.R., Landree, M.A., and Cooper, T.A. (1997). Identification of a new calss of exonic splicing enhancers by in vivo selection. Mol Cell Biol *17*, 2143-2150.

Darnell, R.B. (2006). Developing global insight into RNA regulation. Cold Spring Harb Symp Quant Biol *71*, 321-327.

Das, R., and Reed, R. (1999). Resolution of the mammalian E complex and the ATP-dependent spliceosomal complexes on native agarose mini-gels. Rna *5*, 1504-1508.

Das, R., Zhou, Z., and Reed, R. (2000). Functional association of U2 snRNP with the ATP-independent spliceosomal complex E. Mol Cell *5*, 779-787.

Dawes, R., Hennig, B., Irving, W., Petrova, S., Boxall, S., Ward, V., Wallace, D., Macallan, D.C., Thursz, M., Hill, A.*, et al.* (2006). Altered CD45 expression in C77G carriers influences immune function and outcome of hepatitis C infection. J Med Genet *43*, 678-684.

Deckert, J., Hartmuth, K., Boehringer, D., Behzadnia, N., Will, C.L., Kastner, B., Stark, H., Urlab, H., and Luhrmann, R. (2006). Protein composition and electron microscopy structure of affinity-purified human spliceosomal B complexes isolated under physiological conditions. Mol Cell Biol *26*, 5528-5543.

Donmez, G., Hartmuth, K., Kastner, B., Will, C.L., and Luhrmann, R. (2007). The 5' end of U2 snRNA is in close proximity to U1 and functional sites of the pre-mRNA in early spliceosomal complexes. Mol Cell *25*, 399-411.

Dredge, B.K., Stefani, G., Engelhard, C.C., and Darnell, R.B. (2005). Nova autoregulation reveals dual functions in neuronal splicing. EMBO J *in press*.

Dreyfuss, G., Kim, V.N., and Kataoka, N. (2002). Messenger-RNA-binding proteins and the messages they carry. Nat Rev Mol Cell Biol *3*, 195-205.

Dreyfuss, G., Matunis, M.J., Pinol-Roma, S., and Burd, C.G. (1993). hnRNP proteins and the biogenesis of mRNA. Annu Rev Biochem *62*, 289-321.

Eldridge, A.G., Li, Y., Sharp, P.A., and Blencowe, B.J. (1999). The SRm160/300 splicing coactivator is required for exon-enhancer function. Proc Natl Acad Sci U S A *96*, 6125-6130.

Expert-Bezancon, A., Le Caer, J.P., and Marie, J. (2002). Hetergeneous nuclear ribonucleoprotein (hnRNP) K is a component of an intronic splicing enchancer complex that activates the splicing of the alternative exon 6A from chicken beta-tropomyosin pre-mRNA. J Biol Chem *277*, 16614-16623.

Fairbrother, W.G., and Chasin, L.A. (2000). Human genomic sequences that inhibit splicing. Mol Cell Biol *20*, 6816-6825.

Fairbrother, W.G., Yeh, R.F., Sharp, P.A., and Burge, C.B. (2002). Predictive identification of exonic splicing enhancers in human genes. Science *297*, 1007-1013.

Forch, P., Puig, O., Martinez, C., Seraphin, B., and Valcarcel, J. (2002). The splicing regulator TIA-1 interacts with U1-C to promote U1 snRNP recruitment to 5' splice sites. Embo J *21*, 6882-6892.

Fu, X.D. (2004). Towards a splicing code. Cell *119*, 736-738.

Gamarnik, A.V., and Andino, R. (1997). Two functional complexes formed by KH domain containing proteins with the 5' noncoding region of poliovirus RNA. Rna *3*, 882-892.

Giles, K.E., and Beemon, K.L. (2005). Retroviral splicing suppressor sequesters a 3' splice site in a 50S aberrant splicing complex. Mol Cell Biol *25*, 4397-4405.

Gozani, O., Potashkin, J., and Reed, R. (1998). A potential role for U2AF-SAP 155 interactions in recruiting U2 snRNP to the branch site. Mol Cell Biol *18*, 4752-4760.

Graveley, B. (2005). Mutually exclusive splicing of the insect Dscam pre-mRNA directed by competing intronic RNA secondary structures. Cell *123*, 65-73.

Han, K., Yeo, G., An, P., Burge, C.B., and Grabowski, P.J. (2005). A combinatorial code for splicing silencing: UAGG and GGG motifs. PLoS Biol *3*, e158.

Hermiston, M.L., Xu, Z., Majeti, R., and Weiss, A. (2002). Reciprocal regulation of lymphocyte activation by tyrosine kinases and phosphatases. J Clin Invest *109*, 9-14.

Hermiston, M.L., Xu, Z., and Weiss, A. (2003). CD45: a critical regulator of signaling threshold in immune cells. Annu Rev Immunol *21*, 107-137.

Hertel, K.J. (2007). J Biol Chem.

Hilliker, A.K., Mefford, M.A., and Staley, J.P. (2007). U2 toggles iteratively between the stem IIa and stem Iic conformations to promote pre-mRNA splicing. Genes Dev *21*, 821-834.

House, A.E., and Lynch, K.W. (2006). An exonic splicing silencer represses spliceosome assembly after ATP-dependent exon recognition. Nat Struct Mol Biol *13*, 937-944.

Hui, J., and Bindereif, A. (2005). Alternative pre-mRNA splicing in the human system: unexpected role of repetitive sequences as regulatory elements. Biol Chem *386*, 1265-1271.

Hui, J., Hung, L.H., Sheiner, M., Schreiner, S., Neumuller, N., Reither, G., Haas, S.A., and Bindereif, A. (2005). Intronic CA-repeat and CA-rich elements: a new class of regulators of mammalian alternative splicing. Embo J *24*, 1988-1998.

Hui, J., Stangl, K., Lane, W.S., and Bindereif, A. (2003). HnRNP L stimulates splicing of the eNOS gene by binding to variable-length CA repeats. Nat Struct Biol *10*, 33-37.

Ip, J.Y., Tong, A., Pan, Q., Topp, J.D., Blencowe, B.J., and Lynch, K.W. (2007). Global analysis of alternative splicing during T-cell activation. RNA *13*, 563-572.

Ishiura, S., Kino, Y., Nezu, Y., Onishi, H., Ohno, E., and Sasagawa, N. (2005). Regulation of splicing by MBNL and CELF family of RNA-binding protein. Acta Myol *24*, 74-77.

Izquierdo, J.M., Majos, N., Bonnal, S., Martinez, C., Castelo, R., Guigo, R., Bilbao, D., and Valcarcel, J. (2005). Regulation of Fas alternative splicing by antagonistic effects of TIA-1 and PTB on exon definition. Mol Cell *19*, 475-484.

Johnson, J.M., Castle, J., Garrett-Engele, P., Kan, Z., Loerch, P.M., Armour, C.D., Santos, R., Schadt, E.E., Stoughton, R., and Shoemaker, D.D. (2003). Genome-wide survey of human alternative pre-mRNA splicing with exon junction microarrays. Science *302*, 2141-2144.

Jurica, M.S. (2005). Purification of Intermediate-Containing Spliceosomes. In Organelles and Cellular Structures (Elsevier Science), pp. 109-114.

Jurica, M.S., Licklider, L.J., Gygi, S.R., Grigorieff, N., and Moore, M.J. (2002). Purification and characterization of native spliceosomes suitable for three-dimensional structural analysis. Rna *8*, 426-439.

Jurica, M.S., and Moore, M.J. (2002). Capturing splicing complexes to study structure and mechanism. Methods *28*, 336-345.

Jurica, M.S., and Moore, M.J. (2003). Pre-mRNA splicing: awash in a sea of proteins. Mol Cell *12*, 5-14.

Jurica, M.S., Sousa, D., Moore, M.J., and Grigorieff, N. (2004). Three-dimensional structure of C complex spliceosomes by electron microscopy. Nat Struct Mol Biol *11*, 265-269.

Kameoka, S., Duque, P., and Konarska, M.M. (2004). p54(nrb) associates with the 5' splice site within large transcritpion/splicing complexes. EMBO J *23*, 1782-1791.

Kan, J.L.C., and Green, M.R. (1999). Pre-mRNA splicing of IgM exons M1 and M2 is dierected by a juxtaposed splicing enhancer and inhibitor. Genes Dev *13*, 462-471.

Kim, J.H., Hahm, B., Kim, Y.K., Choi, M., and Jang, S.K. (2000). Protein-protein interaction among hnRNPs shuttling between nucleus and cytoplasm. J Mol Biol *298*, 395-405.

Kishihara, K., Penninger, J., Wallace, V.A., Kundig, T.M., Kawai, K., Wakenham, A., Timms, E., Pfeffer, K., Ohashi, P.S., and Thomas, M.L. (1993). Normal B lymphocyte development but impaired T cell maturation in CD45-exon 6 protein tyrosine phosphatase-deficient mice. Cell *74*, 143-156.

Kohtz, J.D., Jamison, S.F., Will, C.L., Zuo, P., Luhrmann, R., Garcia-Blanco, M.A., and Manley, J.L. (1994). Protein-protein interactions and 5'-splice-site recognition in mammalian mRNA precursors. Nature *368*, 119-124.

Konarska, M.M., and Query, C.C. (2005). Insights into the mechanisms of splicing: more lessons from the ribosome. Genes Dev *19*, 2255-2260.

Konarska, M.M., and Sharp, P.A. (1986). Electrophoretic separation of complexes involved in the splicing of precursors to mRNAs. Cell *46*, 845-855.

Konarska, M.M., and Sharp, P.A. (1987). Interactions between small nuclear ribonucleoprotein particles in formation of spliceosomes. Cell *49*, 763-774.

Konforti, B.B., and Konarska, M.M. (1994). U4/U5/U6 snRNP recognizes the 5' splice site in the absence of U2 snRNP. Genes Dev *8*, 1962-1973.

Kornblihtt, A.R. (2006). Chromatin, transcript elongation and alternative splicing. Nat Struct Mol Biol *13*, 5-7.

Krecic, A.M., and Swanson, M.S. (1999). hnRNP complexes: composition, structure, and function. Curr Opin Cell Biol *11*, 363-371.

Kung, C., Pingel, J.T., Heikinheimo, M., Klemola, T., Varkila, K., Yoo, L.I., Vuopala, K., Poyhonen, M., Uhari, M., Rogers, M.*, et al.* (2000). Mutations in the tyrosine phosphatase CD45 gene in a child with severe combined immunodeficiency disease. Nat Med *6*, 343-345.

Lallena, M.J., Chalmers, K.J., Llamazares, S., Lamond, A.I., and Valcarcel, J. (2002). Splicing regulation at the second catalytic step by Sex-lethal involves 3' splice site recognition by SPF45. Cell *109*, 285-296.

Leffers, H., Dejgaard, K., and Celis, J.E. (1995). Characterisation of two major cellular poly(rC)-binding human proteins, each containing three K-homologous (KH) domains. Eur J Biochem *230*, 447-453.

Li, Q., Lee, J.A., and Black, D.L. (2007). Neuronal regulation of alternative pre-mRNA splicing. Nat Rev Neurosci.

Li, Y., and Blencowe, B.J. (1999). Distinct factor requirements for exonic splicing enhancer function and binding of U2Af to the polypyrimidine tract. J Biol Chem *274*, 35074-35079.

Lim, L.P., and Burge, C.B. (2001). A computational analysis of sequence features involved in recongition of short introns. Proc Natl Acad Sci U S A *98*, 11193-11198.

Lim, S.R., and Hertel, K.J. (2004). Commitment to splice site pairing coincides with A complex formation. Mol Cell *15*, 477-483.

Lin, S., and Fu, X.D. (2007). In:. In Alternative Splicing in the Postgenomic Era, B.J. Blencowe, and B. Graveley, eds. (Landes Biosciences).

Liu, H.-X., Chew, S.L., Cartegni, L., Zhang, M., and Krainer, A.R. (2000). Exonic splicing enhancer motif recognized by SC35 under splicing conditions. Mol Cell Biol *20*, 1063-1071.

Liu, H.-X., Zhang, M., and Krainer, A.R. (1998). identification of functional exonic splicing enhancer motifs recognized by inidividual SR proteins. Genes Dev *12*, 1998-2012.

Lutz, C.S., Cooke, C., O'Connor, J.P., Kobayashi, R., and Alwine, J.C. (1998). The snRNP-free U1A (SF-A) complex(es): identification of the largest subunit as PSF, the polypyrimidine-tract binding protein-associated splicing factor. RNA *4*, 1493-1499.

Lynch, K.W. (2004a). Consequences of regulated pre-mRNA splicing in the immune system. Nat Rev Immunol *4*, 931-940.

Lynch, K.W. (2004b). Consequences of regulated pre-mRNA splicing in the immune system. Nat Rev Immunol *4*, 931-940.

Lynch, K.W. (2007). Regulation of Alternative Splicing by Signal Transduction Pathways. In Alternative Splicing in the Postgenomic Era, B.J. Blencowe, and B. Graveley, eds. (Landes Bioscience).

Lynch, K.W., and Maniatis, T. (1996). Assembly of specific SR protein complexes on distinct regulatory elements of the *Drosophila* doublesex splicing enhancer. Genes Dev *10*, 2089-2101.

Lynch, K.W., and Weiss, A. (2000). A model system for the activation-induced alternative-splicing of CD45 implicates protein kinase C and Ras. Mol Cell Biol *20*, 70-80.

Lynch, K.W., and Weiss, A. (2001). A CD45 polymorphism associated with Muliple Sclerosis disrupts an exonic splicng silencer. J Biol Chem *276*, 24341-24347.

Martinez-Contreras, R., Cloutier, P., Shkreta, L., Fisette, J.F., Revil, T., and Chabot, B. (2007). In:. In Alternative Splicing in the Postgenomic Era, B.J. Blencowe, and B. Graveley, eds. (Landes Biosciences).

Martinez-Contreras, R., Fisette, J.F., Nasim, F.H., Madden, R., Cordeau, M., and Chabot, B. (2006). Intronic binding sites for hnRNP A/B and hnRNP F/H proteins stimulate pre-mRNA splicing. PLoS Biol *4*, e21.

Matlin, A.J., Clark, F., and Smith, C.W. (2005). Understanding alternative splicing: towards a cellular code. Nat Rev Mol Cell Biol *6*, 386-398.

Matlin, A.J., and Moore, M.J. (2007). In Alternative Splicing in the Postgenomic Era, B.J. Blencowe, and B.R. Graveley, eds. (Landes Biosciences).

Mayas, R.M., Maita, H., and Staley, J.P. (2006). Exon ligation is proofread by the DExD/H-box ATPase Prp22p. Nat Struct Mol Biol *13*, 482-490.

McNeill, L., Salmond, R.J., Cooper, J.C., Carret, C.K., Cassady-Cain, R.L., Roche-Molina, M., Tandon, P., Holmes, N., and Alexander, D.R. (2007). The Differential Regulation of Lck Kinase Phosphorylation Sites by CD45 is Critical for T Cell Receptor Signaling Responses. Immunity *27*, 425-437.

Mee, P.J., Turner, M., Basson, M.A., Costello, P.S., Zamoyska, R., and Tybulewicz, V.L. (1999). Greatly reduced efficiency of both positive and negative selection of thymocytes in CD45 tyrosince phosphatase-deficient mice. Eur J Immuno *29*, 2923-2933.

Melton, A.A., Jackson, J., Wang, J., and Lynch, K.W. (2007). Combinatorial Control of Signal-Induced exon Repression by hnRNP L and PSF. Mol Cell Biol *27*, 6972-6984.

Modafferi, E.F., and Black, D.L. (1997). A complex intronic splicing enhancer from the c-src pre-mRNA activates inclusion of a heterologous exon. Mol Cell Biol *17*, 6537-6545.

Modafferi, E.F., and Black, D.L. (1999). Combinatorial control of a neuron-specific exon. RNA *5*, 687-706.

Modrek, B., and Lee, C. (2002). A genomic view of alternative splicing. Nat Genet *30*, 13-19.

Moore, M.J., and Sharp, P.A. (1993). Evidence for two active sites in the spliceosome provided by stereochemistry of pre-mRNA splicing. Nature *365*, 364-368.

Nakielny, S., and Dreyfuss, G. (1999). Transport of proteins and RNAs in and out of the nucleus. Cell *99*, 677-690.

Nasim, F.H., Hutchison, S., Cordeau, M., and Chabot, B. (2002). High-affinity hnRNP A1 binding sites and duplex-forming inverted repeats have similar effects on 5' splice site selection in support of a common looping out and repression mechanism. RNA *8*, 1078-1089.

Park, J.W., Parisky, K., Celotto, A.M., Reenan, R.A., and Graveley, B.R. (2004). Identification of alternative splicing regulators by RNA interference in Drosophila. Proc Natl Acad Sci U S A *101*, 15974-15979.

Peng, R., Dye, B.T., Perez, I., Barnard, D.C., Thompson, A.B., and Patton, J.G. (2002). PSF and p54nrb bind a conserved stem in U5 snRNA. RNA *8*, 1334-1347.

Peng, R., Hawkins, I., Link, A.J., and Patton, J.G. (2006). The splicing factor PSF is part of a large complex that assembles in the absence of pre-mRNA and contains all five snRNPs. RNA Biol *3*, 69-76.

Perriman, R.J., and Ares, M., Jr. (2007). Rearrangement of competing U2 RNA helices within the spliceosome promotes multiple steps in splicing. Genes Dev *21*, 811-820.

Pleiss, J.A., Whitworth, G.A., Bergkessel, M., and Guthrie, C. (2007). Transcript Specificity in Yeast Pre-mRNA Splicing Revealed by Mutations in Core Spliceosomal Components. PLoS *5*.

Query, C.C., and Konarska, M.M. (2006). Splicing fidelity revisited. Nat Struct Mol Biol *13*, 472-474.

Reed, R. (2000). Mechanisms of fidelity in pre-mRNA splicing. Curr Opin Cell Biol *12*, 340-345.

Rooke, N., Markovtsov, V., Cagavi, E., and Black, D.L. (1999). Roles for SR proteins and hnRNP A1 in the regulation of c-crs exon N1. Mol Cell Biol *23*, 1874-1884.

Roscigno, R.F., and Garcia-Blanco, M.A. (1995). SR proteins escort the U4/U6.U5 tri-snRNP to the spliceosome. RNA *1*, 692-706.

Rothrock, C., Cannon, B., Hahm, B., and Lynch, K.W. (2003). A conserved signal-responsive sequence mediates activation-induced alternative splicing of CD45. Mol Cell *12*, 1317-1324.

Rothrock, C.R., House, A.E., and Lynch, K.W. (2005). HnRNP L represses exon splicing via a regulated exonic splicing silencer. Embo J.

Schaal, T.D., and Maniatis, T. (1999a). Multiple distinct splicing enhancers in the protein-coding sequences of a constitutively spliced pre-mRNA. Mol Cell Biol *19*, 261-273.

Schaal, T.D., and Maniatis, T. (1999b). Selection and characterization of pre-mRNA splicing enhancers: idntification of novel SR protein-specific enhancer sequences. Mol Cell Biol *19*, 1705-1719.

Seiwert, S.D., and Steitz, J.A. (1993). Uncoupling Two Functions of the U1 Small Nuclear Ribonucleoprotein Particle during In Vitro Splicing. Mol Cell Biol *13*, 3135-3145.

Sharma, S., Falick, A.M., and Black, D.L. (2005). Polypyrimidine tract binding protein blocks the 5' splice site-dependent assembly of U2AF and the prespliceosomal E complex. Mol Cell *19*, 485-496.

Sharp, P.A. (1987). Splicing of messenger RNA precurssors. Science *235*, 766-771.

Shen, H., and Green, M.R. (2006). RS domains contact splicing signals and promote splicing by a common mechanism in yeast through humans. Genes Dev *20*, 1755-1765.

Shen, H., and Green, M.R. (2007). RS domain-splicing signal interactions in splicing of U12-type and U2-type introns. Nat Struct Mol Biol *14*, 597-603.

Siebel, C.W., Fresco, L.D., and Rio, D.C. (1992). The mechanism of somatic inhibition: multiprotein complexes at an exon pseudo-5' splice site control U1 snRNP binding. Genes Dev *6*, 1386-1401.

Singh, N.N., Singh, R.N., and Androphy, E.J. (2007). Modulating role of RNA structure in alternative splicing of a critical exon in the spinal muscular atrophy genes. Nucleic Acids Res *35*, 371-389.

Small, E.C., Leggert, S.R., Winans, A.A., and Staley, J.P. (2006). The EF-G-like GTPase Snu114p Regulates Spliceosome Dynamics Mediated by Brr2p, a DExD/H Box ATPase. Molecular Cell *23*, 389-399.

Soares, L.M., Zanier, K., Mackereth, C., Sattler, M., and Valcarcel, J. (2006). Intron Removal requires Proofreading of U2AF/3' Splice Site Recognition by DEK. Science *312*, 1961-1964.

Stadler, M.B., Shomron, N., Yeo, G.W., Schneider, A., Xiao, X., and Burge, C.B. (2006). Inference of splicing regulatory activities by sequence neighborhood analysis. PLoS Genet *2*, e191.

Staley, J.P., and Guthrie, C. (1998). Mechanical devices of the spliceosome: motors, clocks, springs, and things. Cell *92*, 315-326.

Staley, J.P., and Guthrie, C. (1999). An RNA switch at the 5' splice site requires ATP and the DEAD box protein Prp28p. Mol Cell *3*, 55-64.

Steitz, T.A., and Steitz, J.A. (1993). A general two-metal-ion mechanism for catalytic RNA. Proc Natl Acad Sci U S A *90*, 6498-6502.

Tacke, R., and Manley, J.L. (1999). Functions of SR and Tra2 proteins in pre-mRNA splicing regulation. Proc Natl Acad Sci U S A *220*, 59-63.

Tackenberg, B., Nitschke, M., Willcox, N., Ziegler, A., Nessler, S., Schumm, F., Oertel, W.H., Hemmer, B., and Sommer, N. (2003). CD45 isoform expression in autoimmune myasthenia gravis. Autoimmunity *36*, 117-121.

Tardiff, D.F., and Rosbash, M. (2005). Arrested yeast splicing complexes indicate stepwise snRNP recruitment during in vivo spliceosome assembly. RNA *12*, 968-979.

Tarn, W.Y. (2007). Cellular signals modulate alternative splicing. J Biomed Sci *14*, 517-522.

Tchilian, E.Z., Wallace, D.L., Dawes, R., Imami, N., Burton, C., Gotch, F., and Beverley, P.C. (2001). A point mutation in CD45 may be associated with an increased risk of HIV-1 infection. Aids *15*, 1892-1894.

Tong, A., Nguyen, J., and Lynch, K.W. (2005). Differential expression of CD45 isoforms is controlled by the combined activity of basal and inducible splicing-regulatory elements in each of the variable exons. J Biol Chem *280*, 38297-38304.

Trowbridge, I.S., and Thomas, M.L. (1994). CD45: An emerging role as a protein tyrosine phosphatase required for lymphocyte activation and development. Annu Rev Immunol *12*, 85-116.

Valadkhan, S. (2007). The spliceosome: caught in a web of shifting interactions. Curr Opin Struct Biol *17*, 310-315.

Valcarcel, J., Singh, R., Zamore, P.D., and Green, M.R. (1993). The protein Sex-lethal antagonizes the splicing factor U2AF to regulate alternative splicing of transformer pre-mRNA. Nature *362*, 171-175.

Wagner, E.J., and Garcia-Blanco, M.A. (2001). Polypyrimidine tract binding protein antagonizes exon definition. Mol Cell Biol *21*, 3281-3288.

Wang, H.-Y., Xu, X., Ding, J.-H., Bermingham, J.R., and Fu, X.-D. (2001). SC35 plays a role in T cell development and alternative splicing of CD45. Mol Cell *7*, 331-342.

Wang, Z., Rolish, M.E., Yeo, G., Tung, V., Mawson, M., and Burge, C.B. (2004). Systematic identification and analysis of exonic splicing silencers. Cell *119*, 831-845.

Watakabe, A., Tanaka, K., and Shimura, Y. (1993). The role of exon sequences in splice site selection. Genes Dev *7*, 407-418.

Wilkinson, K.A., Merino, E.J., and Weeks, K.M. (2006). Selective 2'-hydroxyl acylation analyzed by primer extension (SHAPE): quantitative RNA structure analysis at single nucleotide resolution. Nat Protoc *1*, 1610-1616.

Woerfel, G., and Bindereif, A. (2001). In vitro selection of exonic splicing enhancer sequences: identification of novel CD44 enhancers. Nucleic Acids Res *29*, 3204-3211.

Wu, J.Y., and Maniatis, T. (1993). Specific interactions between porteins implicated in splice site selection and regulated alternative splicing. Cell *75*, 1061-1070.

Xie, J., and Black, D.L. (2001). A CaMK IV responsive RNA element mediates depolarization-induced alternative splicing of ion channels. Nature *410*, 936-939.

Xu, Z., and Weiss, A. (2002). Negative regulation of CD45 by differential homodimerization of the alternatively spliced isoforms. Nat Immunol *3*, 764-771.

Zahler, A.M., Damgaard, C.K., Kjems, J., and Caputi, M. (2004). SC35 and heterogeneous nuclear ribonucleoprotein A/B proteins bind to a juxtaposed exonic splicing enhancer/exonic splicing silencer element to regulate HIV-1 tat exon 2 splicing. J Biol Chem *279*, 10077-10084.

Zhang, X.H., and Chasin, L.A. (2004). Computational definition of sequence motifs governing constitutive exon splicing. Genes Dev *18*, 1241-1250.

Zheng, Z.M. (2004). Regulation of alternative RNA splicing by exon definition and exon sequences in viral and mammalian gene expression. J Biomed Sci *11*, 278-294.

Zhou, Z., Licklider, L.J., Gygi, S.R., and Reed, R. (2002). Comprehensive proteomic analysis of the human spliceosome. Nature *419*, 182-185.

Zhu, H., Hasman, R.A., Young, K.M., Kedersha, N.L., and Lou, H. (2003). U1 snRNP-dependent function of TIAR in the regulation of alternative RNA processing of the human calcitonin/CGRP pre-mRNA. Mol Cell Biol *23*, 5959-5971.

Zhu, J., Mayeda, A., and Krainer, A.R. (2001). Exon identity established through differential antagonism between exonic splicing silencer-bound hnRNP A1 and enhancer-bound SR proteins. Mol Cell *8*, 1351-1361.

Zuo, P., and Maniatis, T. (1996). The splicing factor U2AF35 mediates critical protein-protein interactions in constitutive and enhancer-dependent splicing. Genes Dev *10*, 1356-1368.

VITAE

Amy Elizabeth House was born in Hagerstown, Maryland on July 20, 1980, the daughter of Brenda Kay Murphy House and David Arnold House. After receiving her diploma from Middletown High School in Middletown, Maryland in June 1998, she began her studies at the University of Maryland, College Park in August 1998. She received the degree of Bachelor of Science with a major in Cell Molecular Biology and Genetics in from the University of Maryland in May 2002. In August 2002 she entered the Graduate School of Biomedical Sciences at the University of Texas Southwestern Medical Center at Dallas.

Permanent Address: 1409 Marker Road
                                   Middletown, Maryland